AD_____

Award Number: DAMD17-97-1-7180

TITLE: Cell Cycle Analysis of the BRCA1 Gene Product

PRINCIPAL INVESTIGATOR: Dennis M. Lynch, M.D, Ph.D.

CONTRACTING ORGANIZATION: Dana Farber Cancer Institute
Boston, Massachusetts 02115

REPORT DATE: September 2000

TYPE OF REPORT: Final

PREPARED FOR: U.S. Army Medical Research and Materiel Command
Fort Detrick, Maryland 21702-5012

REPORT DOCUMENTATION PAGE

Form Approved
OMB No. 074-0188

1. AGENCY USE ONLY (Leave blank)	2. REPORT DATE	3. REPORT TYPE AND DATES COVERED
	September 2000	Final (15 Aug 97 - 14 Aug 00)

4. TITLE AND SUBTITLE
Cell Cycle Analysis of the BRCA1 Gene Product

5. FUNDING NUMBERS
DAMD17-97-1-7180

6. AUTHOR(S)
Dennis M. Lynch, M.D, Ph.D.

7. PERFORMING ORGANIZATION NAME(S) AND ADDRESS(ES)
Dana Farber Cancer Institute
Boston, Massachusetts 02115

E-MAIL:
dennis_lynch@dfci.harvard.edu

8. PERFORMING ORGANIZATION REPORT NUMBER

9. SPONSORING / MONITORING AGENCY NAME(S) AND ADDRESS(ES)
U.S. Army Medical Research and Materiel Command
Fort Detrick, Maryland 21702-5012

10. SPONSORING / MONITORING AGENCY REPORT NUMBER

11. SUPPLEMENTARY NOTES
Report contains color.

12a. DISTRIBUTION / AVAILABILITY STATEMENT
Approved for public release; distribution unlimited

12b. DISTRIBUTION CODE

13. ABSTRACT *(Maximum 200 Words)*

This project is focused upon a functional analysis of BRCA1, the hereditary breast/ovarian cancer susceptibility gene. Our aims were to identify proteins that interact with BRCA1 and to determine the functional significance of such interactions. To this end, we discovered that BRCA1 interacts with the product of the second major hereditary breast/ovarian cancer gene, BRCA2. Each of these proteins interacts with the recombination protein, Rad51, suggesting a role for BRCA1 and BRCA2 in double strand break repair (DSBR). We developed a functional assay capable of distinguishing between wild-type and mutant alleles of BRCA1. Wild-type but not mutant alleles of BRCA1 were able to restore efficient DSBR to a BRCA1 -/- cell line, HCC1937. Finally, we cloned a novel helicase, termed BACH1, that interacts specifically and directly with the BRCT motifs of BRCA1. Our data suggest that the interaction of BRCA1 with BACH1 is required for efficient DSBR, and that mutation of BACH1 may contribute to human breast cancer susceptibilty.

14. SUBJECT TERMS	15. NUMBER OF PAGES
Breast Cancer	65
	16. PRICE CODE

17. SECURITY CLASSIFICATION OF REPORT	18. SECURITY CLASSIFICATION OF THIS PAGE	19. SECURITY CLASSIFICATION OF ABSTRACT	20. LIMITATION OF ABSTRACT
Unclassified	Unclassified	Unclassified	Unlimited

NSN 7540-01-280-5500

Standard Form 298 (Rev. 2-89)
Prescribed by ANSI Std. Z39-18
298-102

FOREWORD

Opinions, interpretations, conclusions and recommendations are those of the author and are not necessarily endorsed by the U.S. Army.

———	Where copyrighted material is quoted, permission has been obtained to use such material.
———	Where material from documents designated for limited distribution is quoted, permission has been obtained to use the material.
———	Citations of commercial organizations and trade names in this report do not constitute an official Department of the Army endorsement or approval of the products or services of these organizations.
X	In conducting research using animals, the investigator(s) adhered to the "Guide for the Care and Use of Laboratory Animals," prepared by the Committee on Care and Use of Laboratory Animals of the Institute of Laboratory Animal Resources, National Research Council (NIH Publication No. 86-23, Revised 1985).
X	For the protection of human subjects, the investigator(s) adhered to policies of applicable Federal Law 45 CFR 46.
X	In conducting research utilizing recombinant DNA, the investigator(s) adhered to the NIH Guidelines for Research Involving Recombinant DNA Molecules.
N/A	In the conduct of research involving hazardous organisms, the investigator(s) adhered to the CDC-NIH Guide for Biosafety in Microbiological and Biomedical Laboratories.

Dennis C. Lynch, M.D., Ph.D.

Table of Contents

5. INTRODUCTION

The goal of this research is to understand the mechanism of function of the major hereditary breast/ovarian cancer predisposition gene, BRCA1. To this end, we have undertaken a number of investigations aimed at identification of BRCA1 interaction partners. The full extent of this project has been completed, and has resulted in the identification of several novel BRCA1-interaction partners. In addition, we have developed a functional assay for BRCA1, which points to a tumor suppressor function for this gene in the repair of double strand DNA breaks.

6. BODY

The search for BRCA1 interacting proteins had previously indicated that BRCA1 interacts with the recombination protein, Rad51. BRCA1 and Rad51 were found to co-localize in subnuclear foci (1) and to relocalize to PCNA structures in S phase following exposure of cells to certain genotoxic agents (2). We found that BRCA1 also colocalizes with BRCA2, the product of the second major hereditary breast/ovarian cancer predisposition gene (3). BRCA1 and BRCA2 were found to co-immunoprecipitate in a complex with Rad51. Consistent with these findings, BRCA1 and BRCA2 also colocalized on meiotic chromosomes.

A major unanswered question at the outset of this research program was to identify cellular and biochemical functions of BRCA1 that might be relevant to tumor suppression. This became accessible to careful study once a cell line lacking wild-type BRCA1, HCC1937, became available (4). By use of retroviral transduction, we raised populations of this cell line in which either wild-type or clinically described mutant alleles of BRCA1 were expressed stably, at approximately physiological levels (5). Wild-type but not mutant alleles of BRCA1 were found to reverse sensitivity of HCC1937 cells to gamma radiation, a form of ionizing radiation (IR) known to induce double strand DNA breaks (DSB). A thorough analysis of the mechanisms underlying this reversal revealed that HCC1937 cells exhibited defective kinetics of DSBR, and that introduction of wild-type BRCA1 had restored DSBR to normal rapid kinetics. Dramatically, multiple missense mutant alleles of BRCA1, expressed stably in HCC1937 cells, each failed to complement the DSBR defect (5). Therefore, this work provided genetic evidence of a role for BRCA1 in DSBR and suggested that this is a significant tumor suppressor function of BRCA1.

Using conventional protein interaction screens, we have recently cloned a novel helicase-like protein, which interacts specifically and directly with the C terminal BRCT motifs of BRCA1 (manuscript submitted). This 130kDa protein has been termed BACH-1 (BRCA1-associated C terminal-binding helicase-1). Clinically described, loss-of function disease predisposing mutation of the BRCA1 BRCT region abrogates BRCA1-BACH1 binding. A novel sequence in the C terminus of BACH-1 is necessary and sufficient for BRCA1 binding. BACH-1 colocalized with BRCA1 in somatic cell subnuclear foci. Indeed, the localization of BACH-1 to characteristic foci was dependent upon BRCA1.

We asked whether fragments or mutant forms of BACH-1, when overexpressed, might exhibit "dominant negative" properties. In view of the recently developed functional assay for BRCA1 that revealed a role for BRCA1 in DSBR, we determined whether such BACH-1 derivatives could disturb DSBR in repair competent cells. A mutant form of BACH-1, engineered so as to lose the ATP-binding residue characteristic of all active helicase proteins, disturbed DSBR in the repair-competent cell line, U2OS. Indeed, the kinetics of DSBR in such cases resembled that of the BRCA1-mutant cell line, HCC1937. This suggested that BRCA1 DSBR function is exerted, in part, by its interaction with BACH-1.

In collaboration with Dr. Daniel Haber (Massachusetts General Hospital and Harvard Medical School), we examined families suffering high incidence of hereditary breast/ovarian cancer, specifically excluding those linked to BRCA1 or BRCA2. Sequencing of the BACH-1 gene in such families revealed one allele, present in one such family but not in the general population, that appeared to destabilize (and thereby inactivate) the BACH-1 protein. Thus, mutation of BACH-1 may be relevant to hereditary breast/ovarian cancer predisposition.

7. KEY RESEARCH ACCOMPLISHMENTS

- Discovery of a physiological interaction between BRCA1 and BRCA2
- Development of a functional assay for BRCA1, indicating that its tumor suppressor function is enacted in DSBR.
- Cloning of a novel BRCA1 interaction partner, BACH-1

8. REPORTABLE OUTCOMES

Chen J, Silver DP, Walpita D, Cantor SB, Gazdar AF, Tomlinson G, Minna JD, Couch FJ, Weber BL, Ashley T, Livingston DM, Scully R. Stable interaction the products of the BRCA1 and BRCA2 tumor suppressor genes in mitotic and meiotic cells. Mol Cell 1998; 2:317-328.

Chen, J, Silver DP, Walpita D, Cantor SB, Gazdar AF, Tomlinson G, Minna JD, Couch FJ, Weber BL, Ashley T, Livingston DM, Scully R. The products of the BRCA1 and BRCA2 tumor suppressor genes interact stably in mitotic and meiotic cells. CSH Meeting on Cancer Genetics and Tumor Suppressor Genes, Cold Spring Harbor, NY, Aug 19-23, 1998. (

Livingston DM. Invited Speaker, Columbia University College of Physician and Surgeons, December 17, 1998: "Functional Analysis of the BRCA1 and 2 Tumor Suppressor Gene Products." (No text available)

Livingston*, DM, Cantor, S, Chen J, Joukov V, Scully R, Liver D, Wu X. "Insights into the molecular basis for BRCA1 and BRCA2 Function," The Genetics Society of America Meeting on "DNA Repair: Bacteria to Humans," Arlie House Conference Center, Warrenton, VA, April 16-19, 1998. *speaker (No text available)

Livingston*, DM, Chen J, Scully S, Silver DP, Cantor S, Joukov, V. "Functional analysis of the BRCA1 and BRCA2 tumor suppressor gene products." The American Society of Hematology Annual Meeting, Miami Beach, Fl, Dec 4-8, 1998.. (no text available)
*speaker

Scully, R, Ganesan, S, Vlasakova, K, Chen, J, Socolovsky, M and Livingston, DM. Genetic Analysis of BRCA1 Function in a Defined Tumor Cell Line. Molecular Cell 1999; 4: 1093–1099

Cantor S, Ganesan S, Kass E, Livingston DM. "A Novel Helicase, BAH1 Interacts with a Tumor Suppression Domain of BRCA1 and Contributes to Its Double Strand Break Repair Function". CSH meeting on Cancer Genetics and Tumor Suppressor Genes, Cold Spring Harbor, NY August 16-20, 2000

Livingston *DM Cantor S, Chen J, Ganesan S, Joukov V, Scully R, Elshamy W, Silver D, Wu X, Yang Y-L,. "Functional Analysis of the BRCA1 Gene Product". 65th Cold Spring Harbor Symposium on Quantative Biology. "Biological Responses to DNA Damage" May 31-June 5, 2000.

Scully R, Ganesan S, Vlasakova K, Chen J, Socolovsky M, and Livingston DM. "Development of a Functional Assay for BRCA1". Era of Hope Meeting, Atlanta, Georgia. June 8-12, 2000.

9. CONCLUSIONS: The work reported here has contributed to the first coherent framework for understanding the function of BRCA1. This work unifies a view of hereditary breast/ovarian cancer predisposition and suggests that defects in genome integrity maintenance, specifically in recombination pathways that contribute to DSBR, are causal in such cancer predisposition syndromes. We have identified a tightly interacting helicase, BACH-1, which promises to allow us to understand BRCA1 function in strict biochemical terms. Ultimately, this work is likely to have impact in shaping the prevention of breast cancer, and may lead to new treatments for this disease.

10. REFERENCES

1. R. Scully, et al., *Cell* 88, 265-75 (1997).
2. R. Scully, et al., *Cell* 90, 425-35 (1997).
3. J. Chen, et al., *Mol Cell* 2, 317-28 (1998).
4. G. E. Tomlinson, et al., *Cancer Res* 58, 3237-42 (1998).
5. R. Scully, et al., *Mol Cell* 4, 1093-9 (1999).

Tasks

Tasks 1-7 Completed in 1996, prior to onset of Grant. Published in:
Scully R, *et al.* Cell 1997; 88: 265-275
Scully R, *et al.* Cell 1997; 90: 425-435.

Task 8 Completed and submitted

Tasks 9-10 Completed in 1996, prior to onset of Grant. Published in:
Scully R, *et al.* Cell 1997; 88: 265-275
Scully R, *et al.* Cell 1997; 90: 425-435.

Tasks 11-14 Specific co-immunoprecipitation of BRCA1 with Rad51 was obtained, thereby bypassing the need to perform these tasks.

Task 15 Completed and submitted

Tasks 16-17 Completed in 1996, prior to onset of Grant. Published in:
Scully R, *et al.* Cell 1997; 88: 265-275. However, two attempts to generate monoclonal antibodies specific to Rad51 failed. Identification of a novel BRCA1-interacting protein BACH1, was performed under these tasks, published in Cantor, S et al. Cell 2001;105: 149-160.

Task 19-21 For BRCA1-Rad51 interaction, Completed in 1996, prior to onset of Grant. Published in:
Scully R, *et al.* Cell 1997; 88: 265-275
Scully, R, *et al.* Molecular Cell 1999; 4: 1093–1099
For BRCA1-BACH1 interaction, published in Cantor, S et al. Cell 2001;105: 149-160.

DEVELOPMENT OF A FUNCTIONAL ASSAY FOR BRCA1

R. Scully, S. Ganesan, K. Vlasakova, J. Chen, M. Socolovsky[§] and D. M. Livingston

Dana-Farber Cancer Institute/Harvard Medical School, Boston, MA; [§]Whitehead Institute/Massachusetts Institute of Technology, Cambridge, MA

Ralph_scully@dfci.harvard.edu

Predisposition to breast and/or ovarian cancer may arise from germ line mutations in either of two tumor suppressor genes, BRCA1 and BRCA2. Our previous work demonstrated an in vivo physical interaction between BRCA1 and the recombination protein, Rad51. BRCA1 and Rad51 colocalized in S/G2 phase subnuclear dots in somatic cells, and on the developing synaptonemal complex in meiotic cells, suggesting a role for BRCA1 in DNA recombination. BRCA2 was also shown to interact with Rad51.

Work performed during the tenure of this award pointed to a specific role for BRCA1 during S phase: certain types of DNA damage caused S phase-specific phosphorylation of BRCA1 and its recruitment to sites of damaged, replicating DNA. We showed that BRCA1 and BRCA2 form a stable complex in somatic cells. This work has received support from numerous gene targeting experiments in the mouse. Mouse embryos that lack wt BRCA1 or 2 function undergo early embryonic arrest, likely associated with activation of one or more cell cycle checkpoints. Primary cells from such embryos reveal radiation hypersensitivity, as well as spontaneous chromosomal anomalies in the absence of extrinsic DNA damage.

These observations point to a role for BRCA1 in the control of genomic integrity and homologous recombination. However, the lack of an assay that permits ready functional analysis of BRCA1 has, in the past, impeded the comparative study of wt and selected mutant species. In an effort to remedy this problem, we used retroviral transduction to express wild-type BRCA1 in a human breast cancer cell line, HCC1937, which lacks wild-type BRCA1. Wild-type BRCA1 was expressed stably at levels equivalent to those seen in human breast cancer cell lines expressing endogenous wild-type BRCA1. This decreased the gamma radiation (IR) sensitivity and increased the efficiency of double strand DNA break repair (DSBR) of the HCC1937 cell line. It also reduced its susceptibility to DSB generation by IR. By contrast, multiple, clinically-validated, missense mutant BRCA1 products were non-functional in these assays. These data constitute the basis for a tractable, in vivo functional assay for BRCA1 and suggest that efficient repair of double strand DNA breaks is linked to its tumor suppression function. This work was recently published.

References available upon request.

The U. S. Army Medical Research and Materiel Command under DAMD17-97-1-7180 supported this work.

Molecular Cell, Vol. 4, 1093–1099, December, 1999, Copyright ©1999 by Cell Press

Genetic Analysis of BRCA1 Function in a Defined Tumor Cell Line

Ralph Scully,*§ Shridar Ganesan,*§
Katerina Vlasakova,* Junjie Chen,*‖
Merav Socolovsky,† and David M. Livingston*‡
*Dana-Farber Cancer Institute and
Harvard Medical School
Boston, Massachusetts 02115
†Whitehead Institute and
Massachusetts Institute of Technology
Cambridge, Massachusetts 02138

Summary

Retrovirally expressed, wild-type BRCA1 decreased the γ radiation (IR) sensitivity and increased the efficiency of double-strand DNA break repair (DSBR) of the *BRCA1*$^{-/-}$ human breast cancer line, HCC1937. It also reduced its susceptibility to DSB generation by IR. By contrast, multiple, clinically validated, missense mutant *BRCA1* products were nonfunctional in these assays. These data constitute the basis for a BRCA1 functional assay and suggest that efficient repair of double-strand DNA breaks is linked to BRCA1 tumor suppression function.

Introduction

Predisposition to breast and/or ovarian cancer may arise from germline mutations in either of two tumor suppressor genes, *BRCA1* and *BRCA2* (reviewed in Weber, 1998). Biochemical and cell biological data suggest a role for BRCA1 and BRCA2 in DNA recombination (Scully et al., 1997a, 1997c; Sharan et al., 1997; Chen et al., 1998; Moynahan et al., 1999; Zhong et al., 1999; X. Wu et al., submitted).

Mouse embryos that lack wild-type BRCA1 or 2 function undergo early embryonic arrest, most likely associated with activation of one or more cell cycle checkpoints (Hakem et al., 1996, 1997; Ludwig et al., 1997; Sharan et al., 1997). Moreover, primary cells from such embryos reveal spontaneous chromosomal anomalies in the absence of extrinsic DNA damage (Patel et al., 1998; Shen et al., 1998; Xu et al., 1999a). Furthermore, murine *BRCA1*-induced tumorigenesis is promoted by preexisting inactivation of *p53* (Cressman et al., 1999; Xu et al., 1999b), consistent with the hypothesis that checkpoint inactivation is necessary for cellular tolerance of BRCA1 loss and may precede BRCA1 inactivation during tumorigenesis (Scully et al., 1997a).

The lack of an assay that permits ready functional analysis of BRCA1 has impeded the comparative study of wild-type and selected mutant species. Data reported here constitute the basis for such an assay, which is also capable of supporting detailed BRCA1 genetic analysis.

‡To whom correspondence should be addressed (e-mail: david_livingston@dfci.harvard.edu).
§These authors contributed equally to this work.
‖Present address: Mayo Clinic, 200 First Street SW, Rochester, Minnesota 55905.

Results

Characterization of HCC1937 Cells

The *BRCA1*-mutated breast cancer cell line, HCC1937, has been described previously (Tomlinson et al., 1998). It synthesizes a truncated BRCA1 protein that is the product of a disease-producing mutant allele (*5382insC*) and no wild-type protein (Chen et al., 1998; Figure 1B). Levels of BARD1, BRCA2, Rad51, and Rad50/MRE11/NBS1—all BRCA1-interacting proteins—were normal in these cells (data not shown). All but BARD1 were normally localized in S+G2 phase nuclear dot structures (X. Wu et al., submitted, and data not shown). Like BARD1, the indigenous mutant BRCA1 protein was absent from nuclear dots in these cells (Figure 1D).

In view of a potential role for BRCA1 in recombination, we compared the γ irradiation (IR) sensitivity of HCC1937 with that of other human cell lines expressing endogenous wild-type *BRCA1*. HCC1937 cells were considerably more IR sensitive than the other lines tested (Figure 2A), as has also been noted by others (Abbott et al., 1999; Cortez et al., 1999).

Stable Expression of Wild-Type *BRCA1* in HCC1937 Cells

To determine the contribution of the absence of intact BRCA1 to the IR sensitivity profile of HCC1937, we sought to express the wild-type protein in these cells. Acute elevations in BRCA1 can induce cellular toxicity (Wilson et al., 1997), apoptosis (Shao et al., 1996; Harkin et al., 1999), or cell cycle arrest (Somasundaram et al., 1997). We, therefore, sought stable expression of *BRCA1* alleles at levels close to those of the wild-type protein observed in other, well-characterized human cell lines (see below). Moreover, expression was attempted in uncloned pools of these cells, in an effort to avoid the effects of clonal selection.

HCC1937 cells were stably transfected with the murine ecotropic receptor (EcoR), which rendered them susceptible to infection with ecotropic retrovirus (Hua et al., 1998, and data not shown). High titer virus, encoding wild-type BRCA1 and green fluorescent protein (GFP) in a bicistronic array, was generated (Figure 1A). Retroviral integration into HCC1937 allowed GFP to report *BRCA1* expression.

A specific coculture method permitted infection of EcoR$^+$ cells with this vector. EcoR$^+$ cells were first infected with ecotropic retrovirus carrying a puromycin resistance gene and selected in puromycin, generating EcoR$^+$puroR cells. The puromycin-sensitive packaging cell line, VE23.6 (Socolovsky et al., 1997), was transiently transfected with *BRCA1-GFP* retroviral DNA (Figure 1A) and then cocultivated with EcoR$^+$puroR cells. After 72 hr of coculture, puromycin was added to selectively eliminate the packaging cells. Cell sorting was used to

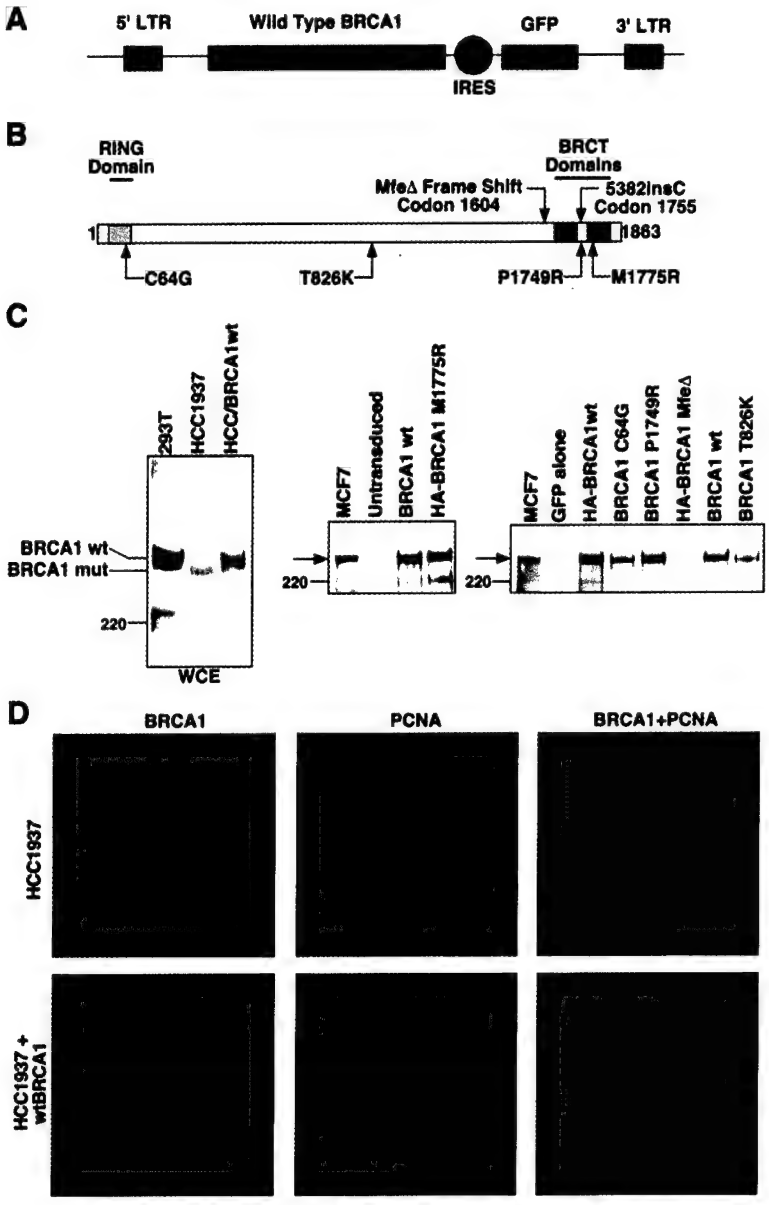

Figure 1. Reexpression of Wild-Type *BRCA1* in HCC1937 Cells Following Recombinant Retroviral Infection

(A) Schematic of the bicistronic retroviral vector. The full-length, wild-type *BRCA1* cDNA was positioned 5′ of the internal ribosomal entry signal (IRES). Translation initiation at the IRES resulted in the production of green fluorescent protein (GFP).

(B) Sites of frameshifted or missense mutant *BRCA1* alleles used in these experiments (not to scale). The RING domain is lightly stippled. The BRCT repeats are heavily stippled.

(C) Steady-state levels of retrovirally encoded *BRCA1* products in HCC1937 cells. Left panel: extracts of 293T, uninfected HCC1937, and HCC1937/BRCA1wt cells were normalized for protein content, separated by 5% SDS-PAGE, and immunoblotted for BRCA1 with mAb MS110 (Scully et al., 1996). Wild-type BRCA1 and the *5382insC* product (BRCA1-mut) are indicated. Middle and right panel: steady-state levels of BRCA1wt and mutant proteins in HCC1937 cells. Cell extracts from HCC1937-derived cultures were normalized for protein, then subjected to IP with mAb SG11, and immunoblotted with mAb MS110 (middle panel) or mAb SD118 (right panel). Full-length BRCA1 is indicated with an arrow. The total protein in the control MCF7 extracts was adjusted to be half that of the HCC1937 extracts.

(D) Localization of wild-type BRCA1 in HCC1937 cells. Uninfected HCC1937 cells (upper row) and HCC1937/BRCA1wt cells (lower row) were immunostained for BRCA1 and PCNA. Left panels: stained with BRCA1 mAb SD118 (FITC, green). Middle panels: stained with PCNA Ab "AK" (rhodamine, red). Right panels: combined images showing localization of wild-type BRCA1 but not mutant BRCA1 in S+G2 phase nuclear dots.

purify pools of GFP$^+$ wild-type BRCA1-producing cells to approximately 90% homogeneity.

The steady-state level of wild-type BRCA1 protein in HCC1937/BRCA1wt cells was approximately 2- to 3-fold higher than that of the *5382insC* product, 2- to 4-fold lower than wild-type BRCA1 levels in 293T cells, and approximately the same as that noted in another human breast cancer cell line, MCF-7 (Figure 1C). Thus, the method yielded cells producing quantities of steady-state BRCA1 within the range detected in other human cell lines.

To confirm the identity of the product detected in HCC1937/BRCA1wt cells, extracts of MCF7, HCC1937, and HCC1937/BRCA1wt cells were subjected to immunoprecipitation (IP) with the C terminal BRCA1 mAb, SG11, and immunoblotting with mAbs specific to other BRCA1 epitopes (Figure 1C). As expected, uninfected HCC1937 extracts revealed no signal, given the absence of an SG11 epitope in the *5382insC* product (Chen et al., 1998; Tomlinson et al., 1998; Figure 1C). In contrast, HCC1937/BRCA1wt cells contained a full-length, approximately 220 kDa BRCA1 protein (Figure 1C).

Wild-type BRCA1 in HCC1937 localized in discrete S and G2 phase dots (Figure 1D, bottom row panels; Scully et al., 1997a). In contrast, the endogenous *5382insC* product was detected in a weakly staining, stippled pattern, even in S phase cells (Figure 1D, top row panels).

Suppression of Radiation Hypersensitivity by Wild-Type BRCA1

The doubling time, cell cycle distribution, and plating efficiency (~5%) of HCC1937/BRCA1wt cells were similar to those of parental HCC1937. However, they were significantly less sensitive to IR in colony formation assays (Figure 2B). To further assess this property, we prepared a (1:8) mixture of HCC1937/BRCA1wt (GFP$^+$)

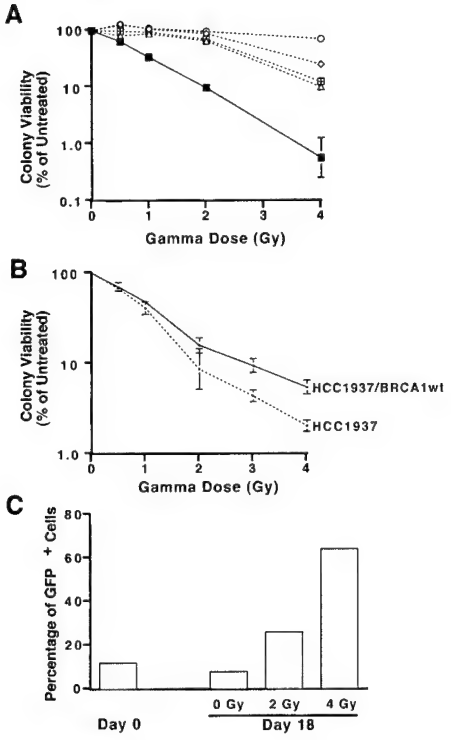

Figure 2. Wild-Type BRCA1 Decreases the γ Radiation Sensitivity of HCC1937 Cells

(A) Comparison of radiation sensitivity of HCC1937 cells with unrelated human cell lines synthesizing wild-type BRCA1. Cells were plated, γ irradiated, and scored for colony formation as described in the Experimental Procedures. Cells were identified as follows: closed squares, HCC1937; open circles, MDA MB435S; open diamonds, T47D; crossed squares, U2OS; open triangles, MDA MB231.

(B) Reconstitution with wild-type BRCA1 reverses γ sensitivity of HCC1937. γ irradiation and colony formation assays were performed as described in the Experimental Procedures. Error bars represent standard error of triplicate measurements.

(C) γ irradiation produces enrichment of wild-type BRCA1$^+$GFP$^+$ cells within a mixture of HCC1937/BRCA1wt and HCC1937 cells. The values indicate the percentage of GFP$^+$ cells in the culture after exposure to 0, 2Gy, or 4Gy at day 0 or day 18 after irradiation.

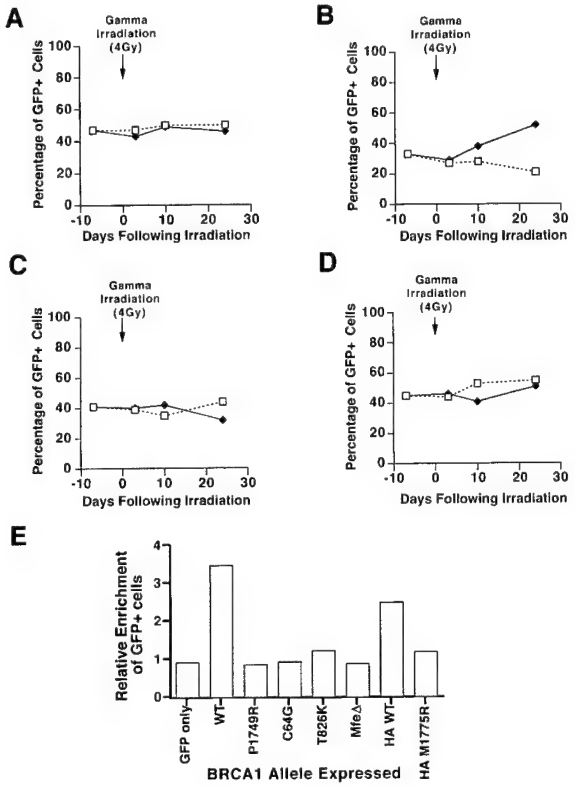

Figure 3. Wild-Type, but Not Mutant, BRCA1 Enhances IR Resistance of HCC1937 Cells

Pools of GFP$^+$ cells expressing various *BRCA1* alleles were mixed with parental HCC1937 cells. Cell mixtures were either γ-irradiated (4Gy) or left untreated, and the percentage of GFP$^+$ cells in the culture was assessed at the times shown. Closed diamonds, irradiated mixed cultures. Open symbols, parallel unirradiated cultures.

(A) Cells infected with *GFP* alone.

(B) Cells infected with *HA-BRCA1wt*.

(C) Cells infected with *BRCA1 P1749R*.

(D) Cells infected with *BRCA1 C64G*.

(E) Summary of the data at day 24 in (A–D) and the inclusion of additional data obtained in the same experiment as (A–D) with GFP$^+$ cultures producing untagged wild-type, T826K, HA MfeΔ, and HA M1775R BRCA1. A ratio (of the percentage of GFP$^+$ cells in the irradiated culture divided by that in the unirradiated control) of greater than 1 implies enhancement of γ resistance.

and parental HCC1937 (GFP$^-$) cells and subjected aliquots to either no irradiation, 2Gy, or 4Gy. The fate of the two populations after irradiation was followed by determining the relative proportion of GFP$^+$:GFP$^-$ cells in the relevant cultures (Figure 2C). After 18 days of coculture, the unirradiated, mixed culture contained 8% GFP$^+$ cells, little different from the starting mixture. By contrast, the 2Gy-treated culture contained 26% GFP$^+$ cells, and the 4Gy-treated culture 64% GFP$^+$ cells (Figure 2C), further evidence that wild-type *BRCA1* expression promotes survival after IR.

Structural Motifs of BRCA1 Contributing to Post-IR Survival

The retroviral transduction method was also applied to a genetic analysis of BRCA1 function. Pools of EcoR$^+$ cells were infected, in parallel, with retroviruses encoding wild-type and various mutant *BRCA1* products. The relevant products included: wild-type BRCA1; the RING domain mutant, C64G; the C terminal mutant, P1749R; N terminal influenza hemagglutinin (HA)–tagged wild-type BRCA1; the HA-BRCA1 C terminal mutant, M1775R; the exon 11 mutant, T826K; and the HA-BRCA1 mutant, MfeΔ, which is frameshifted at codon 1604 (Figure 1B). A viral vector carrying IRES-*GFP* but no *BRCA1* allele served as a negative control. Once again, infected populations were sorted to contain approximately 90% GFP$^+$ cells. Cultures synthesizing C64G, P1749R, M1775R, or T826K contained full-length (point mutant) BRCA1 proteins, the steady-state levels of which were similar to those of a wild-type BRCA1-expressing culture (Figure 1C). Despite high expression levels of *BRCA1 MfeΔ* in HCC1937 (as judged by the GFP signal), we were repeatedly unable to detect the expected HA-tagged protein product in vivo, using mAbs capable of recognizing the in vitro–translated *MfeΔ* product (data not shown). Possibly, this protein is unstable in HCC1937.

As before, specifically mixed cultures of HCC1937

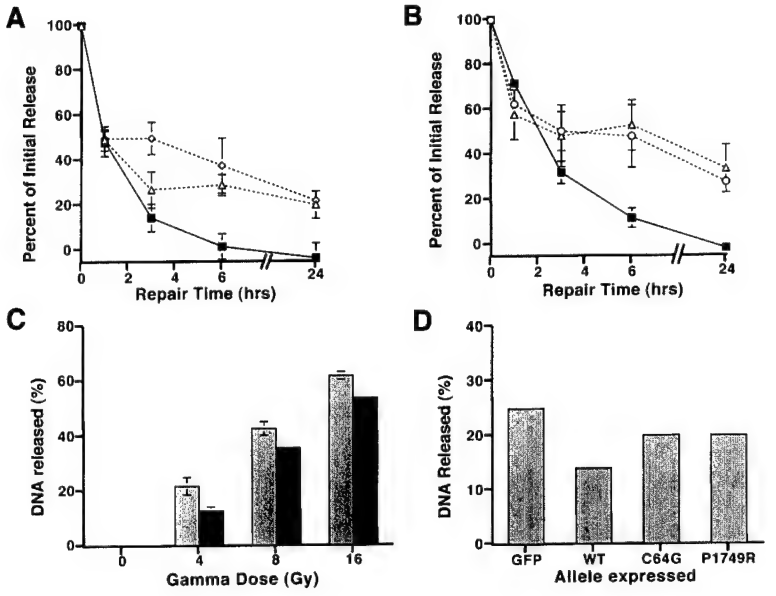

Figure 4. Introduction of Wild-Type BRCA1 into HCC1937 Alters the Kinetics of DSBR

(A) HCC1937 expressing either HA-BRCA1wt (closed squares), GFP alone (open diamonds), or BRCA1 mutant P1749R (open triangles) were treated with 8Gy and harvested at the times indicated. Residual DSBs were determined as described in the Experimental Procedures. Each point represents the mean and standard error of at least three independent measurements within one experiment.

(B) HCC1937 synthesizing BRCA1 mutants C64G (open circles), T826K (open triangles), or untagged BRCA1wt (closed squares, different culture to Figure 4A) were treated with 8Gy and processed as described above. Where no error bars are shown they are too small for clear representation.

(C) Comparison of the induction of double-stranded breaks in HCC1937/GFP (light stippling) versus HCC1937/HA-BRCA1wt cells (heavy stippling). Cultures were treated as described in the Experimental Procedures. The data shown represent the percent of total DNA released into the pulsed field gel at the γ dose shown. Where no error bars are shown, they are too small for clear representation.

(D) Comparison of induction of DSBs by 4Gy IR in HCC1937/BRCA1 cells expressing the alleles shown. Values are the mean of duplicate samples, obtained in a separate experiment to that described in Figure 4C.

(GFP$^-$) and HCC1937/BRCA1wt (GFP$^+$) or mutant protein-producing (GFP$^+$) cells were prepared and either irradiated (4Gy) or left untreated. Cells were analyzed by FACS for quantitative GFP status 3, 10, and 24 days after irradiation (Figure 3). Cells transduced with GFP alone showed no growth advantage relative to parental HCC1937, whether irradiated or unirradiated (Figure 3A). By contrast, cells synthesizing wild-type BRCA1 or HA-tagged wild-type BRCA1 showed, as before, a relative growth advantage in the irradiated mixed culture, but not in the unirradiated control (Figures 3B and 3E). GFP$^+$ cells synthesizing BRCA1 P1749R, C64G, M1775R, T826K, or MfeΔ failed to exhibit an IR-specific growth advantage after exposure to 4Gy (Figures 3C–3E). Therefore, reversal of the IR sensitivity phenotype by BRCA1 requires, at a minimum, an intact RING domain, BRCT motifs, and certain structures encoded by exon 11. Of note, unirradiated, uncloned cells producing the T826K mutant protein outproliferated similarly untreated parental cells (data not shown).

Cell Cycle Checkpoint Function

DNA damage-dependent checkpoint function can contribute to IR resistance. However, HCC1937 cells revealed functional S phase deceleration and G2/M checkpoints, but no G1 checkpoint response, in keeping with the absence of p53 in these cells (Lu and Lane, 1993). In the same experiments, ataxia-telangiectasia (AT) cells revealed the expected radioresistant DNA synthesis phenotype (Painter and Young, 1980). None of these HCC1937 phenotypes were modified by reexpression of wild-type *BRCA1* (data not shown). Therefore, absence of the protein is not associated with alterations in two cell cycle checkpoints. On the other hand, a post-IR mitotic checkpoint defect was noted in primary cells producing a *BRCA1* allele lacking exon 11 (Xu et al., 1999a). Conceivably, the *5382insC* gene product can perform or induce certain checkpoint functions that an internally deleted protein cannot.

Wild-Type, but Not Mutant, BRCA1 Restores Double-Strand Break Repair

Of the various DNA lesions generated by IR, the double-strand break (DSB) is most closely correlated with cell lethality (reviewed in Foray et al., 1997). In order to determine whether BRCA1 makes a contribution to double-strand break repair (DSBR), its kinetics in HCC1937/BRCA1wt were compared with those of vector-infected HCC1937 ("HCC1937/GFP"). After exposure to 8Gy, repair kinetics were similar during the first hour (Figure 4A). Thereafter, HCC1937/GFP cells failed to repair DSBs efficiently, seen most strikingly after 3 hr (Figure 4A). In contrast, the repair of DSBs in HCC1937/BRCA1wt cells was nearly complete within the first 6 hr (Figure 4A), a time course characteristic of repair-proficient cell lines that synthesize endogenous wild-type BRCA1 (Nevaldine et al., 1993).

In the same experiment, we examined the kinetics of DSBR in HCC1937-expressing BRCA1 missense mutant alleles that had failed to reverse γ sensitivity (BRCA1 P1749R, BRCA1 C64G, and BRCA1 T826K; see above). HCC1937/BRCA1 P1749R, HCC1937/BRCA1 C64G, and HCC1937/BRCA1 T826K cells showed repair kinetics similar to those of HCC1937/GFP cells (Figures 4A and 4B), indicating a failure by all to complement the DSBR defect of HCC1937.

Wild-Type BRCA1 Protects against the Development of Radiation-Induced DSBs

In the DSBR assay, described above, the initial release of DNA into the gel after IR is a measure of the number of induced DSBs. For a given dose of IR, HCC1937/GFP

cells consistently released a greater fraction of genomic DNA into the gel than did HCC1937/BRCA1wt cells (Figure 4C). Therefore, reconstitution with wild-type BRCA1 reduced the sensitivity of HCC1937 chromosomal DNA to radiation-induced breakage. By contrast, equivalent expression of two missense mutants (C64G and P1749R) failed to suppress effectively the "hypernickability" phenotype (Figure 4D).

Discussion

HCC1937 represents a tool for investigating various functions of BRCA1. IR hypersensitivity has previously been observed in this and other *BRCA1* and *BRCA2* mutant cell types (Connor et al., 1997; Sharan et al., 1997; Gowen et al., 1998; Patel et al., 1998; Shen et al., 1998; Abbott et al., 1999; Cortez et al., 1999). To determine whether this property was linked to the absence of normal BRCA1 function in this line, HCC1937 was infected with a retrovirus-encoding wild-type BRCA1 protein that led to its synthesis in uncloned cell populations under nonoverexpression conditions. The protein significantly, albeit incompletely, suppressed HCC1937 γ sensitivity, consistent with results of Cortez et al. (1999). The basis for the residual γ sensitivity of BRCA1-reconstituted cells is unclear.

The retroviral expression approach also permitted new, valid comparisons of function among a collection of wild-type and clinically relevant, missense mutant alleles. Three different missense mutants, each defective in what have been speculated to be biochemically unrelated domains—the RING domain (Wu et al., 1996), the BRCT repeats (Chapman and Verma, 1996; Monteiro et al., 1996; Scully et al., 1997b; Yu et al., 1998), and one or more structures encoded by exon 11—each failed to restore radiation resistance. These three distinctive structural elements, therefore, cooperate to promote postirradiation survival and might interact in as yet unappreciated ways. The exon 11 observations are consistent with the data of Xu et al. (1999a), who analyzed cells from mice carrying exon 11–deleted alleles and demonstrated spontaneous chromosomal rearrangements. Interestingly, G2/M checkpoint abnormalities were also detected in these cells (Xu et al., 1999a).

HCC1937 exhibits relatively slow kinetics of DSBR, in keeping with recent results of Moynihan et al. (1999) obtained in *BRCA1*$^{-/-}$ murine ES cells. We further noted that stable expression of wild-type *BRCA1* increased the efficiency of this process dramatically, while equivalent levels of three clinically relevant missense mutant proteins did not. This is evidence of a direct and specific contribution of full-length, wild-type BRCA1 to a defined, endogenous biochemical process (i.e., DSBR) in which, once again, three regions of the polypeptide cooperate to effect a normal outcome.

For a given dose of γ radiation, HCC1937 produced more DNA breaks than HCC1937/BRCA1wt cells, and certain missense mutants also failed to correct this defect. This phenotype is similar to that detected in several radiosensitive cell types, including AT cells, and has been interpreted as a defect in chromatin organization (Painter, 1982; Smith, 1984). Alternatively, this could reflect differences in "daughter strand gap repair." These hypotheses are testable with the use of the internally controlled BRCA1 assay system described here.

Since HCC1937 cells synthesize a truncated BRCA1 protein, the opportunity was potentially there for collaborative interaction between this endogenous C terminal truncated protein and, for example, a mutant BRCA1 polypeptide with an intact C terminus (e.g., C64G, T826K). That this form of interallelic complementation was not observed suggests that, at a minimum, intact RING, BRCT, and exon 11–encoded regions must be present on one BRCA1 molecule for it to function in DSBR. If so, the contribution of BRCA1 to DSBR may be integrative, suggesting that it performs a scaffolding function.

The data presented here offer an assay that can distinguish the biological and biochemical behavior of wild type from that of clinically validated, missense mutant alleles of *BRCA1* expressed at levels within a range observed in multiple, human cell lines. An analysis of BRCA1 radiation rescue and of DSBR in HCC cells has also been performed by others (Abbott et al., 1999). Their experiments relied upon overexpression of various, functionally defective mutant proteins in the absence of an intact, wild-type BRCA1 control, thereby limiting its usefulness as an assay method. Our structure–function analysis reveals a close correlation between failure of BRCA1 to perform DSBR, to protect the genome from excessive IR-mediated DS breakage, and to protect breast and ovarian cells from developing into malignant tumors.

Experimental Procedures

Cell Culture, IP, Immunoblotting, and Immunostaining

HCC1937 cells (from Dr. Adi Gazdar) were maintained in ACL4 medium with 10% FBS (Hyclone), as described in Tomlinson et al. (1998). Other cell lines (ATCC) were maintained in DMEM/10% FBS. Other procedures were performed as described previously (Scully et al., 1997c).

Plasmids and In Vitro Translation

Mutations in *BRCA1* were generated as follows. For the C64G mutant, wild-type *BRCA1* in vector pcDNA3β (Scully et al., 1997a) was used as template for PCR generation of the missense point mutant, C64G, using external PCR primers: 1, 5′-GGGCCCAAGCTTACCATGGATTTATCTGCTCTTCG-3′; 2, 5′-ATAGTCGACTTCCAGCCCATCTGTTATGT-3′; and internal PCR primers: 3, 5′-CCAGAAGAAAGGGCCCTCACAGTGTCCTTTAGGTAAGAATGATATAACC-3′; and 4, 5′-GGTTATATCATTCTTACCTAAAGGACACTGTGAGGGCCCTTTCTTCTGG-3′. Products were generated using pair 1 and 4 and pair 2 and 3, then reamplified using primers 1 and 2. The product was subcloned into the HindIII–EcoRI sites of a pcDNA3β/BRCAwt vector and screened for the new ApaI site (underlined in primers 3 and 4). Mutant PCR products were validated by sequencing.

T826K mutant was generated using the same template as above and PCR primers: 1, 5′-GGGGGATCCCGGGTACCTGGTACTGATTATGGC-3′; and 2, 5′-CCCGACTGTGGTTAACTTCATGTCCTAGGGGATACTTAAAGCCTTCTTTGTCATTTCTATCTTTGG-3′. The PCR product was digested with KpnI and HpaI and ligated into EcoRI-HpaI-digested pcDNA3β/BRCA1wt, with a second insert *BRCA1wt* fragment, EcoRI–KpnI. The product of the triple ligation was tested for presence of a new AvrII site (underlined in PCR product 2), and the PCR region confirmed to be correct by sequencing. The P1749R and M1775R mutants were kindly supplied by Dr. Fergus Couch; XbaI-digested mutant C terminus–encoding fragments were subcloned into pcDNA3β/BRCA1 vector linearized by XbaI digestion. *BRCA1* cDNA species (wild type or mutant) were subcloned into the retroviral expression vector in two steps. First, the 3′ segment

(~5 kb) was subcloned between the EcoRI and XhoI sites of the vector, MSIG1.1SK (Socolovsky et al., 1999). Second, the 5′ segment was prepared by digestion of the relevant *BRCA1* cDNA with HindIII followed by Klenow treatment to generate a blunt end. EcoRI digestion released the approximately 1 kb 5′ *BRCA1* fragment, which was subcloned into the NotI–EcoRI sites of the MSIG1.1SK vector (the NotI site was Klenow fragment treated prior to subcloning). The MfeΔ mutant was generated by digesting MSIG1.1SK/HA-BRCA1wt with MfeI. After Klenow fragment treatment, the residual sequences were religated, generating a frameshift mutation at codon 1604.

In vitro transcription translation reactions were performed using a TNT kit (Promega), according to the manufacturer's protocol, using ^{35}S-methionine to label plasmid-encoded protein. The MSIG1.1SK vector has a T3 RNA polymerase site 5′ of the multiple cloning site, which permitted subcloned inserts to be transcribed/translated in vitro.

Retroviral Infections

HCC1937 cells were transfected with murine ecotropic receptor (EcoR)-IRES-neo vector (Hua et al., 1998), by use of calcium phosphate transfection, and selected in G418 (GIBCO-BRL) at 400 mcg/ml. Stable transfectants were exposed to high titer retrovirus encoding a puromycin resistance gene and then selected in puromycin (Sigma) at 2 mcg/ml final concentration. The resulting puromycin-resistant (puroR) cells (HCC1937EcoR$^+$puroR) had, thereby, demonstrated functionality of the stably expressed, ecotropic receptor.

Production of *BRCA1*-IRES-*GFP* recombinant retrovirus was achieved by calcium phosphate-mediated transfection of the ecotropic packaging cell line, VE23.6 (Socolovsky et al., 1997), with MSIG1.1SK/BRCA1 vector. In this plasmid, wild-type *BRCA1* cDNA was cloned immediately upstream of an IRES, which in turn separates it from a *GFP* allele. The medium was changed 5–6 hr later. VE23.6 cells (~5×10^6) were cocultured 12 hr after transfection with approximately 10^6 recipient HCC1937EcoR$^+$puroR cells in a 100 mm dish in 5 ml of ACL4/FBS medium, with added Polybrene (Sigma; 4 mcg/ml). Half of the medium was replaced daily in order to maintain a relatively stable retroviral titer. After 72 hr of cocultivation, puromycin (2 mcg/ml) was added to eliminate the VE23.6 cells. HCC1937 EcoR$^+$puroR cells were subjected to flow cytometry 48 hr or more later, and GFP$^+$ cells were selected. Infection rates for MSIG1.1SK vector alone of up to 70% were observed by this method. In contrast, the larger *BRCA1*-IRES-*GFP* vector permitted stable retroviral transduction rates of approximately 5%. GFP$^+$ cells were resorted by use of a Vantage FACS Sorter (Becton Dickenson) to achieve approximately 90% GFP$^+$ populations.

Assays for IR Sensitivity

All cell lines tested were assayed for plating efficiency. HCC1937 cells, HCC1937/BRCA1wt, and mutant-producing cells revealed a plating efficiency of approximately 5% across a range of cell densities. For colony formation assays, cells were plated so as to produce approximately 30–100 colonies per 60 mm dish at the final count. Plates were blindly scored. HCC1937 colony formation assays were performed in triplicate and the data presented as mean and standard error values.

Mixed culture irradiation experiments were performed as described in the text. At the times of FACS analysis, cells were trypsinized, and aliquots were analyzed for their content of GFP$^+$ cells. The remaining aliquots were allowed to continue growing until the next experimental time point.

Double-Strand Break Repair Assay

Cells were irradiated with a ^{137}Cs source at 4°C and allowed to repair DNA breaks at 37°C. At the indicated times, cellular DNA was analyzed by pulse field gel electrophoresis as described (Badie et al., 1995). After electrophoresis, the gel was processed and stained with SYBR green as described (Kiltie and Ryan, 1997). Fluorescence was quantitated with a Molecular Dynamics Storm Scanner using the blue fluorescence channel and ImageQuant software (Molecular Dynamics). The fraction of DNA entering the gel was measured using the formula: Percent release = (signal in lane)/[(signal in lane) + (signal in plug)] × 100. The quantity of signal present in unirradiated, parallel control cultures (<10% of total input DNA in a given lane) was taken as a measure of background signal and subtracted from the measured values. For kinetic studies, the data presented were normalized to the percent released at T = 0. Each data point in these kinetic experiments reflects the mean and standard error of at least three independent measurements. For experiments that examined induction of DSB at different doses of γ irradiation, the cells were trypsinized and kept at 4°C before casting into plugs.

Acknowledgments

We are grateful to our laboratory colleagues for many helpful discussions and for numerous reagents. We also express sincere thanks to Drs. Nicolas Foray and Jean Feunteun for sharing their expertise in pulsed field gel electrophoresis and to Dr. Harvey Lodish for his support of M. S. (NIH grant HL 32262). This work was supported by grants from the NCI and by a US DOD IDEA Award (to D. M. L.), a Howard Temin Award from the NCI (to R. S.), a grant from the Susan B. Komen Foundation (to D. M. L.), and an HHMI fellowship for physicians (to S. G.).

Received October 21, 1999; revised November 16, 1999.

References

Abbott, D.W., Thompson, M.E., Robinson-Benion, C., Tomlinson, G., Jensen, R.A., and Holt, J.T. (1999). *BRCA1* expression restores radiation resistance in *BRCA1*-defective cancer cells through enhancement of transcription-coupled DNA repair. J. Biol. Chem. *274*, 18808–18812.

Badie, C., Iliakis, G., Foray, N., Alsbeih, G., Cedervall, B., et al. (1995). Induction and rejoining of DNA double-strand breaks and interphase chromosome breaks after exposure to X rays in one normal and two hypersensitive human fibroblast cell lines. Radiat. Res. *144*, 26–35.

Chapman, M.S., and Verma, I.M. (1996). Transcriptional activation by BRCA1. Nature *382*, 678–679.

Chen, J., Silver, D.P., Walpita, D., Cantor, S.B., Gazdar, A.F., et al. (1998). Stable interaction between the products of the *BRCA1* and *BRCA2* tumor suppressor genes in mitotic and meiotic cells. Mol. Cell *2*, 317–328.

Connor, F., Bertwistle, D., Mee, P.J., Ross, G.M., Swift, S., et al. (1997). Tumorigenesis and a DNA repair defect in mice with a truncating *Brca2* mutation. Nat. Genet. *17*, 423–430.

Cortez, D., Wang, Y., Qin, J., and Elledge, S.J. (1999). Requirement of ATM-dependent phosphorylation of Brca1 in the DNA damage response to double-strand breaks. Science *286*, 1162–1166.

Cressman, V.L., Backlund, D.C., Hicks, E.M., Gowen, L.C., Godfrey, V., and Koller, B.H. (1999). Mammary tumor formation in *p53*- and *BRCA1*-deficient mice. Cell Growth Differ. *10*, 1–10.

Foray, N., Arlett, C.F., and Malaise, E.P. (1997). Radiation-induced DNA double-strand breaks and the radiosensitivity of human cells: a closer look. Biochimie *79*, 567–575.

Gowen, L.C., Avrutskaya, A.V., Latour, A.M., Koller, B.H., and Leadon, S.A. (1998). *BRCA1* required for transcription-coupled repair of oxidative DNA damage. Science *281*, 1009–1012.

Hakem, R., de la Pompa, J.L., Sirard, C., Mo, R., Woo, M., et al. (1996). The tumor suppressor gene *Brca1* is required for embryonic cellular proliferation in the mouse. Cell *85*, 1009–1023.

Hakem, R., de la Pompa, J.L., Elia, A., Potter, J., and Mak, T.W. (1997). Partial rescue of *Brca1* (5–6) early embryonic lethality by *p53* or *p21* null mutation. Nat. Genet. *16*, 298–302.

Harkin, D.P., Bean, J.M., Miklos, D., Song, Y.H., Truong, V.B., et al. (1999). Induction of *GADD45* and JNK/SAPK-dependent apoptosis following inducible expression of *BRCA1*. Cell *97*, 575–586.

Hua, X., Liu, X., Ansari, D.O., and Lodish, H.F. (1998). Synergistic cooperation of TFE3 and smad proteins in TGF-β-induced transcription of the plasminogen activator inhibitor-1 gene. Gen. Dev. *12*, 3084–3095.

Kiltie, A.E., and Ryan, A.J. (1997). SYBR green I staining of pulsed field agarose gels is a sensitive and inexpensive way of quantitating

DNA double-strand breaks in mammalian cells. Nucleic Acids Res. *25*, 2945–2946.

Lu, X., and Lane, D.P. (1993). Differential induction of transcriptionally active p53 following UV or ionizing radiation: defects in chromosome instability syndromes? Cell *75*, 765–778.

Ludwig, T., Chapman, D.L., Papaioannou, V.E., and Efstratiadis, A. (1997). Targeted mutations of breast cancer susceptibility gene homologs in mice: lethal phenotypes of *Brca1*, *Brca2*, *Brca1/Brca2*, *Brca1/p53*, and *Brca2/p53* nullizygous embryos. Gen. Dev. *11*, 1226–1241.

Monteiro, A.N., August, A., and Hanafusa, H. (1996). Evidence for a transcriptional activation function of BRCA1 C-terminal region. Proc. Natl. Acad. Sci. USA *93*, 13595–13599.

Moynahan, M.E., Chiu, J.W., Koller, B.H., and Jasin, M. (1999). *Brca1* controls homology-directed DNA repair. Mol. Cell *4*, 511–518.

Nevaldine, B., Longo, J.A., King, G.A., Vilenchik, M., Sagerman, R.H., and Hahn, P.J. (1993). Induction and repair of DNA double-strand breaks. Radiat. Res. *133*, 370–374.

Painter, R.B. (1982). Structural changes in chromatin as the basis for radiosensitivity in ataxia telangiectasia. Cytogenet. Cell Genet. *33*, 139–144.

Painter, R.B., and Young, B.R. (1980). Radiosensitivity in ataxia-telangiectasia: a new explanation. Proc. Natl. Acad. Sci. USA *77*, 7315–7317.

Patel, K.J., Yu, V.P.C.C., Lee, H., Corcoran, A., Thistlethwaite, F.C., et al. (1998). Involvement of *Brca2* in DNA repair. Mol. Cell *1*, 347–357.

Scully, R., Ganesan, S., Brown, M., De Caprio, J.A., Cannistra, S.A., Feunteun, J., Schnitt, S., and Livingston, D.M. (1996). Location of BRCA1 in human breast and ovarian cancer cells. Science *272*, 123–126.

Scully, R., Chen, J., Plug, A., Xiao, Y., Weaver, D., Feunteun, J., Ashley, T., and Livingston, D.M. (1997a). Association of BRCA1 with Rad51 in mitotic and meiotic cells. Cell *88*, 265–275.

Scully, R., Anderson, S.F., Chao, D.M., Wei, W., Ye, L., Young, R.A., Livingston, D.M., and Parvin, J.D. (1997b). BRCA1 is a component of the RNA polymerase II holoenzyme. Proc. Natl. Acad. Sci. USA *94*, 5605–5610.

Scully, R., Chen, J., Ochs, R.L., Keegan, K., Hoekstra, M., Feunteun, J., and Livingston, D.M. (1997c). Dynamic changes of BRCA1 subnuclear location and phosphorylation state are initiated by DNA damage. Cell *90*, 425–435.

Shao, N., Chai, Y.L., Shyam, E., Reddy, P., and Rao, V.N. (1996). Induction of apoptosis by the tumor suppressor protein BRCA1. Oncogene *13*, 1–7.

Sharan, S.K., Morimatsu, M., Albrecht, U., Lim, D.S., Regel, E., Dinh, C., Sands, A., Eichele, G., Hasty, P., and Bradley, A. (1997). Embryonic lethality and radiation hypersensitivity mediated by Rad51 in mice lacking *Brca2*. Nature *386*, 804–810.

Shen, S.X., Weaver, Z., Xu, X., Li, C., Weinstein, M., Chen, L., Guan, X.Y., Ried, T., and Deng, C.X. (1998). A targeted disruption of the murine *Brca1* gene causes gamma-irradiation hypersensitivity and genetic instability. Oncogene *17*, 3115–3124.

Smith, P.J. (1984). Relationship between a chromatin anomaly in ataxia-telangiectasia cells and enhanced sensitivity to DNA damage. Carcinogenesis *5*, 1345–1350.

Socolovsky, M., Dusanter-Fourt, I., and Lodish, H.F. (1997). The prolactin receptor and severely truncated erythropoietin receptors support differentiation of erythroid progenitors. J. Biol. Chem. *272*, 14009–14012.

Socolovsky, M., Fallon, A.E., Wang, S., Brugnara, C., and Lodish, H.F. (1999). Fetal anemia and apoptosis of red cell progenitors in *Stat5a*$^{-/-}$*5b*$^{-/-}$ mice: a direct role for Stat5 in *Bcl-X(L)* induction. Cell *98*, 181–191.

Somasundaram, K., Zhang, H., Zeng, Y.X., Houvras, Y., Peng, Y., et al. (1997). Arrest of the cell cycle by the tumour-suppressor BRCA1 requires the CDK-inhibitor p21WAF1/CiP1. Nature *389*, 187–190.

Tomlinson, G.E., Chen, T.T., Stastny, V.A., Virmani, A.K., Spillman, M.A., et al. (1998). Characterization of a breast cancer cell line derived from a germ-line *BRCA1* mutation carrier. Cancer Res. *58*, 3237–3242.

Weber, B.L. (1998). Update on breast cancer susceptibility genes. Recent Results Cancer Res. *152*, 49–59.

Wilson, C.A., Payton, M.N., Elliott, G.S., Buaas, F.W., Cajulis, E.E., et al. (1997). Differential subcellular localization, expression and biological toxicity of BRCA1 and the splice variant BRCA1-delta11b. Oncogene *14*, 1–16.

Wu, L.C., Wang, Z.W., Tsan, J.T., Spillman, M.A., Phung, A., et al. (1996). Identification of a RING protein that can interact in vivo with the BRCA1 gene product. Nat. Genet. *14*, 430–440.

Xu, X., Weaver, Z., Linke, S.P., Li, C., Gotay, J., Wang, X.W., Harris, C.C., Ried, T., and Deng, C.X. (1999a). Centrosome amplification and a defective G2-M cell cycle checkpoint induce genetic instability in *BRCA1* exon 11 isoform-deficient cells. Mol. Cell *3*, 389–395.

Xu, X., Wagner, K.U., Larson, D., Weaver, Z., Li, C., Ried, T., Hennighausen, L., Wynshaw-Boris, A., and Deng, C.X. (1999b). Conditional mutation of *Brca1* in mammary epithelial cells results in blunted ductal morphogenesis and tumour formation. Nat. Genet. *22*, 37–43.

Yu, X., Wu, L.C., Bowcock, A.M., Aronheim, A., and Baer, R. (1998). The C-terminal (BRCT) domains of BRCA1 interact in vivo with CtIP, a protein implicated in the CtBP pathway of transcriptional repression. J. Biol. Chem. *273*, 25388–25392.

Zhong, Q., Chen, C.F., Li, S., Chen, Y., Wang, C.C., Xiao, J., Chen, P.L., Sharp, Z.D., and Lee, W.H. (1999). Association of BRCA1 with the hRad50-hMre11-p95 complex and the DNA damage response. Science *285*, 747–750.

Cell, Vol. 88, 265–275, January 24, 1997, Copyright ©1997 by Cell Press

Association of BRCA1 with Rad51 in Mitotic and Meiotic Cells

Ralph Scully,* Junjie Chen,*§ Annemieke Plug,†§ Yonghong Xiao,* David Weaver,* Jean Feunteun,‡ Terry Ashley,† and David M. Livingston*
*The Dana-Farber Cancer Institute
Harvard Medical School
Boston, Massachusetts 02115
†Department of Genetics
Yale University School of Medicine
New Haven, Connecticut 06520–8005
‡Centre National de la Recherche Scientifique
Institut Gustave-Roussy
Cedex 94805 Villejuif
France

Summary

BRCA1 immunostaining reveals discrete, nuclear foci during S phase of the cell cycle. Human Rad51, a homolog of bacterial RecA, behaves similarly. The two proteins were found to colocalize in vivo and to coimmunoprecipitate. BRCA1 residues 758–1064 alone formed Rad51-containing complexes in vitro. Rad51 is also specifically associated with developing synaptonemal complexes in meiotic cells, and BRCA1 and Rad51 were both detected on asynapsed (axial) elements of human synaptonemal complexes. These findings suggest a functional interaction between BRCA1 and Rad51 in the meiotic and mitotic cell cycles, which, in turn, suggests a role for BRCA1 in the control of recombination and of genome integrity.

Introduction

Between 5% and 10% of all breast cancers and 10% of ovarian cancers can be attributed to mutations of highly penetrant, autosomal dominant susceptibility genes (Newman et al., 1988; Claus et al., 1991). One of these is *BRCA1*, which maps to 17q21 (Hall et al., 1990; Narod et al., 1991; reviewed in Feunteun and Lenoir, 1996). *BRCA1* mutations are responsible for almost all families with inherited breast and ovarian cancer and for approximately half of the families with breast cancer only (Easton et al., 1993). The detection of LOH affecting the wild-type *BRCA1* allele in tumors from *BRCA1* mutation carriers implies that *BRCA1* is a tumor suppressor gene (Smith et al., 1992; Neuhausen and Marshall, 1994).

The *BRCA1* cDNA encodes an 1863 residue polypeptide of as yet unknown biochemical function (Miki et al., 1994). The BRCA1 sequence includes an N-terminal RING domain (reviewed in Freemont, 1993; Saurin et al., 1996), a negatively charged region in its C terminus, and C-terminal sequences partially homologous to yeast RAD9 and to a cloned p53 binding protein (Koonin et al., 1996). The negatively charged segment may contribute to transcription-inducing activity of a GAL4–BRCA1 fusion protein (Chapman and Verma, 1996; Monteiro et al., 1996). Whether BRCA1 enacts a transcriptional control function is not yet known.

To date, more than 100 unique, naturally occurring *BRCA1* germline mutations have been identified (Castilla et al., 1994; Friedman et al., 1994; Simard et al., 1994; Shattuck-Eidens et al., 1995). Somatic *BRCA1* mutations have not been detected in sporadic breast cancer and are rare in sporadic ovarian cancer (Merajver et al., 1995). Approximately 90% of breast or ovarian cancer–linked *BRCA1* mutations leads to truncated products. The pattern of truncations and missense mutations suggests that multiple regions of the protein structure contribute to its tumor suppression function.

Multiple BRCA1-specific antibodies detect a protein migrating at ~220 kDa in various cell lines (Chen et al., 1995; Scully et al., 1996). This polypeptide comigrates with and has a peptide map indistinguishable from that of the 220 kDa clonal BRCA1 in vitro translation product (Chapman and Verma, 1996; Scully and Livingston, unpublished data). Several reports indicate that p220 BRCA1 is a nuclear protein in cultured cells and normal tissues (Chen et al., 1995; Chapman and Verma, 1996; Chen et al., 1996; Scully et al., 1996).

The developmental pattern of murine *BRCA1* expression (Lane et al., 1995; Marquis et al., 1995) and its cell cycle–regulated expression (Gudas et al., 1995; Gudas et al., 1996; Vaughn et al., 1996) suggest a relationship between BRCA1 function and cellular proliferation (e.g., in the mammary gland in response to ovarian hormones). Loss of BRCA1 function is a lethal event during murine embryogenesis (Gowen et al., 1996; Hakem et al., 1996; Liu et al., 1996). Some *BRCA1*$^{-/-}$ embryos revealed an early (~E7.5) proliferation block with elevated levels of p21 mRNA at E4 (Hakem et al., 1996).

There are also reports of growth- and transformation-suppressing behavior, as well as death of cells that acutely overproduce BRCA1 (Holt et al., 1996; Rao et al., 1996; Shao et al., 1996; Wilson et al., 1996). However, these studies do not reveal the mechanism underlying these effects.

We have reported that BRCA1 immunostaining is characterized by a "nuclear dot" pattern (Scully et al., 1996). As suggested by the work of Chen et al. (1996) and as defined below, BRCA1 nuclear dots appear in S phase of the cell cycle. Among nuclear proteins known to be characterized by dot-like staining is human Rad51 (hRad51), a homolog of bacterial RecA. hRad51 nuclear dots also appear in S phase (Tashiro et al., 1996).

hRad51 is a member of a protein family known to mediate DNA strand–exchange functions leading to normal recombination (Kowalczykowski, 1991; Radding, 1991; Sung, 1994; Sung and Robberson, 1995; Baumann et al., 1996). Although yeast, mutated for *RAD51*, cannot perform normal meiotic recombination and double-stranded break repair, they are viable (Shinohara et al., 1992). In contrast, mice bearing homozygous, loss-of-function *RAD51* mutations died early in embryogenesis. Moreover, like *BRCA1*$^{-/-}$ embryos, cells of *RAD51*$^{-/-}$ embryos revealed a proliferation defect, suggesting an

§These authors contributed equally to this work.

additional role for Rad51 in cell growth control (Lim and Hasty, 1996; Tsuzuki et al., 1996). Here, we report that BRCA1 and hRad51 colocalize in S phase cells, interact physically, and, in keeping with previous reports of the behavior of hRad51 (Ashley et al., 1995; Plug et al., 1996), share common space on the surfaces of zygotene and pachytene meiotic chromosomes. These observations identify a biochemical pathway involving BRCA1 and suggest that BRCA1 participates in nuclear processes that lead to normal chromosomal recombination and genome integrity control.

Results

S Phase Nuclear Dot Pattern of BRCA1

The identification of discrete, nuclear dot–like structures as loci of endogenous BRCA1 protein in multiple cell lines and diploid human fibroblasts has been established previously, using seven different BRCA1 monoclonal antibodies (MAb's) and an affinity-purified BRCA1 polyclonal Ab (Scully et al., 1996). BRCA1 nuclear dots were observed in only a fraction of asynchronous cells. The remaining cells revealed a weaker, more diffuse nuclear signal (data not shown). This suggested that the dot-like staining might be cell cycle–dependent. Serum starvation and synchronous release were used to synchronize populations of the breast cancer cell line, MCF7, which were then subjected to BRCA1 immunostaining. In cultures enriched for S phase cells (t = 24 hr population; see Figure 1), most cells scored positively for BRCA1 nuclear dots, while a G1-enriched population presented weaker and largely diffuse nuclear staining (t = 12 hr; see Figure 1 and see also Chen et al., 1996). Analysis of the same cultures with irrelevant MAb revealed no nuclear staining (Scully et al., 1996; data not shown). These and other results not shown here indicate that the BRCA1 nuclear dot pattern is S phase–specific.

Colocalization of the BRCA1 and Rad51 Immunostaining Patterns in S Phase Nuclei

Rad51, a mammalian RecA homolog, has been shown previously to form S phase–specific nuclear foci (Tashiro et al., 1996). Given the apparent similarity in the timing of appearance of Rad51 and BRCA1 nuclear dots, we asked whether Rad51 and BRCA1 staining colocalize in the same structures. Two-color confocal immunostaining with a BRCA1 monoclonal antibody and an affinity-purified, rabbit polyclonal antiserum raised against clonal human Rad51 (Haaf et al., 1995; Plug et al., 1996) revealed significant, albeit not complete, colocalization of the BRCA1 and the Rad51 nuclear dot patterns (Figure 2). Figure 2 also illustrates cell-to-cell variability in colocalization between BRCA1 and Rad51 signals. In some cells, colocalization of dot signals was extensive (e.g., Figures 2D–2F). In others, the overlap was incomplete (e.g., Figures 2A–2C, top cell). This suggested that the colocalization of BRCA1 and Rad51 is conditional or transient, even in S phase cells. Similar colocalization results were obtained in WI38 and CV-1 cells. These observations raised the possibility that BRCA1 and Rad51 physically interact.

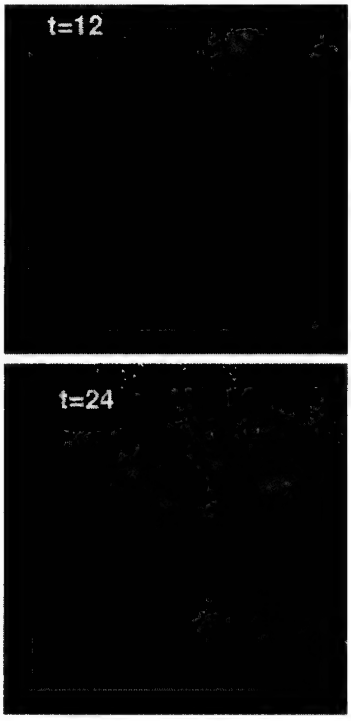

Figure 1. BRCA1 Nuclear Dot Pattern Arises in S Phase

MCF7 cells were serum-starved and released, as described in Experimental Procedures. The figure depicts immunostaining using BRCA1 MAb MS13. Identical results were obtained using two other BRCA1 MAb's (MS110 and AP16). (t = 12), cells 12 hr after serum release (83% G1, 9% S); (t = 24), cells 24 hr after serum release (30% G1, 62% S).

The specificity of the affinity-purified Rad51 antiserum was assessed. Immunoblotting of an MCF7 cell extract with this antiserum revealed a single band, migrating at 38 kDa, the expected size of hRad51 (data not shown). This band disappeared after preabsorbing the antiserum with clonal GST–hRad51 but not with 10-fold more unfused GST. The same was true for the nuclear immunofluorescence signal generated with this Ab. No reaction between this antiserum and authentic BRCA1 was detected by immunoblotting (data not shown).

Biochemical Evidence of an In Vivo BRCA1–Rad51 Interaction

MCF7, 293T, and HeLa cell immunoprecipitates generated with the BRCA1 MAb, SG11, contained endogenous, 38 kDa Rad51, as determined by immunoblotting (Figure 3A and data not shown). The Rad51 and BRCA1 signals detected in SG11 immunoprecipitates were suppressed by preincubation of this BRCA1 antibody with the immunizing BRCA1 peptide. Only a fraction of the ambient Rad51 coimmunoprecipitated with BRCA1 by this method. Although S phase extracts contained more BRCA1–Rad51 complexes than G1 extracts (data not shown), even in S phase–enriched fractions, there was incomplete coprecipitation of hRad51 with BRCA1. Whether this results from the presence of an excess of

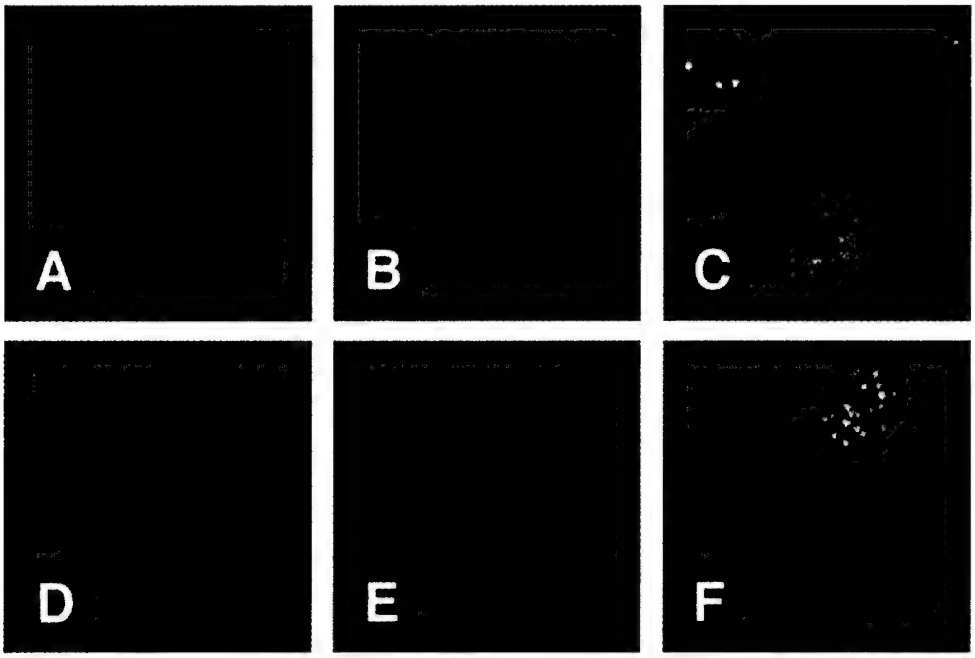

Figure 2. BRCA1 and Rad51 Colocalize in Discrete Nuclear Foci

MCF7 cells were double-stained with BRCA1 MAb MS13 (green) and anti-Rad51 (red). (A) and (D), BRCA1 stain; (B) and (E), Rad51 stain; and (C) and (F), composite BRCA1 and Rad51 stains. Where green and red signals overlap, a yellow pattern is seen, indicating colocalization of BRCA1 and Rad51.

(A–C) Staining of asynchronously growing MCF7 cells, depicting the location of BRCA1 and Rad51 in a BRCA1 dot-containing cell and in a cell exhibiting a more diffuse BRCA1 signal.

(D–E) Staining of serum-starved MCF7 cells, illustrating the rare (5%) S phase cell with a BRCA1 nuclear dot pattern.

Rad51 over BRCA1 and/or only a fraction of Rad51 is competent to bind, directly or indirectly, to BRCA1 is not known.

In an effort to confirm the existence of a physical interaction between BRCA1 and Rad51, we asked whether BRCA1 would complex with epitope-tagged, ectopic Rad51. Figure 3B shows that, after transient transfection of HA-tagged Rad51 into 293T cells, both endogenous BRCA1 and HA-tagged Rad51 were detected in an anti-BRCA1 immunoprecipitate. The coprecipitating band, identified as HA-Rad51, comigrated with bands precipitated from the same extract with either HA or Rad51 antibody. No such band precipitated from untransfected cells with anti-HA MAb (Figure 3B). In addition, transiently overproduced HA–E2F4 was not detected in BRCA1 immunoprecipitates, despite the fact that its concentration was similar to that of HA–Rad51 (data not shown). Hence, the BRCA1 MAb used here did not recognize the HA tag. Moreover, this BRCA1 MAb failed to recognize in vitro translated HA-tagged Rad51 synthesized in a wheat germ extract (data not shown). Hence, it did not appear to recognize Rad51 independently.

In a reciprocal experiment, anti-Rad51 immunoprecipitation of a HA-BRCA1-transfected 293T cell extract coprecipitated BRCA1 (Figure 3C). Despite the presence of higher levels of two HA-tagged control nuclear proteins—the p300 nuclear coactivator and the p130 pocket protein—in parallel transfections of the same cell line, neither protein was detected in anti-Rad51 immunoprecipitates (Figure 3C). Thus, further evidence of specific complex formation between Rad51 and BRCA1 was obtained in transiently transfected cells containing definitively tagged gene products.

BRCA1 Exon 11 Encodes Sequences That Mediate Rad51 Binding

Six overlapping BRCA1 fragments spanning the entire *BRCA1* open reading frame were synthesized as GST fusion proteins (Figures 4A and 4B). Approximately equal amounts of each protein, bound to glutathione-sepharose beads, were incubated with an extract of BJAB (Burkitt's lymphoma–derived) cells. Bead-bound proteins were recovered and separated electrophoretically. The separated proteins were immunoblotted for Rad51 (Figure 4C). GST–BRCA1 fragment #4, corresponding to BRCA1 residues 758–1064, which are encoded by a portion of exon 11, repeatedly bound a 38 kDa immunoreactive Rad51 comigrating band. Identical results were obtained using cell lines MCF7, 293T, and U2OS.

To distinguish between bona fide hRad51 and a comigrating 38 kDa band supplied by the bacterial extract, the same experiment was performed with an extract of ^{35}S-methionine-labeled MCF7 cells (Figure 4D). After incubation of the various bead-bound GST proteins with

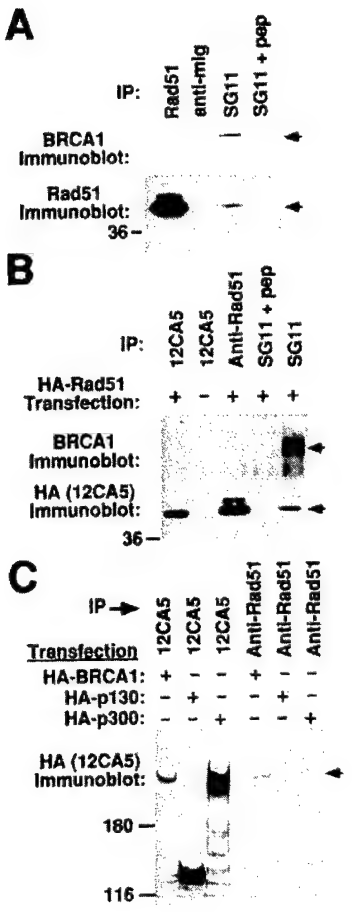

Figure 3. Coimmunoprecipitation of BRCA1 and Rad51

(A) Association in untransfected cells. MCF7 cultures were enriched for S phase (see Experimental Procedures). Extracts (5×10^6 cells per lane) were immunoprecipitated with the antibodies shown. Immunoprecipitated proteins were separated by SDS–PAGE and immunoblotted with MAb MS110 (anti-BRCA1, upper panel; arrow signals the migration position of p220 BRCA1 [Scully et al., 1996]) and with the Rad51 antiserum (arrow signals the presence of the 38 kDa protein). Control antibodies included the rabbit anti-mouse IgG secondary immunoprecipitation antibody ("anti-mIg") and MAb SG11 that had been preincubated with a 10-fold molar excess of the peptide against which it was raised.

(B) Coimmunoprecipitation of ectopic, HA-tagged Rad51 with BRCA1. 293T cells were transfected with an HA-Rad51 expression plasmid. Extracts of the transfected cultures ($\sim 10^7$ cells per lane) were subjected to immunoprecipitation 48 hr later. After SDS–PAGE, immunoblotting for p220 BRCA1 (using MAb MS110, upper panel) and for the HA tag (using MAb 12CA5, lower panel) was performed. Immunoblots of whole cell extracts clearly showed an HA-Rad51-specific doublet migrating at 40–42 kDa (data not shown). The absence of this doublet from an extract of untransfected cells indicated that the 40–42 kDa $12CA5^+$ species depicted in the lower panel are HA–Rad51 products.

(C) Coimmunoprecipitation of ectopic HA-BRCA1 with Rad51. 293T cells were transfected, in parallel, with expression plasmids encoding HA–BRCA1, HA–p130, or HA–p300, as shown. Transfected cell extracts ($\sim 10^7$ cells per lane) were immunoprecipitated. After SDS–PAGE, anti-HA immunoblotting (using MAb 12CA5) was performed. Note that the nominal molecular weights of BRCA1 (220 kDa) and p300 (300 kDa) are not reflected in the relative migration rates of these proteins, which, even in the untagged state, migrate close to one another.

this extract and washing, we eluted the bead-bound proteins. After dilution of the individual eluates to reduce the ambient SDS concentration, the eluted proteins were reimmunoprecipitated with the Rad51 antiserum. A labeled 38 kDa band did reimmunoprecipitate from an eluate of the same lot of GST–BRCA1 #4 fragment-bound beads that yielded the Rad51 immunoreactive band in the earlier experiment (Figure 4C). No such band appeared in the eluates of GST beads alone. Hence, the protein recovered by the BRCA1 #4 fragment is Rad51 and originated in the mammalian and not the bacterial extract.

Taken together, the data indicate that *BRCA1* exon 11 encodes a sequence(s) that can serve as a specific binding site for Rad51. Whether the BRCA1 interaction with Rad51 is direct or depends upon BRCA1 binding to an intermediate protein(s) is not clear at present.

Presence of BRCA1 on Meiotic Chromosomes

The association of BRCA1 and Rad51 in mitotic cells and the known presence of Rad51 on synaptonemal complexes of various organisms (Bishop, 1994; Ashley et al., 1995; Terasawa et al., 1995; Plug et al., 1996) suggested that the two proteins might also colocalize during meiotic prophase. *BRCA1* mRNA is highly expressed in spermatocytes during meiotic prophase (Zabludoff et al., 1996).

The pairing of homologous chromosomes during meiosis is accompanied by the appearance of unique, meiosis-specific DNA- and protein-bearing structures, termed synaptonemal complexes. Following DNA replication in premeiotic S phase, meiotic chromosomes begin to condense and a protein-containing core, or axial element, forms between sister chromatids. As homologous chromosomes synapse in zygonema to form a bivalent, the axial elements align and are joined by transverse filaments. Finally, a discrete central element forms between the two axial elements, completing the structure of the synaptonemal complex. In the current study, we used an antibody to SCP3, a component of the axial/synaptic elements of this structure (Lammers et al., 1994), to visualize the progression of meiotic prophase.

In nuclei of zygotene spermatocytes obtained from fresh, human testis, BRCA1 staining (in red) was observed with three different MAb's (MS13, MS110, and SG11 [Scully et al., 1996]). Chromosomal axes doubly stained with MAb MS110 (red) and Ab to SCP3 (white) are shown in Figure 5. BRCA1 staining was detected in an uneven pattern. On those structures where the specific details of chromosomal anatomy were most clearly discernible, a significant fraction of the staining was noted along unsynapsed axial elements (small arrows, Figure 5A), as well as at axes that were in the process of synapsing (larger arrows, Figure 5A). BRCA1 staining was also detected on unsynapsed centromeric heterochromatin (arrowheads, Figure 5B), on remaining univalents (e.g., small arrow, Figure 5B), and at pairing forks (e.g., larger arrow, Figure 5B). Figure 5D highlights the

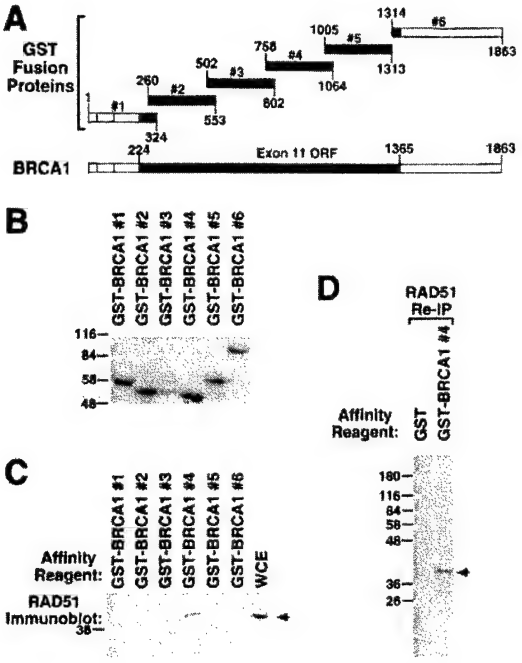

Figure 4. In Vitro Binding of a Segment of BRCA1 to Rad51

Six GST–BRCA1 fusion proteins were generated in E. coli. (A) The schematic diagram of these fusion proteins is not drawn to scale. BRCA1 exon 11 products are indicated by dense stippling. The amino-terminal BRCA1 RING domain is shown by light stippling. BRCA1 residues are marked relative to the translation initiation site.

(B) Synthesis of GST–BRCA1 fusion proteins in E. coli. Individual GST–BRCA1 fusion proteins were prepared as described in Experimental Procedures. The figure depicts a Coomassie blue–stained SDS acrylamide gel, showing the relative abundance of each fusion protein used in Figure 4C. Note that GST–BRCA1 protein #3 was consistently found to be unstable.

(C) Rad51 antiserum recognizes a 38 kDa protein bound to GST–BRCA1 #4. GST–BRCA1 affinity beads were incubated briefly with an unlabeled BJAB extract. After washing, bound proteins were electrophoresed and immunoblotted using the Rad51 antiserum as probe. The figure shows a 38 kDa band, comigrating with Rad51 detected in whole cell extracts (WCE), specifically associated with GST–BRCA1 #4.

(D) The 38 kDa protein bound to GST–BRCA1 #4 is a product of the human cell extract and can be reimmunoprecipitated with Rad51 antiserum. Beads containing GST–BRCA1 #4 and excess GST-containing affinity beads were incubated, in parallel, with extracts of ^{35}S-methionine-labeled MCF7. After washing, bound proteins were solubilized by boiling in SDS buffer. Diluted eluates were then immunoprecipitated with Rad51 antiserum, and the ensuing precipitates were analyzed by SDS–PAGE and autoradiography. The specific 38 kDa band (indicated with an arrow) was found in another experiment to comigrate with the 38 kDa Rad51 protein, as identified by immunoblotting. Furthermore, an anti-Rad51 reimmunoprecipitate from an initial anti-Rad51 precipitate of MCF7 cells yielded only a ^{35}S-labeled 38 kDa species (not shown).

existence of BRCA1 staining on unsynapsed axial elements (small arrows). Arrowheads mark examples of synapsed regions of the indicated synaptonemal complexes. Identical results were obtained with all three BRCA1 Ab's, strongly suggesting that the observed signals resulted from the presence of BRCA1.

Many fewer chromosomes revealed detectable BRCA1 staining in pachynema (Figure 5C). By contrast, BRCA1 staining persisted on the asynapsed X-axis during this period (Figure 5C). Indeed, as pachynema progressed, the BRCA1 signal seemed to be present in a less interrupted manner on late-synapsing autosomal axes (arrows, Figure 5C) and on the X chromosome (see Figure 6), which has no homolog in males. These data imply that the appearance of BRCA1 staining is a synchronous event during meiotic prophase.

The BRCA1 MAb MS13 was raised against a defined segment of the N-terminal region of the cloned protein (residues 1–304, Scully et al., 1996). As another test of specificity, we preincubated MAb MS13, in parallel, with each of two purified BRCA1 fragments. One was the initial MS13 immunogen. The other contained residues 1313–1863. These preincubated preparations were used, in parallel, to stain pachytene spermatocytes. Both Rad51 Ab and a second BRCA1 MAb, MS110, costained the unsynapsed axis of the X chromosome (data not shown). MAb MS13, preincubated with the C-terminal BRCA1 fragment, noted above, also stained the unsynapsed axis of the X chromosome (Figure 6B), which was simultaneously costained with SCP3 Ab (Figure 6A). In contrast, MAb MS13, preincubated with the relevant, immunizing N-terminal polypeptide, yielded no signal despite the presence of the X in that spread (Figures 6C [SCP3 staining] and 6D).

The same experiment was performed with MAb MS110 (which, like MS13, was raised against BRCA1 residues 1–304) with identical results (data not shown). MAb SG11, a third BRCA1 monoclonal Ab, led to a staining pattern identical to that of MS13 and MS110. However, as predicted, SG11 staining was blocked by preincubation with a C-terminal BRCA1 polypeptide containing the SG11 epitope (data not shown). Therefore, the immunostaining obtained with these MAb's likely reflects specific interactions of these MAb's with BRCA1.

A further indication of the specifity of the BRCA1 staining pattern is given by the failure of monoclonal antibodies specific to other nuclear proteins, such as the retinoblastoma protein and the nuclear coactivator, p300, to elicit any signal on human synaptonemal complexes. Furthermore, testis spreads, prepared in this manner, stained positively for DNA (with DAPI) throughout the nucleus. In S phase spermatocytes, nuclei also stained with Ab to the replication protein, RPA, throughout, indicating that the method of preparation does not extract non-SC-bound proteins from the spreads (A. Plug and T. Ashley, unpublished data). The unsynapsed/axial elements, therefore, appear to be the only sites of BRCA1 concentration in zygotene and pachytene spermatocytes.

Simultaneous BRCA1 and Rad51 Staining of Meiotic Chromosomes

Plug et al. (1996) showed that Rad51 is present in premeiotic S phase nuclear foci. During zygonema, Rad51 staining organizes into discrete structures along axial elements. Homologous synapsis is completed in early pachynema, and Rad51 foci remain evident along the

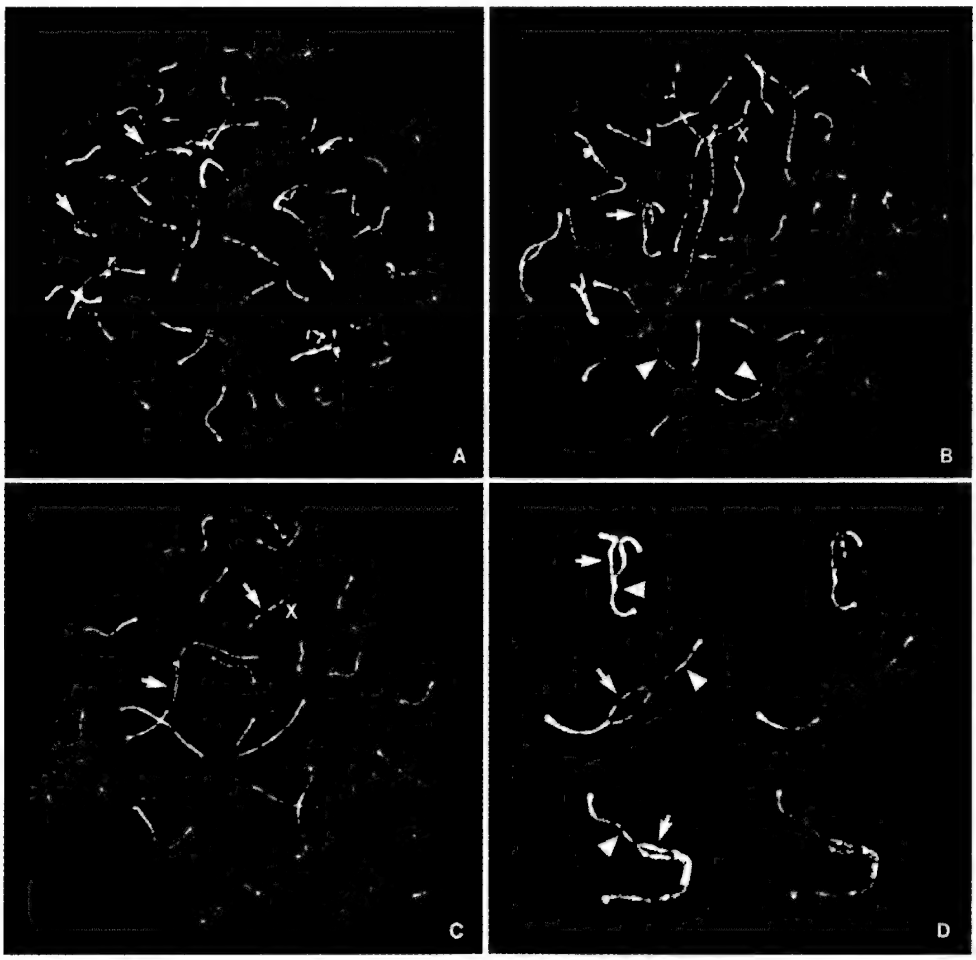

Figure 5. Localization of BRCA1 Staining to Meiotic Chromosomes

(A) Axial and synapsed segments (using Ab SCP3, white) in a human zygotene nucleus. BRCA1 (stained with MAb MS110, red) localized to discrete sites along unsynapsed axial elements (examples noted by small arrows) and axes that are in the process of synapsing (examples noted by larger arrows).

(B) Localization of BRCA1 to sites along unsynapsed axes of regions delayed in synapsis (examples noted by arrowheads), pairing forks (example noted by arrow), and remaining univalents (examples noted by small arrows).

(C) Pachytene nucleus showing the presence of BRCA1 staining on the unsynapsed X chromosome and a delayed pairing fork (arrows).

(D) BRCA1 staining on unsynapsed axial elements (enlarged images taken, in part, from [B]). Arrows indicate examples of unsynapsed segments; arrowheads indicate examples of synapsed regions. SCP3 staining (white) is shown on the left; SCP3 and BRCA 1 costaining (white and red, respectively) are shown on the right. The lowermost complexes of the three are from another zygotene spread, where BRCA1 staining was obtained with MS13.

length of the synaptonemal complex. Shortly after completion of synapsis of most chromosomes, Rad51 foci begin to disappear from the synaptonemal complex. In contrast, Rad51 foci remain associated with the unsynapsed axial element of the X chromosome in spermatocytes (Ashley et al., 1995; Plug et al., 1996). Rad51 foci also remain associated with a few autosomal axes in which synapsis is delayed (Plug et al., unpublished data). In coimmunostaining experiments, much of the BRCA1 staining (red, Figure 7B) and much, albeit not all, of the Rad51 staining (green, Figure 7A; composite image, Figure 7C) appeared in the same general locations on developing synaptonemal complexes during zygonema. In multiple spreads, some foci of Rad51 staining were not associated with a BRCA1 signal at all (Figure 7 and data not shown). One interpretation of the Rad51 and BRCA1 staining patterns, described above, is that a significant fraction of both the BRCA1 and the Rad51 staining, i.e., that which appears in the same general chromosomal locations, is concentrated at unsynapsed chromosomal sites.

Discussion

The data presented here show, for the first time, that BRCA1 associates with Rad51, a human homolog of

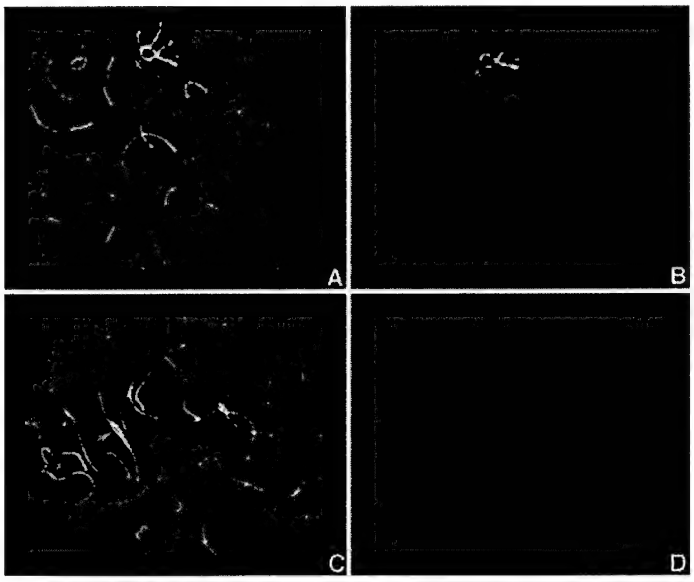

Figure 6. Specificity of BRCA1 Staining of Synaptonemal Complexes

(A) SCP3 staining of pachytene chromosomes.

(B) BRCA1 costaining of this spread with MAb MS13 that had been preincubated with a C-terminal GST–BRCA1 fusion protein, which lacks the MS13 epitope. BRCA1 staining is limited to the unsynapsed axes of the X chromosome.

(C) SCP3 staining of pachytene chromosomes. A prominent X-chromosomal axis is present.

(D) The same spread costained with MS13 preincubated with an N-terminal GST–BRCA1 fusion protein that contains the MS13 epitope.

bacterial RecA. In mitotic cells, this association was marked by colocalization in S phase nuclear foci and coimmunoprecipitation. Furthermore, during meiotic prophase in primary human spermatocytes, the proteins occupied the same general regions of developing synaptonemal complexes. These findings suggest a functional relationship between these two proteins. This conclusion was strengthened by the mapping of a Rad51 interaction domain to BRCA1 residues 758–1064, the site of at least one naturally occurring, loss-of-function missense mutation (Shattuck-Eidens et al., 1995).

Like Rad51, BRCA1 was detected in the nuclei of human spermatocytes on the axial (unsynapsed) elements of developing synaptonemal complexes. This is consistent with the prior observation that *BRCA1* mRNA levels are greatly elevated in zygotene/pachytene spermatocytes (Zabludoff et al., 1996). Since recombination, per se, occurs in synapsed regions, one might speculate that BRCA1 does not act directly in meiotic crossing-over. If that were true, it is possible that BRCA1 acts prior to the initiation of recombination, e.g., as an upstream regulator of this process. Alternatively, since its association with meiotic structures developed and ended synchronously, one could argue that it functions only when it is detected on the meiotic chromosome, e.g., during a period when the search for homologous sequences initiates and proceeds and/or when double-strand breaks appear (reviewed in Kleckner, 1996). The relatively synchronous manner in which BRCA1 appeared on meiotic chromosomes and formed dot structures in mitotic cells suggests a role in both mitotic and meiotic cell cycle control.

Recently, the *ATR* and *ATM* gene products were detected on mutually exclusive regions of the synaptonemal complex (Keegan et al., 1996). Like BRCA1, Atr was found on axial elements, together with Rad51. Atm, the product of another gene whose germ line inactivation may predispose to breast cancer (Swift et al., 1987), was present on synapsed regions. Atr is a homolog of Mec-1 (S. cerevisiae), Rad3 (S. pombe), and mei-41 (Drosophila), and mutations affecting these proteins lead to defects in DNA damage–induced cell cycle responses, radiation hypersensitivity, and defective meiosis (Al-Khodairy and Carr, 1992; Jiminez et al., 1992; Rowley et al., 1992; Cimprich et al., 1996). These large proteins are protein kinases, and, where studied, kinase function was essential to their normal biological activity (Bentley et al., 1996). This, in turn, suggests a role for these proteins in one or more signal transduction cascades, one product of which is proper meiotic and mitotic checkpoint control (reviewed in Carr, 1996).

The question of whether BRCA1 and Atr interact is now clearly relevant. Their similar locations on meiotic chromosomes, the known contribution of Atr to DNA damage control, and its possible role in meiotic cell cycle regulation (Keegan et al., 1996) suggest a related role for BRCA1. The Atr equivalent function in mitotic cells could be monitoring intersister chromatid interactions during S and G2 (Kleckner, 1996). One wonders, then, whether Atr and, possibly, BRCA1 participate in monitoring the progress of DNA replication and/or normal recombination-linked functions.

Tumorigenesis can arise from defects in DNA repair, e.g., in the case of hereditary nonpolyposis colon cancer. There, the defects lie in certain mismatch repair genes (reviewed in Kolodner, 1996). The products of some of these genes are also present on synaptonemal complexes and participate in normal meiosis (Baker et al., 1995; Baker et al., 1996; Edelmann et al., 1996). That BRCA1 and the product(s) of a second class of tumor suppressor genes that play a role in maintaining genome integrity are intimately associated with synaptonemal complexes raises the question of whether they communicate with one another.

What might be the outcome of a specific BRCA1 interaction with Rad51? In yeast, Rad51 participates in double-stranded break repair and meiotic recombination

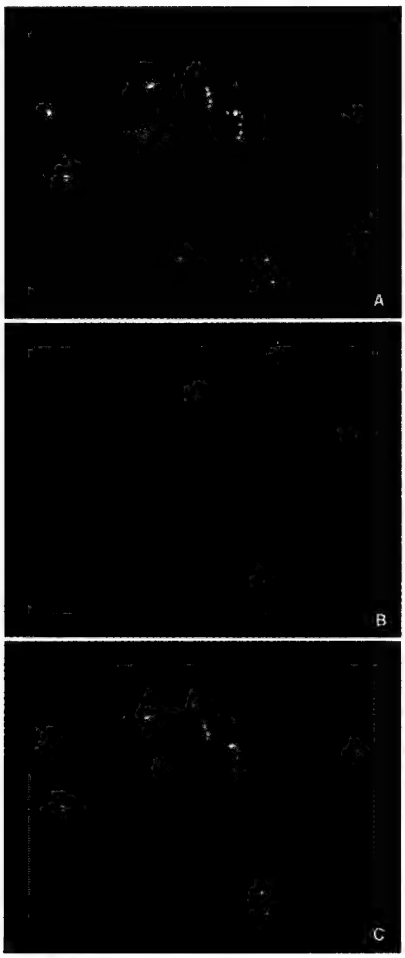

Figure 7. Colocalization of BRCA1 and Rad51 on Meiotic Chromosomes

(A) Rad51 immunostaining (green).

(B) BRCA1 immunostaining (red, MS13).

(C) Rad51 and BRCA1 costaining (colocalization is reflected by yellow images).

(Shinohara et al., 1992). Indeed, it must also play some role in the normal replication of mammalian embryonic cells, since *Rad51*$^{-/-}$ murine zygotes undergo early replication arrest (Lim and Hasty, 1996; Tsuzuki et al., 1996). Finally, RecA function is essential for the SOS response, a bacterial DNA damage control pathway dependent upon the activated transcription of certain genes (reviewed in Echols and Goodman, 1991).

Given these facts, one outcome of the Rad51–BRCA1 interaction could be orderly cell cycle progression, high fidelity DNA replication, and/or events that lead to the maintenance of genomic integrity. Indeed, BRCA1 breast tumors are characterized by a greater degree of genome plasticity than those arising in patients with mutations in the *BRCA2* gene (Marcus et al., 1996). Similarly, given the essential role of RecA in the SOS response and the apparent transcription activation function of certain BRCA1 fusion proteins (Chapman and Verma, 1996; Monteiro et al., 1996), one wonders whether BRCA1 plays a role in mediating a response to mammalian DNA damage in a Rad51/transcription–dependent manner. Notable in this regard is the finding of Reinberg and his coworkers of hRad51 in a fraction of RNA polymerase II holoenzyme (Maldonado et al., 1996).

Importantly, Rad51 and p53, another tumor suppressor with a central role in the response to DNA damage, interact, specifically, in vivo (Sturzbecher et al., 1996). There is a putative p53 interaction sequence in BRCA1 (Koonin et al., 1996) that is distinct from the apparent Rad51 interacting region of BRCA1. p53 also serves as an hereditary breast cancer–inducing gene in patients with the Li-Fraumeni Syndrome (Malkin et al., 1990).

On the face of it, the phenotype (i.e., cell cycle arrest) of *BRCA1* knockout embryos would seem to run counter to a proposed tumor suppressing role for this protein. On the other hand, if BRCA1 has a role in the maintenance of genome integrity, loss of its function might result in genome errors and the subsequent activation of checkpoint genome guardian functions, the outcome of which might be cell cycle arrest. Perhaps only those cells that are already defective in monitoring genome integrity and/or responding to a defect therein can escape the proliferation defect of BRCA1 loss. If this is the case, then loss of BRCA1 function, per se, may not initiate tumorigenesis, but rather accelerate its progression in cells that have already sustained damage to such a checkpoint function.

Interestingly, only trophoblast cells of *BRCA1* knockout embryos developed normally (Hakem et al., 1996). This tissue is unusual in that it normally undergoes endoreplication. If BRCA1 loss trips a normal S phase checkpoint, these cells may not be susceptible to it.

Rad51 loss is lethal in mice but not in yeast, a unicellular organism that may not be subjected to all of the same checkpoint and cell cycle controls as multicellular organisms. Interestingly, yeast also lack a *BRCA1* gene.

Experimental Procedures

Tissue Culture Methods and Preparation of Cell Extracts

Cells were cultured in DMEM-10% fetal bovine serum (FBS), or 10% Fetal Clone I (Hyclone labs). For synchronization studies of MCF7 cells, asynchronous cultures were cultivated for 24 hr in DMEM/0.05% BSA to induce G1 arrest. After release into 20% FBS, cell cycle progression was measured by FACS analysis. Maximum S phase enrichment was seen 24 hr after serum release. For transfection, a standard calcium phosphate precipitation method was used (Wigler et al., 1977). Immunoprecipitation (typically ~2 μg Ab per reaction) and immunoblotting were performed as described previously (Scully et al., 1996), with the exception of the extraction buffer, which contained only NP-40 (0.5%) as detergent.

Immunostaining of Adherent Cells

Cells were fixed and permeablized as described previously (Eckner et al., 1994). Primary antibodies were incubated in a humidified atmosphere at 37°C for 20 min. Species-specific, fluorochrome-conjugated secondary antibodies (Jackson Immunoresearch) were incubated in a similar fashion. Immunofluorescence was recorded using a Zeiss confocal microscope.

Preparation and Immunostaining of Human Synaptonemal Complexes

Preparation of "spreads" of human spermatocytes was perfomed as described by Peters et al. (1997). Antibody incubation and detection

were performed as described previously (Moens et al., 1987; Ashley et al., 1995). BRCA1 MAb's were detected with anti-mouse IgG rhodamine conjugate (Pierce), and SCP3 polyclonal antibodies with anti-rabbit IgG FITC conjugate (Pierce). Preparations were counterstained with 4′,6′ diamino-2-phenylindole (DAPI, Sigma), mounted in a DABCO (Sigma) antifade solution, and examined on a Zeiss Axioskop (63-X and 100-X, 1.2 Plan Neofluor oil immersion objective). Each fluorochrome image was captured separately as an 8-bit source image using a computer-assisted cooled CCD camera (Photometrics CH 220). The separate images were 24-bit pseudocolored and merged with custom software developed by Tim Rand (Ried et al., 1992).

Construction of *BRCA1* and *Rad51* Expression Vectors

To optimize in vivo expression of *BRCA1* cDNA, a rabbit β-globin intron was inserted into pcDNA3 (Invitrogen). The insert was generated by PCR from vector pSG5 (Stratagene), using the primers: 5′-GGGCCAAGCTTGCGTCTAGAGTCGATCCTGAGAACTTCAG GGTG-3′ and 5′-GGGGGATCCGCCCGGGCCAAGCTTGGGGTCGA CAGCACAATAACCAGCACGTTGCCC-3′. The pcDNA3 HindIII restriction site was converted to a unique NheI site using HindIII digestion, Klenow treatment, and religation. The insert was digested with XbaI and BamHI and subcloned into the NheI–BamHI sites of pcDNA3. Full sequencing of the insert showed that nucleotides AATAA (underlined above) had been replaced by the sequence AAA. No other errors were found. This vector was termed "pcDNA3β."

Derivation of the wild-type human cDNA for BRCA1 has been described previously (Scully et al., 1996). An amino-terminal HA–BRCA1 expression vector was generated by PCR of BRCA1 cDNA (using primers 5′-GGGGGATCCATGGATTTATCTGCTCTTCGCG-3′ and 5′-GGGTCAGAATTCAGCCTTTTCTACATTCATTCTGTC-3′). A BamHI–BstXI fragment of this product was subcloned into the same sites of a partial *BRCA1* cDNA, and the full-length cDNA was reassembled into pcDNA3β containing a previously subcloned HA tag-coding sequence (Krek et al., 1993) located between HindIII and BamHI sites. The PCR-derived part was confirmed correct by direct sequencing.

An amino-terminal HA-tagged *hRad51* expression construct was generated in a similar fashion. A full-length *hRad51* cDNA, housing a BamHI site immediately upstream of the open reading frame, was generated by using Pfu polymerase and PCR primers: 5′-GGG CCCGGATCCATGGCAATGCAGATGCAGC-3′ and 5′-GGGCCCCAA TTGGATATCATTCAGTCTTTGGCATCTCCCACTCC-3′. Restriction digests confirmed the identity of the cloned fragment, which was subcloned into BamHI–EcoRV sites of a pcDNA3/HA vector, as described above. Expression vectors for HA-p300 and HA-p130 have been described previously (Eckner et al., 1994; Vairo et al., 1995).

Construction and Expression of Bacterial GST-Fusion Proteins

Constructs corresponding to GST–BRCA1 #1–#5 (see text) were made using the vector pGEX-5X3 (Pharmacia). Inserts were generated by PCR using Pfu polymerase and the following pairs of primers: (#1) 5′-ATAGGATCCAAATGGATTTATCTGCTCTTCGC-3′ and 5′-ATAGTCGACTTCCAGCCCATCTGTTATGT-3′; (#2) 5′-ATAGGAT CCAGGGTAGTTCTGTTTCAAACTTG-3′ and 5′-ATAGTCGACCACT ATTAGTAATATTCATCACT-3′; (#3) 5′-ATAGGATCCGTAAAAGGAG ACCTACATCAG-3′ and 5′-ATAGTCGACTCACACATTTATTTGGTT CTG-3′; (#4) 5′-ATAGGATCCAAACTGAAAGATCTGTAGAGAGT-3′ and 5′-ATAGTCGACTGGAACCTATTTCATTAATAC-3′; and (#5) 5′-ATAGGATCCCATTCAATGTCACCTGAAAGA-3′ and 5′-ATAGTCGA CTGGGTGTTTGTATTTGCAGTCAA-3′.

GST–BRCA1 fragment #6 was described previously (Scully et al., 1996). GST–hRad51 was generated using the *Rad51* cDNA described above. Synthesis of GST fusion proteins and their partial purification on glutathione-sepharose beads was performed as described (Kaelin et al., 1992). Where GST fusion proteins were used for specificity controls, they were used as glutathione-eluted protein (10 μg per sample) or as affinity beads.

Acknowledgments

We are especially indebted to Drs. Nancy Kleckner, Bill Kaelin, Jim DeCaprio, Myles Brown, and Richard Kolodner for stimulating and helpful discussions. We are grateful to Drs. Adam Kibel and Jerome Ritchie for their expert help in obtaining testis tissue for these experiments. Drs. Charles Radding, Efim Golub, Gurucharan Reddy, and Oleg Kovalenko generously provided affinity-purified hRad51 antibody, and we thank them enthusiastically for it. We also thank Dr. Christa Heyting for her generosity in supplying SCP3 antibody and Mr. Phillipe Male for processing meiosis photographs. This work was supported by grants from the National Institutes of Health and the Dana-Farber Women's Cancer Program.

Received December 2, 1996; revised December 20, 1996.

References

Al-Khodairy, F., and Carr, A.M. (1992). DNA repair mutants defining G2 checkpoint pathways in Schizosaccharomyces pombe. EMBO J. *11*, 1343–1350.

Ashley, T., Plug, A.W., Xu, J., Solari, A.J., Reddy, G., Golub, E.I., and Ward, D.C. (1995). Dynamic changes in Rad51 distribution on chromatin during meiosis in male and female vertebrates. Chromosoma *104*, 19–28.

Baker, S.M., Bronner, C.E., Zhang, L., Plug, A.W., Robatzek, M., Warren, G., Elliott, E.A., Yu, J., et al. (1995). Male mice defective in the DNA mismatch repair gene PMS2 exhibit abnormal chromosome synapsis in meiosis. Cell *82*, 309–319.

Baker, S.M., Plug, A.W., Prolla, T.A., Bronner, C.E., Harris, A.C., Yao, X., Christie, D.-M., Monell, C., et al. (1996). Involvement of mouse Mlh1 in DNA mismatch repair and meiotic crossing over. Nat. Genet. *13*, 336–342.

Baumann, P., Benson, F.E., and West, S.C. (1996). Human Rad51 protein promotes ATP-dependent homologous pairing and strand transfer reactions in vitro. Cell *87*, 757–766.

Bentley, N.J., Holtzman, D.A., Keegan, K.S., Flaggs, G., DeMaggio, A.J., Ford, J.C., Hoekstra, M.F., and Carr, M. (1996). The Schizosaccharomyces pombe rad3 checkpoint gene. EMBO J., in press.

Bishop, D.K. (1994). RecA homologues Dmc1 and Rad51 interact to form multiple nuclear complexes prior to meiotic chromosome synapsis. Cell *79*, 1081–1092.

Carr, A.M. (1996). Checkpoints take the next step. Science *271*, 314–315.

Castilla, L.H., Couch, F.J., Erdos, M.R., Hoskins, K.F., Calzone, K., and Garber, J.E. (1994). Mutations in the BRCA1 gene in families with early-onset breast and ovarian cancer. Nat. Genet. *8*, 387–391.

Chapman, M.S., and Verma, I.M. (1996). Transcriptional activation by BRCA1. Nature *382*, 678–679.

Chen, Y., Chen, C.-F., Riley, D.J., Allred, D.C., Chen, P.-L., Von Hoff, D., Osborne, C.K., and Lee, W.-H. (1995). Aberrant subcellular localization of BRCA1 in breast cancer. Science *270*, 789–791.

Chen, Y.M., Farmer, A.A., Chen, C.F., Jones, D.C., Chen, P.L., and Lee, W.H. (1996). BRCA1 is a 220-kDa nuclear phosphoprotein that is expressed and phosphorylated in a cell cycle–dependent manner. Cancer Res. *56*, 3168–3172.

Cimprich, K.A., Shin, T.B., Keith, C.T., and Schreiber, S.L. (1996). cDNA cloning and gene mapping of a candidate human cell cycle checkpoint protein. Proc. Natl. Acad. Sci. USA *7*, 2850–2855.

Claus, E.B., Risch, N., and Thompson, W.D. (1991). Genetic analysis of breast cancer in the Cancer and Steroid Hormone Study. Am. J. Hum. Genet. *48*, 232–241.

Easton, D.F., Bishop, T., Ford, D., Crockford, G.P., and The Breast Cancer Linkage Consortium (1993). Genetic linkage analysis in familial breast and ovarian cancer: results from 214 families. Am. J. Hum. Genet. *52*, 678–701.

Echols, H., and Goodman, M.F. (1991). Fidelity mechanisms in DNA replication. Annu. Rev. Biochem. *60*, 477–511.

Eckner, R., Ewen, M.E., Newsome, D., Gerdes, M., DeCaprio, J.A., Lawrence, J.B., and Livingston, D.M. (1994). Molecular cloning and functional analysis of the adenovirus E1A-associated 300-kD protein (p300) reveals a protein with properties of a transcriptional adaptor. Genes Dev. *8*, 869–884.

Edelmann, W., Cohen, P.E., Kane, M., Lau, K., Morrow, B., Bennett, S., Umar, A., Kunkel, T., et al. (1996). Meiotic pachytene arrest in MLH1-deficient mice. Cell *85*, 1125–1134.

Feunteun, J., and Lenoir, G.M. (1996). BRCA1, a gene involved in inherited predisposition to breast and ovarian cancer. Biochem. Biophys. Acta *1242*, 177–180.

Freemont, P.S. (1993). The RING finger. Ann. NY Acad. Sci. *684*, 174–192.

Friedman, L.S., Ostermeyer, E.A., Szabo, C.I., Dowd, P., Lynch, E.D., Rowell, S.E., and King, M.-C. (1994). Confirmation of BRCA1 by analysis of germline mutations linked to breast and ovarian cancer in ten families. Nat. Genet. *8*, 399–404.

Gowen, L.C., Johnson, B.L., Latour, A.M., Sulik, K.K., and Koller, B.H. (1996). BRCA1 deficiency results in early embryonic lethality characterized by neuroepithelial abnormalities. Nat. Genet. *12*, 191–194.

Gudas, J.M., Li, T., Nguyen, H., Jensen, D., Rauscher, F.J.I., and Cowan, K.H. (1996). Cell cycle regulation of BRCA1 messenger RNA in human breast epithelial cells. Cell Growth Differ. *7*, 717–723.

Gudas, J.M., Nguyen, H., Li, T., and Cowan, K. (1995). Hormone-dependent regulation of BRCA1 in human breast cancer cells. Cancer Res. *55*, 4561–4565.

Haaf, T., Golub, E.I., Reddy, G., Radding, C.M., and Ward, D.C. (1995). Nuclear foci of mammalian Rad51 recombination protein in somatic cells after DNA damage and its localization in synaptonemal complexes. Proc. Natl. Acad. Sci. USA *92*, 2298–2302.

Hakem, R., de la Pomba, J.L., Sirard, C., Mo, R., Woo, M., Hakem, A., Wakeham, A., Potter, J., et al. (1996). The tumor suppressor gene *Brca1* is required for embryonic cellular proliferation in the mouse. Cell *85*, 1009–1023.

Hall, J.M., Lee, M.K., and Newmann, B. (1990). Linkage of early-onset breast cancer to chromosome 17q21. Science *250*, 1684–1689.

Holt, J.T., Thompson, M.E., Szabo, C., Robinson-Benion, C., Arteaga, C. L., King, M.-C., and Jensen, R.A. (1996). Growth retardation and tumor inhibition by BRCA1. Nat. Genet. *12*, 298–302.

Jiminez, G., Yucel, J., Rowley, R., and Subramani, S. (1992). The rad3^{+} gene of Schizosaccharomyces pombe is involved in multiple checkpoint functions and in DNA repair. Proc. Natl. Acad. Sci. USA *87*, 4952–4956.

Kaelin, W.G., Jr., Krek, W, Sellers, W.R., DeCaprio, J.A., Ajchenbaum, F., Fuchs, C.S., Chittenden, T., Li, Y., Farnham, P.J., et al. (1992). Expression cloning of a cDNA encoding a retinoblastoma-binding protein with E2F-like properties. Cell *70*, 351–364.

Keegan, K.S., Holtzman, D.A., Plug, A.W., Christenson, E.R., Brainerd, E.E., Flaggs, G., Bentley, N.J., Taylor, E.M., et al. (1996). The Atr and Atm protein kinases associate with different sites along meiotically pairing chromosomes. Genes Dev. *10*, 2423–2437.

Kleckner, N. (1996). Meiosis: how could it work? Proc. Natl. Acad. Sci. USA *93*, 8167–8174.

Kolodner, R. (1996). Biochemistry and genetics of eukaryotic mismatch repair. Genes Dev. *10*, 1433–1442.

Koonin, V.F., Altschul, S.F., and Bork, P. (1996). BRCA1 protein products: functional motifs. Nat. Genet. *13*, 266–267.

Kowalczykowski, S.C. (1991). Biochemistry of genetic recombination: energetics and mechanism of DNA strand exchange. Annu. Rev. Biophys. Chem. *20*, 539–575.

Krek, W., Livingston, D.M., and Shirodkar, S. (1993). Binding to DNA and the retinoblastoma gene product promoted by complex formation of different E2F family members. Science *262*, 1557–1560.

Lammers, J.H.M., Offenberg, H.H., van Aalderen, M., Vink, A.C., Dietrich, A.J., and Heyting, C. (1994). The gene encoding a major component of the lateral element of the synaptonemal complex of the rat is related to X-linked lymphocyte-regulated genes. Mol. Cell. Biol. *14*, 1137–1146.

Lane, T.F., Deng, C., Elson, A., Lyu, M.S., Kozak, C.A., and Leder, P. (1995). Expression of BRCA1 is associated with terminal differentiation of ectodermally and mesodermally derived tissues in mice. Genes Dev. *9*, 2712–2722.

Lim, D.-S., and Hasty, P. (1996). A mutation in mouse rad51 results in an early embryonic lethal that is suppressed by a p53 mutation. Mol. Cell. Biol. *16*, 7133–7143.

Liu, C.Y., Flesken-Nikitin, A., Li, S., Zeng, Y., and Lee, W.-H. (1996). Inactivation of the mouse Brca1 gene leads to failure in the morphogenesis of the egg cylinder in early postimplantation development. Genes Dev. *10*, 1835–1843.

Maldonado, E., Shiekhattar, R., Sheldon, M., Cho, H., Drapkin, R., Rickert, P., Lees, E., Anderson, C.W., Linn, S., and Reinberg, D. (1996). A human RNA polymerase II complex associated with SRB and DNA-repair proteins. Nature *381*, 86–89.

Malkin, D., Li, F.P., Strong, L.C., Fraumeni, J.F., Jr., Nelson, C.E., Kim, D.H., Kassel, J., Gryka, M.A., Bischoff, F.Z., et al. (1990). Germ line p53 mutations in a familial syndrome of breast cancer, sarcomas, and other neoplasms. Science *250*, 1233–1238.

Marcus, J.N., Watson, P., Page, D.L., Narod, S.A., Lenoir, G., Tonin, P., Linder-Stephenson, L., et al. (1996). Hereditary breast cancer: pathobiology, prognosis, and BRCA1 and BRCA2 gene linkage. Cancer *77*, 697–709.

Marquis, S.T., Rajan, J.V., Wynshaw-Boris, A., Xu, J., and Yin, G.-Y. (1995). The developmental pattern of BRCA1 expression implies a role in differentiation of the breast and other tissues. Nat. Genet. *11*, 17–26.

Merajver, S.D., Pham, T.M., Caduff, R.F., Chen, M., Poy, E.L., Cooney, K.A., Weber, B.L., Collins, F.S., et al. (1995). Somatic mutations in the BRCA1 gene in sporadic ovarian tumors. Nat. Genet. *9*, 439–443.

Miki, Y., Swensen, J., Shattuck-Eidens, D., Futreal, P.A., Harshman, K., Tavtigian, S., Liu, Q., Cochran, C., et al. (1994). A strong candidate for the breast and ovarian cancer susceptibility gene BRCA1. Science *266*, 66–71.

Moens, P.B.C., Heyting, C., Dietrich, A.J., van Raamsdonk, W., and Chen, Q. (1987). Synaptonemal complex antigen localization and conservatation. J. Cell Biol. *105*, 93–103.

Monteiro, A.N.A., August, A., and Hanafusa, H. (1996). Evidence for a transcriptional activation function of BRCA1 C-terminal region. Proc. Natl. Acad. Sci. USA *93*, 13595–13599.

Narod, S.A., Feunteun, J., Lynch, H.T., Watson, P., Conway, T., Lynch, J., and Lenoir, G. (1991). Familial breast-ovarian cancer locus on chromosome 17q12–23. Lancet *338*, 82–83.

Neuhausen, S.L., and Marshall, C.J. (1994). Loss of heterozygosity in familial tumors from three BRCA1-linked kindreds. Cancer Res. *54*, 6069–6072.

Newman, B., Austin, M.A., Lee, M., and King, M.-C. (1988). Inheritance of breast cancer: evidence for autosomal dominant transmission in high risk families. Proc. Natl. Acad. Sci. USA *85*, 1–5.

Peters, A.H.F.M., Plug, A.W., van Vugt, M.J. and deBoer, P. (1997). Drying down method for spreading mammalian meiocytes from the male and female germline. Chromosoma *5*, 1–3.

Plug, A.W., Xu, J., Reddy, G., Golub, E.I., and Ashley, T. (1996). Presynaptic association of Rad51 protein with selected sites in meiotic chromatin. Proc. Natl. Acad. Sci. USA *93*, 5920–5924.

Radding, C.M. (1991). Helical interactions in homologous pairing and strand exchange driven by RecA protein. J. Biol. Chem. *266*, 5355–5358.

Rao, V.N., Shao, N., Ahmad, M., and Reddy, E.S. (1996). Antisense RNA to the putative tumor suppressor gene BRCA1 transforms mouse fibroblasts. Oncogene *12*, 523–528.

Ried, T., Baldini, A., Rand, T.C. and Ward, D.C. (1992). Simultaneous visualization of seven different DNA probes by in situ hybridization using combinatorial fluorescence and digital imaging microscopy. Proc. Natl. Acad. Sci. USA *89*, 1388–1392.

Rowley, R., Subramani, S., and Young, P.G. (1992). Checkpoint controls in Schizosaccharomyces pombe, rad 1. EMBO J. *11*, 1335–1342.

Saurin, A.J., Borden, K.L. B., Boddy, M.N., and Freemont, P.S. (1996). Does this have a familiar RING? Trends Biochem. Sci. *21*, 208–214.

Scully, R., Ganesan, S., Brown, M., De Caprio, J.A., Cannistra, S.A., Feunteun, J., Schnitt, S., and Livingston, D.M. (1996). Location of BRCA1 in human breast and ovarian cell lines. Science *272*, 123–125.

Shao, N.S., Chai, Y.L., Shyam, E., Reddy, P., and Rao, N.V. (1996). Induction of apoptosis by the tumor suppressor protein BRCA1. Oncogene *13*, 1–7.

Shattuck-Eidens, D., McClure, M., Simard, J., Labrie, F., Narod, S., Couch, F., Hoskins, K., Weber, B., et al. (1995). A collaborative survey of 80 mutations in the BRCA1 breast and ovarian cancer susceptibility gene. J. Am. Med. Assoc. *273*, 535–541.

Shinohara, A., Ogawa, H., and Ogawa, T. (1992). Rad51 protein involved in repair and recombination in Saccharomyces cerevisiae is a RecA-like protein. Cell *69*, 457–470.

Simard, J., Tonin, P., Durocher, F., Morgan, K., Rommens, J., and Gingras, S. (1994). Common origins of BRCA1 mutations in Canadian breast and ovarian cancer families. Nat. Genet. *8*, 392–398.

Smith, S.A., Easton, D.F., Evans, D.G.R., and Ponder, B.A.J. (1992). Allele losses in the region 17q12–q21 in familial breast and ovarian cancer non-randomly involve the wild-type chromosome. Nat. Genet. *2*, 128–131.

Sturzbecher, H.-W., Donzelmann, B., Henning, W., Knippschild, U., and Buchop, S. (1996). p53 is linked directly to homologous recombination processes via RAD51/RecA protein interaction. EMBO J. *15*, 1992–2002.

Sung, P. (1994). Catalysis of ATP-dependent homologous DNA pairing and strand exchange by yeast Rad51 protein. Science *265*, 1241–1243.

Sung, P., and Robberson, D.L. (1995). DNA strand exchange mediated by a Rad51–ssDNA nucleoprotein filament with polarity opposite to that of RecA. Cell *82*, 453–461.

Swift, M., Reitnauer, P.J., Morrell, D., and Chase, C.L. (1987). Breast and other cancers in families with Ataxia-Telangiectasia. N. Engl. J. Med. *316*, 1289–1294.

Tashiro, S., Kotomura, N., Shinohara, A., Tanaka, K., Ueda, K., and Kamada, N. (1996). S phase specific formation of the human Rad51 protein nuclear foci in lymphocytes. Oncogene *12*, 2165–2170.

Terasawa, M., Shinohara, A., Hotta, Y., Ogawa, H., and Ogawa, T. (1995). Localization of RecA-like recombination proteins on chromosomes of lily at various meiotic stages. Genes Dev. *9*, 925–934.

Tsuzuki, T., Fujii, Y., Sakumi, K., Tominaga, Y., Nakao, K., Sekiguchi, M., Matsushiro, A., Yoshimura, Y., and Morita, T. (1996). Targeted disruption of the Rad51 gene leads to lethality in embryonic mice. Proc. Natl. Acad. Sci. USA *93*, 6236–6240.

Vairo, G., Livingston, D.M., and Ginsberg, D. (1995). Functional interaction between E2F-4 and p130: evidence for distinct mechanisms underlying growth suppression by different retinoblastoma protein family members. Genes Dev. *9*, 869–881.

Vaughn, J.P., Davis, P.L., Jarboe, M.D., Huper, G., Evans, A.C., Wiseman, R.W., Berchuck, A., Iglehart, J.D., et al. (1996). BRCA1 expression is induced before DNA synthesis in both normal and tumor-derived breast cells. Cell Growth Differ. *7*, 711–715.

Wigler, M., Silverstein, S., Lee, L.S., Pellicer, A., Cheg, Y.C., and Axel, R. (1977). Transfer of purified herpes virus thymidine kinase gene to cultured mouse cells. Cell *11*, 223–232.

Wilson, C.A., Payton, M.N., Elliott, G.S., Buaas, F.W., Cajulis, E.E., Grosshans, D., Ramos, L., Reese, D.M., et al. (1996). Differential subcellular localization, expression and biological toxicity of BRCA1 and the splice variant BRCA1-Δ11b. Oncogene, in press.

Zabludoff, S.D., Wright, W.W., Harshman, K., and Wold, B.J. (1996). BRCA1 mRNA is expressed highly during meiosis and spermiogenesis but not during mitosis of male germ cells. Oncogene *13*, 649–653.

Cell, Vol. 90, 425–435, August 8, 1997, Copyright ©1997 by Cell Press

Dynamic Changes of BRCA1 Subnuclear Location and Phosphorylation State Are Initiated by DNA Damage

Ralph Scully,* Junjie Chen,* Robert L. Ochs,†
Kathleen Keegan,‡ Merl Hoekstra,‡
Jean Feunteun,§ and David M. Livingston*
*The Dana-Farber Cancer Institute
Harvard Medical School
Boston, Massachusetts 02115
†The Scripps Research Institute
La Jolla, California 92037
‡ICOS Corporation
Bothell, Washington 98021
§Centre National de la Recherche Scientifique
Institut Gustave-Roussy
Cedex 94805 Villejuif
France

Summary

BRCA1 localizes to discrete nuclear foci (dots) during S phase. Hydroxyurea-mediated DNA synthesis arrest of S phase MCF7 cells led to a loss of BRCA1 from these structures. Ultraviolet light, mitomycin C, or gamma irradiation produced a similar effect but with no concurrent arrest of DNA synthesis. BARD1 and Rad51, two proteins associated with the BRCA1 dots, behaved similarly. Loss of the BRCA1 foci was accompanied by a specific, dose-dependent change(s) in the state of BRCA1 phosphorylation. Three distinct DNA damaging agents preferentially induced this change in S phase. The S phase BRCA1 phosphorylation response to DNA damage occurred in cells lacking, respectively, two DNA damage-sensing protein kinases, DNA-PK and Atm, implying that neither plays a prime role in this process. Finally, after BRCA1 dot dispersal, BRCA1, BARD1, and Rad51 accumulated, focally, on PCNA$^+$ replication structures, implying an interaction of BRCA1/BARD1/Rad51 containing complexes with damaged, replicating DNA. Taken together, the data imply that the BRCA1 S phase foci are dynamic physiological elements, responsive to DNA damage, and that BRCA1-containing multiprotein complexes participate in a replication checkpoint response.

Introduction

BRCA1 is a tumor suppressor gene that maps to human chromosome 17q 21.3 (Futreal et al., 1994; Hall et al., 1990; Miki et al., 1994; Neuhausen and Marshall, 1994; Smith et al., 1992). When one copy of *BRCA1* is inactivated in the germ line, affected individuals are predisposed to developing breast, ovarian, and other malignant tumors (reviewed in Feunteun and Lenoir, 1996). Until recently, there has been little understanding of how its product operates as a tumor suppressor or in any other capacity.

BRCA1 is an 1863 residue nuclear polypeptide which appears in discrete, nuclear foci (dots) during S phase (Chen et al., 1996; Scully et al., 1996, 1997a). These structures contain at least two other proteins, Rad51 and BARD1, both of which form complexes with BRCA1 in vivo (Scully et al., 1997a; Wu et al., 1996; R. Baer, personal communication and data presented below).

The *BRCA1* gene is widely expressed in developing embryos, with a marked preference for replicating cells (Lane et al., 1995; Marquis et al., 1995). It is essential for early embryonic proliferation and development (Gowen et al., 1996; Hakem et al., 1996; Liu et al., 1996). Recently, its full-length product was found to interact, directly or indirectly, with Rad51, a major participant in eukaryotic double-strand break repair and homologous recombination (Shinohara et al., 1992; Baumann et al., 1996; Scully et al., 1997a). BRCA1/Rad51 interactions have been identified in both mitotic and meiotic cells (Scully et al., 1997a), where Rad51 contributes to meiotic recombination (Ashley et al., 1995; Bishop, 1994; Terasawa et al., 1995). These observations imply that BRCA1 and Rad51 communicate physiologically and further suggest that BRCA1 functions in the maintenance of genome integrity.

In keeping with these findings, Sharan et al. (1997) have reported that another familial breast cancer tumor suppressor gene product, BRCA2, can interact with Rad51, and that murine embryos lacking wild-type *BRCA2* exhibit radiation sensitivity. Collectively, these data suggest that loss of functional BRCA1 or BRCA2 are mutagenic events, and, thereby, accelerate neoplastic transformation. Interestingly, BRCA1 and BARD1 each contain a C-terminal "BRCT" domain, which is found in many DNA repair and cell cycle checkpoint proteins (Bork et al., 1997; Callebaut and Mornon, 1997; Koonin et al., 1996). The generic function of the BRCT domain is not clear. However, this segment of BRCA1 has both transactivation (Chapman and Verma, 1996; Monteiro et al., 1996) and growth suppression properties (Humphrey et al., 1997) and may play a part in docking BRCA1 onto the RNA polymerase II holoenzyme (Scully et al., 1997b).

Although these observations are consistent with a role for BRCA1 in DNA repair and the maintenance of genome stability, there is little evidence that speaks to a dynamic function of BRCA1 in this regard. Here we report that BRCA1/Rad51/BARD1 containing S phase nuclear foci are sensitive to the integrity of the genome, undergoing a major structural change in the face of genotoxic insult. This response to DNA damage is accompanied by a specific change in BRCA1 phosphorylation and by the relocation of BRCA1, BARD1, and Rad51 to sites of "abnormal" (nonduplex) DNA structure in S phase cells. These findings suggest that BRCA1 participates in an S phase, DNA damage-dependent cell cycle checkpoint response.

Results

Disruption of BRCA1 S Phase Nuclear Foci by DNA Damage

A proportion of BRCA1 is localized to nuclear foci in S phase cells. These structures were not detected in

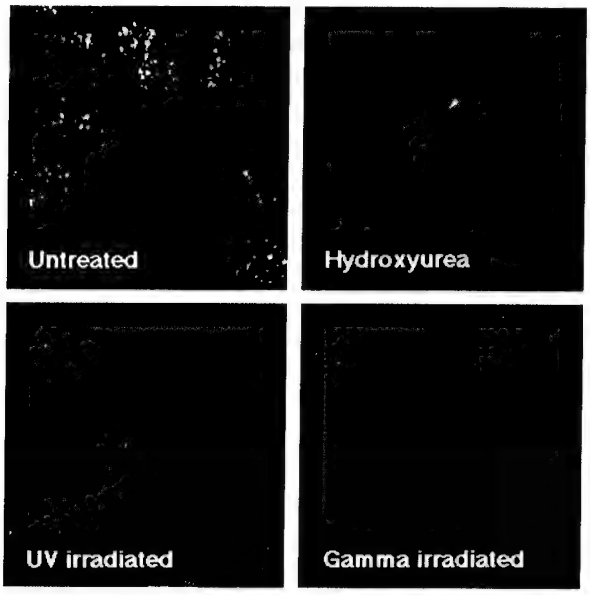

Figure 1. DNA Damage Disperses BRCA1 S Phase Focal Staining

S phase MCF7 cells were treated with DNA damaging agents, as indicated. Immunostaining for BRCA1 was performed using mAb MS13. Cells received either no treatment, HU 1 mM, UV 10 Jm^{-2}, or 5000 Rads and were harvested 1 hr later. The arrow indicates a rare cell in an HU-treated culture which retains some focal staining for BRCA1.

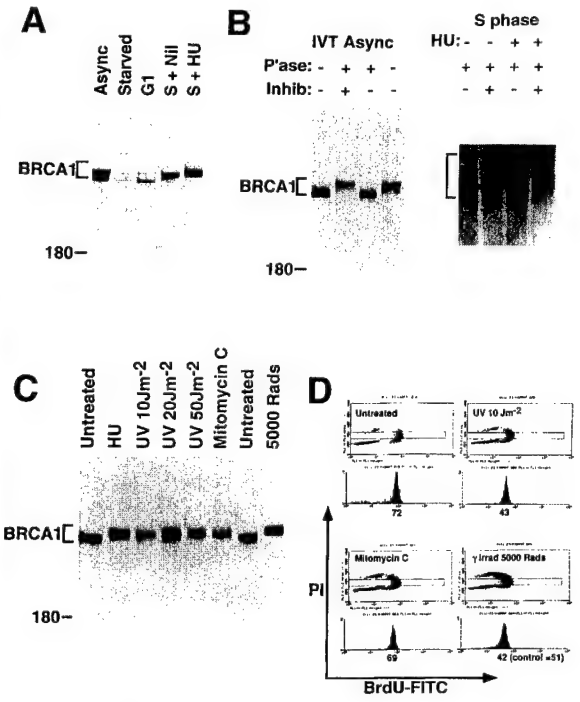

Figure 2. Specific Phosphorylation of BRCA1 following DNA Damage

(A) Cell cycle variation in BRCA1 gel mobility. MCF7 extracts were immunoblotted for BRCA1 using mAb MS110. Migration of BRCA1 is indicated. Async, asynchronous culture (58% G1, 30% S); starved, cells after 24 hr of serum starvation (90% G1, 2.5% S); G1, cells 12 hr after release into high serum (86% G1, 7% S); S + Nil, cells 24 hr after release into high serum (40% G1, 54% S); S + HU, identically treated S phase cells (in parallel) cultured after 24 hr of serum refeeding in HU for 1 hr before harvesting.

(B) Changes in mobility are due to changes in phosphorylation of BRCA1. BRCA1 IPs were treated with λ-phosphatase (see Experimental Procedures) ± phosphatase inhibitors, as indicated, and then immunoblotted for BRCA1. IVT, in vitro translated wild-type BRCA1. Left panel, MCF7 cells were asynchronous. Right panel, similar treatment of S phase MCF7 cells ± HU, as indicated. BRCA1 species are bracketed.

(C) Phosphorylation of BRCA1 in S phase after DNA damage. S phase MCF7 cells were exposed to the treatments shown for 1 hr prior to harvesting. Cell extracts were then immunoblotted for BRCA1.

(D) Cell cycle analysis on samples from (C). BrdU staining and cell cycle FACS analysis were performed as described in Experimental Procedures. To quantitate BrdU incorporation in S phase cells, a FACS gate was used to exclude G1 and G2 populations. Under each panel, the histogram gives the mean BrdU fluorescence intensity of gated (S phase) cells, in arbitrary units. HU-treated S phase cells, which had arrested DNA synthesis, had a mean BrdU fluorescence intensity of 13 in the same experiment.

multiple cell lines during G1, when a less intense nucleoplasmic BRCA1 immunostaining signal was observed (Scully et al., 1997a). They can be detected using many different BRCA1-specific Abs, raised to distinct epitopes, using any of several different fixation methods, or in living cells containing green fluorescent protein (GFP)-tagged BRCA1 (Scully et al., 1996; R. S., D. M. L., J. A. DeCaprio, and P. A. Silver, unpublished observations). Further, BRCA1 foci exist in mouse fibroblast nuclei as shown by immunofluorescence with anti-murine BRCA1 (X. Wu and D. M. L., unpublished observations). Hence, they are general BRCA1 phenomena.

Since BRCA1 is suspected of playing a role in genome integrity maintenance, we asked whether the S phase BRCA1 dots were altered in S phase cells after DNA damage and/or when DNA synthesis is interrupted. Hydroxyurea (HU) was used to induce DNA synthesis arrest of S phase cultures of the human breast cancer cell line, MCF7. BRCA1 immunostaining of HU-treated cells, performed with any of three different BRCA1 monoclonal antibodies, revealed overt dispersal of BRCA1 nuclear foci (Figure 1). Given the likelihood that HU treatment of S phase cells mimics DNA damage (Allen et al., 1994; Carr, 1995; Sanchez et al., 1996; Sun et al., 1996), we asked whether other DNA damaging agents affect the integrity of the S phase BRCA1 dots. Treatment with ultraviolet (UV) irradiation, mitomycin C, or gamma irradiation also led to dispersal of the dots within 1 hr (Figure 1 and data not shown). Untreated or mock-treated S phase cells revealed typical BRCA1 dots (Figure 1 and data not shown). Thus, dispersal of BRCA1 S phase foci might represent a cellular response to DNA damage. A few cells retained BRCA1 foci after HU or UV treatment (e.g., cell indicated by an arrow in Figure 1). The nature of these foci is discussed below (Figures 5 and 6 and accompanying text).

Cell Cycle–Specific Phosphorylation of BRCA1

In an effort to understand the mechanisms governing the migration of BRCA1 into and out of S phase foci, we sought biochemical correlates of the different BRCA1 nuclear immunofluorescence patterns. Immunoblotting for p220 BRCA1 in asynchronous MCF7 cells revealed a doublet (Figure 2A). Each band of the doublet reacted

with BRCA1 monoclonal antibodies (mAbs), MS13, MS110, SG11, and AP16 (data not shown and Figure 2B). Serum-starved MCF7 cells contained reduced levels of BRCA1 (Figure 2A). Cells released into G1 for 12 hr produced an enrichment of the faster migrating band of the doublet (Figure 2A). In contrast, 24 hr after release into high serum, when most cells were in S phase, there was a further increase in BRCA1 protein level, represented primarily by the slower migrating form of the protein (Figure 2A). Similar observations concerning the migration of G1 and S phase associated forms of BRCA1 have been made by Ruffner and Verma (1997).

A parallel culture of S phase MCF7 cells was treated with HU for 1 hr. Immunoblotting revealed the presence of a form of BRCA1 that was not detected in untreated cycling cells but which migrated more slowly than the BRCA1 present in untreated S phase cells (Figure 2A). Thus, endogenous "p220" BRCA1 was detectable in at least three different forms: a rapidly migrating, G1-associated form; a more slowly migrating, S phase form; and an even more slowly migrating form, noted in HU-treated S phase cells.

Thus, BRCA1 might undergo regulated post-translational modifications, such as phosphorylation. Consistent with this, phosphatase treatment of BRCA1 immunoprecipitates (IPs) altered the gel mobility of BRCA1 (Figure 2B). IPs of BRCA1 from asynchronous MCF7 cells, using the C-terminal mAb, SG11, were aliquoted into three fractions. The first was treated with λ-phosphatase in the presence of phosphatase inhibitors; the second with λ-phosphatase in the absence of inhibitors; and the third was left untreated. IPs were immunoblotted using the N-terminal BRCA1 mAb, MS110. Phosphatase treatment in the absence of inhibitors resulted in collapse of the BRCA1 doublet into a single band which comigrated with in vitro synthesized, clonal BRCA1 (Figure 2B). Phosphatase treatment in the presence of inhibitors did not perturb the BRCA1 doublet relative to untreated IPs (Figure 2B), ruling out nonspecific effects of the phosphatase preparation. Similarly, phosphatase treatment of BRCA1 IPs, prepared from HU-treated S phase cells, led to its comigration with the phosphatase-treated BRCA1 species detected in naive S phase cells (Figure 2B). These results strongly suggest that the differential gel mobility of the three forms of BRCA1, noted in G1, S phase, and HU-treated S phase cells, is due to differential phosphorylation.

HU treatment of S phase cells, therefore, led to three measured events: DNA synthesis arrest, dispersal of BRCA1 foci, and phosphorylation of BRCA1. DNA synthesis arrest following brief (2 hr) HU exposure was found to be reversible. Removal of HU after this time led to the resumption of full DNA synthesis. Furthermore, both the BRCA1 foci and the faster migrating S phase BRCA1 band reappeared, while the slower HU-associated band disappeared (data not shown). Therefore, within the time limits of this experiment, all three effects of HU were reversible.

Phosphorylation of BRCA1 after DNA Damage in S Phase without Arrest of Scheduled DNA Synthesis

Exposure of S phase MCF7 cells to UV irradiation, mitomycin C, or gamma irradiation was found to retard the migration of the S phase BRCA1 band, similar to the effect of HU treatment (Figure 2C). This effect, coupled with the above noted dispersal of BRCA1 S phase foci (Figure 1), indicated a similarity between the effect of these DNA damaging agents and HU. However, in contrast to HU-treated cells, the response of S phase cells to two of these three DNA damaging agents did not include acute DNA synthesis arrest. Specifically, mitomycin C–treated and gamma-irradiated S phase MCF7 cells showed no impairment of BrdU incorporation compared with untreated controls, at a time when BRCA1 had already undergone the relevant DNA damage-induced phosphorylation (Figures 2C and 2D). UV treatment led to a dose-dependent inhibition of BrdU uptake, with only a modest impairment of DNA synthesis detectable in cells treated with 10 Jm^{-2}, but near total DNA synthesis arrest seen at 50 Jm^{-2} (Figure 2D and data not shown). Ten joules per square meter did, however, lead to the supershift of the S phase band, as seen following treatment with HU, mitomycin, or gamma irradiation (Figure 2C).

The finding of continued BrdU incorporation into S phase cells that had sustained acute DNA damage could be interpreted as unscheduled DNA synthesis (i.e., repair synthesis) in the context of an arrest of scheduled DNA synthesis. Although some repair process might be expected to be occurring at this time (e.g., to permit resolution of abnormal DNA structures at replication forks), the data are incompatible with the idea that scheduled DNA synthesis itself had ceased. First, BrdU incorporation during repair synthesis should be much less efficient than during normal DNA replication (Li et al., 1996), whereas near normal DNA synthesis levels were noted after acute exposure to mitomycin C, gamma irradiation, or 10 Jm^{-2} UV. Second, if the BrdU incorporation detected were a manifestation of repair synthesis alone, a higher density of DNA lesions should produce a higher level of BrdU incorporation. However, the reverse was true for UV treatment, where increasing doses led to progressive impairment of BrdU incorporation efficiency. Therefore, 1 hr after treatment with either UV irradiation (10 Jm^{-2}), mitomycin C, or gamma irradiation, scheduled DNA synthesis had not yet ceased. Therefore, DNA damage-associated BRCA1 phosphorylation can occur in S phase cells without arrest of scheduled DNA synthesis.

Although three DNA damaging agents and HU had disparate effects upon scheduled DNA synthesis, the feature common to all these treatments is their ability to induce DNA lesions, rather than their effect on the replication machinery per se. HU treatment might be predicted to produce, at least transiently, "abnormal" (i.e., nonduplex) DNA structures at arrested replication forks. The simplest model to explain these phenomena would be one in which "abnormal" DNA structures, generated in S phase, trigger a signaling cascade, one outcome of which is specific BRCA1 phosphorylation.

Time Course of the Response to UV Irradiation

These results suggest a relationship between DNA damage-associated phosphorylation of BRCA1 and dispersal of the BRCA1 dots. This was explored further, using UV as the stimulus. The phosphorylation status

of BRCA1 was followed at 10-min intervals following a pulse of 10 Jm^{-2}, administered to S phase MCF7 cells. A significant alteration in BRCA1 gel mobility was apparent 20–30 min after treatment (Figure 3A). In a similar experiment, the time course of dispersal of BRCA1 foci was followed at 5-min intervals, by scoring, at each time point, four randomly selected confocal microscopic fields for the percentage of cells containing BRCA1 foci. Significant dispersal of BRCA1 foci was not detected until 25 min after the UV pulse (Figure 3B). Thus, at this UV dose (and also at higher doses, data not shown), there was a close temporal correlation between damage-induced phosphorylation of BRCA1 and dispersal of the BRCA1 foci.

Hydroxyurea, Mitomycin C, and UV Treatments Preferentially Target BRCA1 in S Phase

The data, noted above, raise the question of whether BRCA1 is targeted for phosphorylation by DNA damage only in S phase. The migration pattern of MCF7 in asynchronous or G1-enriched cells provided a means to address this question. We had noted (Figure 2A) that there is a faster migrating form of p220 BRCA1 enriched in G1 MCF7 cells and detectable in asynchronous cultures. Asynchronous MCF7 cells were subjected to treatment with HU, UV, or gamma irradiation. One hour later they were harvested and immunoblotted for BRCA1. Consistently, HU treatment or low-dose UV (10 Jm^{-2}) treatment induced the predicted BRCA1 gel shift of the upper (S phase correlated) but not the lower (G1 correlated) BRCA1 band (data not shown). In contrast, gamma irradiation (5000 Rads) appeared to displace both forms of BRCA1. This implied that low-dose UV or HU treatment might produce phosphorylation of BRCA1 in S phase but not in G1.

To test this notion directly, we prepared G1-synchronized MCF7 cells by serum starvation followed by 7 hr of incubation in high serum. These synchronized cells were then exposed to HU, UV, mitomycin C, or gamma irradiation and harvested 1 hr later, while still in G1. Immunoblotting for BRCA1 in unperturbed control G1 cells revealed the presence of the faster-migrating, G1 form of BRCA1, albeit at levels lower than in S phase cells (Figure 3C, left panel). Strikingly, neither HU, mitomycin C, nor low-dose UV treatment (10 Jm^{-2}) led to a change in the mobility of the G1 band (Figure 3C, right panel). Under identical conditions, the S phase band shifted (compare Figures 2C and 3C). Higher doses of UV led to a dose-dependent shift in the G1 form of BRCA1 (Figure 3C) as did gamma irradiation (5000 Rads).

This preferential S phase targeting of BRCA1 for phosphorylation, following HU, low dose UV, or mitomycin C, could be interpreted in two ways. First, the sensor(s) of abnormal DNA structure, or their subsequent amplificatory cascades, might operate differently between S phase and G1. Second, the S phase preference for BRCA1 phosphorylation after UV/mitomycin C could be an attribute of the BRCA1 protein itself, rather than of the signals impinging on it. A hint that the former might be correct came from examination of the response to

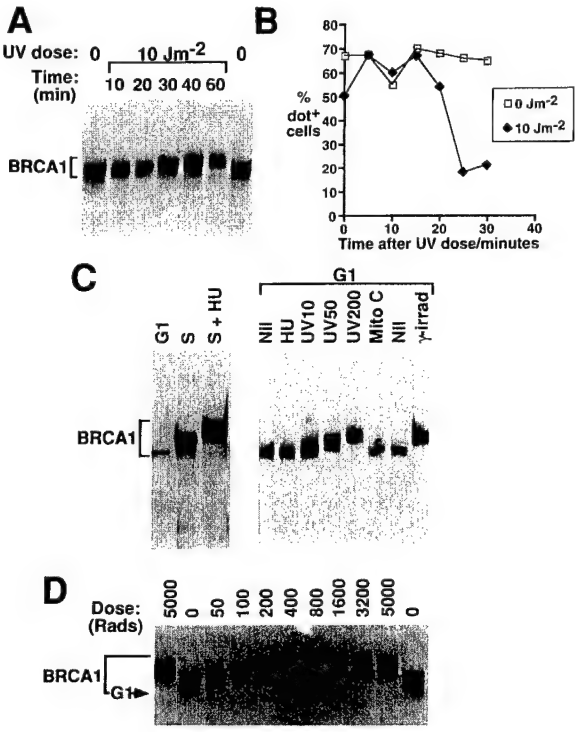

Figure 3. Time Course and Cell Cycle Specificity of the BRCA1/DNA Damage Response

(A) Time course of phosphorylation change after UV irradiation. S phase enriched MCF7 cells were exposed to 10 Jm^{-2} UV light, harvested at the time points indicated, and immunoblotted for BRCA1. The shift in BRCA1 migration is seen ~20–30 min after UV exposure.

(B) Time course of BRCA1 focus dispersal following UV exposure. In a protocol identical to that employed in A, S phase MCF7 cells were exposed to 10 Jm^{-2} UV light (filled diamonds), or mock treated (open squares), and were harvested at the time points indicated. Each coverslip was stained for BRCA1, and cells in four randomly selected confocal fields were scored for the presence or absence of BRCA1 nuclear foci. One hundred and fifteen to 185 cells were scored per time point. Results are presented as the percentage of cells scoring positive for BRCA1 foci.

(C) S phase specificity of the BRCA1 damage response. MCF7 cells were released from serum starvation into G1 for 7 hr. After treatment with DNA damaging agents, as shown, cells were harvested 1 hr later (while still in G1) and immunoblotted for BRCA1. Extracts of S phase MCF7 and HU-treated S phase cells were analyzed in parallel to show the relative migration of the G1, G1/damage, S and S/damage forms of BRCA1. Note that HU, mitomycin C, and low-dose UV treatment (10 Jm^{-2}) each failed to shift the G1 form of BRCA1 under conditions in which the S phase form had undergone damage-induced phosphorylation (compare with Figure 2C).

(D) BRCA1 gel migration change after ionizing radiation. Asynchronously growing MCF7 cells were exposed to metered doses of gamma irradiation, harvested 1 hr later, and then immunoblotted for BRCA1. The lower (G1) band of BRCA1, indicated with an arrow, was noted to disappear at 50 Rads, whereas the S phase band shifted only at doses above 200 Rads.

gamma irradiation. When asynchronous MCF7 cells were exposed to a range of doses of gamma irradiation, the emergence of BRCA1 species migrating slower than the S phase band was apparent only at doses above 200 Rads (Figure 3D). In contrast, exposure to 50 Rads was sufficient to displace the G1 form of the protein (Figure 3D). Therefore, gamma irradiation appeared to

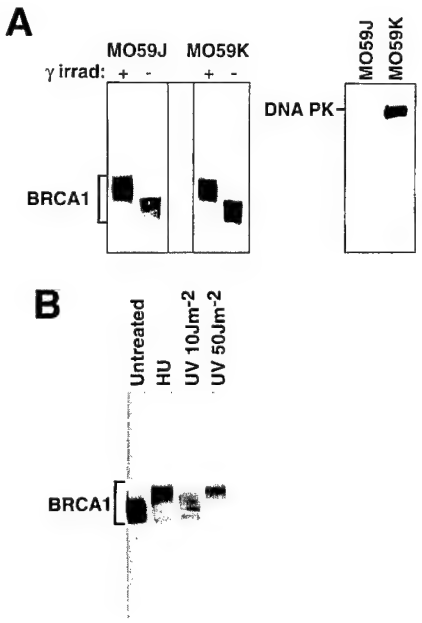

Figure 4. BRCA1 Damage Response in DNA-PK and ATM Mutant Cell Lines

(A) Asynchronously growing human glioma cell lines, MO59J (DNA-PK null) and MO59K (DNA-PK wild type) were exposed to 5000 Rads, or mock treated, and harvested 1 hr later. Immunoblotting for BRCA1 is shown in the left panel, and for DNA-PK in the right panel.

(B) Response of AT fibroblasts to HU and UV treatment. Asynchronous cultures of the AT primary human diploid fibroblast culture, GM02052B, were exposed to DNA damaging agents as shown, harvested 1 hr later, and immunoblotted for BRCA1.

provide an exception to the above-noted preference for S phase in signaling from DNA damage to BRCA1. This suggests that cell cycle specificity in the BRCA1 DNA damage response is a property of the particular sensors of and signaling arising from DNA damage, rather than of the BRCA1 protein itself.

DNA-Dependent Protein Kinase and the Ataxia Telangiectasia Gene Product Are Not Required for DNA Damage-Induced BRCA1 Phosphorylation in S Phase

Genetic and biochemical approaches suggest a role for the PIK family of nuclear protein kinases in linking the detection of DNA damage to cell cycle responses (Bentley et al., 1996; Cimprich et al., 1996; Hari et al., 1995; Hartley et al., 1995; Keith and Schreiber, 1995; Morrow et al., 1995; Savitsky et al., 1995). This family of proteins includes the catalytic subunit of DNA-dependent protein kinase (p460 DNA-PK), Atm, and Atr. Initially, we asked whether a functional copy of DNA-PK was necessary for detection of the BRCA1 DNA damage-phosphorylation response. The human glioma cell line, MO59, has two derivatives, one of which (MO59K) is wild-type for p460 DNA-PK. The other (MO59J) does not express its gene (Lees-Miller et al., 1995). Using gamma irradiation as the stimulus, we asked whether the two cell lines could each respond to DNA damage by phosphorylating BRCA1. Indeed, the two cell lines mounted indistinguishable responses to gamma irradiation (Figure 4A and data not shown). Immunoblotting of whole cell extracts was used to confirm the expression of p460 DNA-PK in MO59K cells and its absence from MO59J cells (Figure 4A). BRCA1 phosphorylation after HU or UV treatment was also detected in both cell lines, and the response to each of these stimuli was indistinguishable between MO59J and MO59K cells (data not shown). These results exclude p460 DNA-PK as a necessary component of the DNA damage-BRCA1 phosphorylation pathway.

To investigate a potential role for Atm, we analyzed primary cultures of Atm homozygous mutant fibroblasts. Both HU and UV exposure elicited a clear retardation in the migration of the S phase BRCA1 band (Figure 4B). A similar response to gamma irradiation was also noted (data not shown), although a quantitative effect of Atm on the DNA damage-BRCA1 signaling pathway has not yet been ruled out.

Recruitment of BRCA1 to PCNA- and DNA-Containing Nuclear Structures after DNA Damage in S Phase

Close examination of the BRCA1 immunostaining pattern after HU treatment or UV irradiation revealed that the frequency of cells, within S phase cultures, containing BRCA1 nuclear foci, although substantially reduced, was not zero (Figures 1 and 3B). In a small proportion of cells, there were characteristic small, punctate BRCA1 dots. In yet others, a qualitatively different BRCA1 focal pattern was detected (see below). The reasons for the presence of these different BRCA1 focal staining patterns became clear when cells were double stained for BRCA1 and proliferating cell nuclear antigen (PCNA), as detailed below.

Under some fixation conditions, PCNA immunostaining is seen only in cells synthesizing DNA, and given that its staining pattern changes during S phase, it can be used as an S phase temporal marker (Bravo, 1986; Bravo and Macdonald-Bravo, 1987). In early/mid–S phase cells, PCNA immunostaining is in a multifocal/diffusely nuclear pattern. In late S phase, the staining pattern changes dramatically and becomes "nodular." Importantly, throughout S phase, the immunostaining pattern of BrdU incorporation into replication forks clearly overlies the PCNA stain (Bravo and Macdonald-Bravo, 1987; Nakamura et al., 1986; Figure 5A). We confirmed, by the use of a mimosine block and release protocol, that these changes in PCNA morphology are similarly correlated with the stage of S phase in MCF7 cells (data not shown).

In synchronized cells, BRCA1 foci first appear in S phase. This raised the question of whether BRCA1 foci coincide with PCNA foci. This was addressed using two-color immunostaining followed by confocal microscopy. Images in Figure 5B depict unperturbed, S phase MCF7 cells doubly stained for BRCA1 (green, fluorescein isothiocyanate [FITC]) and PCNA (red, rhodamine). In repeated experiments, the two immunostaining patterns were found to be distinct, even when the PCNA pattern resembled the nodular one reported for late S phase cells (Bravo and Macdonald-Bravo, 1987; Nakamura et al., 1986). Thus, in conventionally cycling S phase cells, there was no immunocytochemical indication that

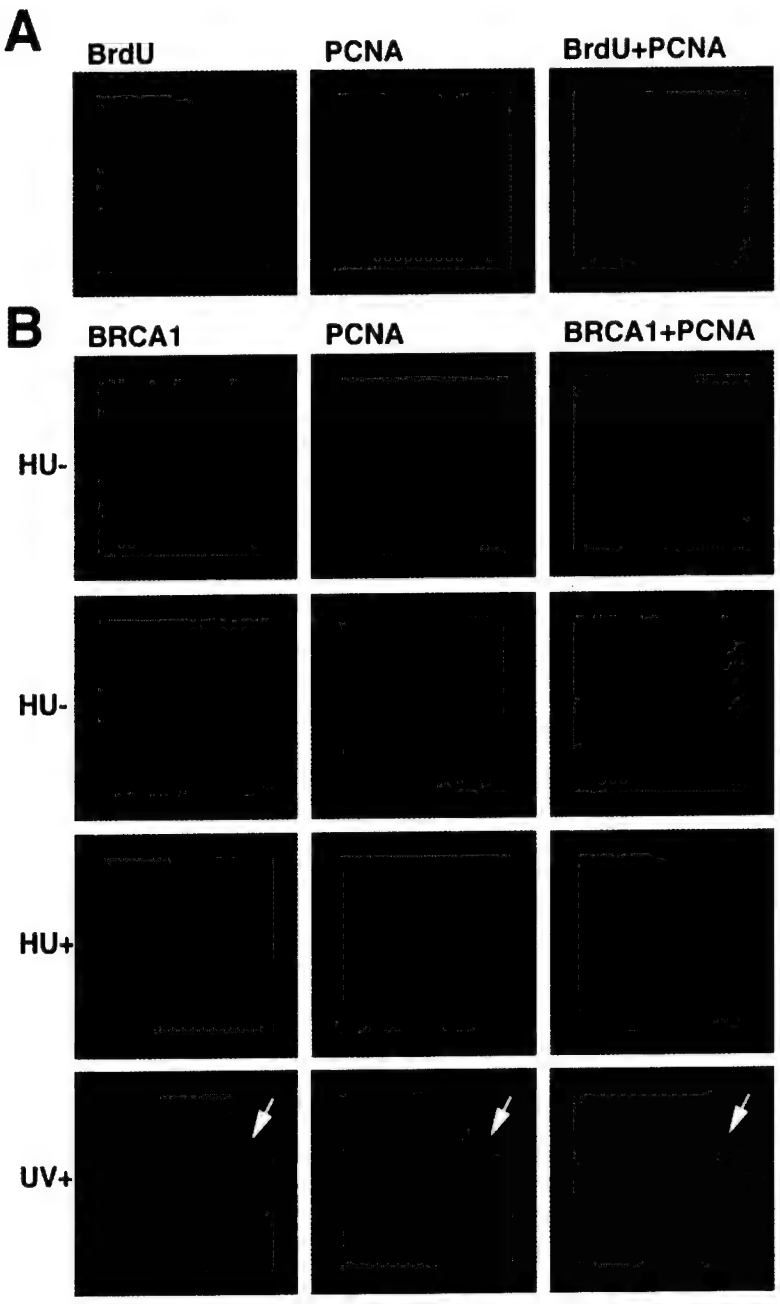

Figure 5. Recruitment of BRCA1 to Replication Structures after HU or UV Treatment

(A) In S phase cells, PCNA immunostaining can be used to locate sites of DNA synthesis. Panels depict S phase MCF7 cells, pulsed with BrdU prior to fixation, double stained with anti-BrdU mAb (green), and anti-PCNA Ab ("AK" serum, red). Where colocalization of the two images is seen, the signal appears in the right hand panel as a yellow signal.

(B) Recruitment of BRCA1 to replication structures after HU treatment. In untreated S phase cells ("HU−"), BRCA1 foci (mAb MS13, green) were not significantly coincident with PCNA (AK Ab, red) in either early S phase (upper row) or late S phase (second row). In contrast, in HU-treated cells ("HU+," third row), BRCA1 colocalizes extensively with PCNA in late S phase nuclei, as shown by the yellow overlap signal of green and red. Similar results were obtained in UV treated cells ("UV+," lowest row). The arrow points to a cell carrying BRCA1 dots and no PCNA staining. This may be a G2 cell.

BRCA1 focally accumulates at replication forks. Further, a small proportion of cells was noted to be positive for BRCA1 foci and negative for PCNA. This population was found to be enriched in late S phase cultures (data not shown), suggesting that the presence of BRCA1 foci is also a feature of some G2 cells.

In contrast, when HU- or UV-treated S phase cultures were similarly examined, a striking colocalization of the BRCA1 staining pattern and the PCNA staining pattern was noted in those rare, late S phase cells in which PCNA immunostaining was clearly nodular or focal (Figure 5B and data not shown). In the majority of S phase nuclei, where the PCNA pattern was diffuse, the BRCA1 stain was also diffuse (data not shown). The overt relocation of BRCA1 to PCNA$^+$ structures after DNA damage suggests that BRCA1 is recruited to replication forks after HU or UV treatment of S phase cells. By contrast, the small subset of nuclei scoring positive for BRCA1 dots but negative for PCNA (presumed G2 cells, as noted above) were not perturbed by either HU or UV treatment (e.g., "UV$^+$" panel in Figure 5B, cell indicated by an arrow).

Colocalization of BRCA1, BARD1, and Rad51 before and after DNA Damage in S Phase

Two proteins associated with BRCA1 in S phase foci—Rad51 and BARD1—were examined during the DNA damage response. Consistent with the described physical interaction between BRCA1 and BARD1 (Wu et al., 1996), BARD1 immunostaining, reflected by binding of multiple antibodies to BARD1, colocalized with BRCA1 in S phase nuclear dots (Figure 6A). This result was

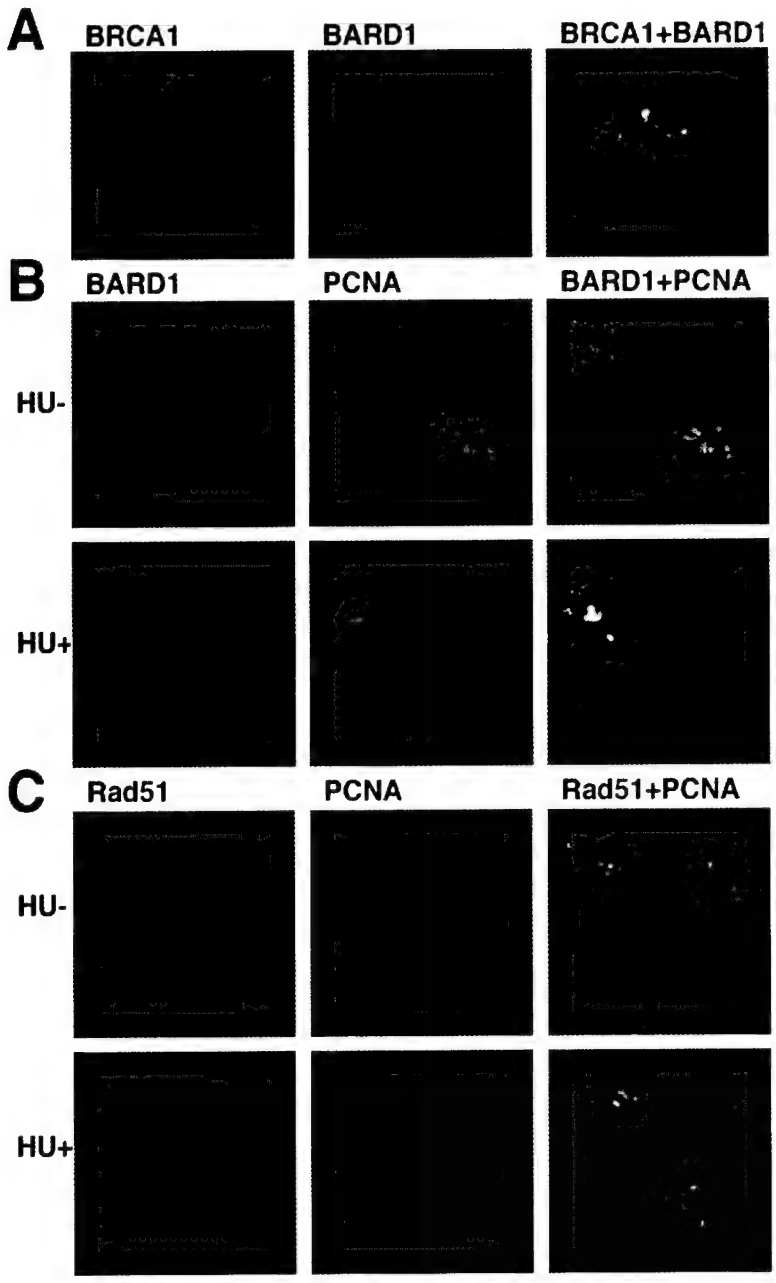

Figure 6. Recruitment of BARD1 and Rad51 to Replication Structures after DNA damage

(A) Colocalization of BRCA1 and BARD1 in S phase nuclear foci. Untreated S phase MCF7 cells, stained with BRCA1 mAb MS13 (green, FITC) and BARD1 Ab (rhodamine, red). Where the two nuclear dot signals overlap, a yellow signal was detected.

(B) Recruitment of BARD1 to replication structures after HU treatment. The upper panel depicts untreated S phase MCF7 cells ("HU−") double stained for BARD1 (using affinity purified polyclonal antiserum to BARD1, red) and PCNA (using mAb PC10, green). No significant colocalization of the green and red signals was noted. The lower panel shows the same, two-color immunstaining experiment, performed on HU-treated MCF7 cells ("HU+"). Where BARD1 and PCNA signals overlap, a yellow color was noted in the right-hand panel.

(C) Recruitment of Rad51 to replication structures after HU treatment. Similar treatments as for (B). Cells were double stained for Rad51 (using affinity purified polyclonal antiserum to Rad51, green) and PCNA (using "AK" antiserum, red), as described in Experimental Procedures. After HU treatment ("HU+"), but not in untreated cells ("HU−"), significant colocalization of Rad51 and PCNA is seen as a yellow overlap.

first obtained by Richard Baer and coworkers (personal communication). S phase ($PCNA^+$) nuclei were examined for BARD1 and Rad51 before and after HU or UV treatment. As was noted for BRCA1, undamaged cells revealed no significant colocalization of either Rad51 or BARD1 with PCNA (Figures 6B and 6C, see HU−). After HU or UV exposure, however, colocalization was seen on PCNA nodules (Figures 6B and 6C, see HU+). In the majority of S phase nuclei, where the PCNA stain was diffuse, Rad51 and BARD1 stains were also found to have become diffuse (data not shown). Thus, BRCA1 and two known associated proteins, BARD1 and Rad51, both concentrate in PCNA-containing, replicating structures after DNA damage. Like BRCA1 dots, BARD1 and Rad51 foci appeared to persist into G2 (data not shown). In addition, as was noted above for BRCA1 foci in G2, the BARD1/Rad51 G2 foci were not perturbed by either UV or HU treatment (data not shown).

These findings strengthen the notion that BRCA1 relocalizes to replication forks after DNA damage, since it does so in the company of two known physiological partners. Hence, either multiprotein BRCA1-containing complexes leave the dots after DNA damage, or the underlying subnuclear structure which constitutes the substance of the S phase foci, itself, undergoes disassembly after DNA damage.

Discussion

These experiments identify the p220 BRCA1 protein as a participant in a DNA damage response of cycling cells, thereby fulfilling the prediction that BRCA1 participates

in the maintenance of genome integrity (Scully et al., 1997a). Within 1 hr of treatment of cells with various DNA damaging agents, two effects were noted in the behavior of the BRCA1 protein. First, S phase cells lost the characteristic BRCA1 nuclear foci. Second, the protein underwent a specific change(s) in phosphorylation. Third, BRCA1 was now associated with PCNA/replicating DNA-containing structures. The timing of these events was closely correlated, suggesting that they are different manifestations of the same cellular response. Taken together, these findings allow one to construct a functional model of BRCA1 behavior, at least during S phase.

First, the BRCA1 dots, which clearly contain BRCA1-containing complexes, given the colocalization of both Rad51 and BARD1, appear to be dynamic physiological structures. Their integrity is, at a minimum, tied to the integrity of the genome. DNA damage leads to signals, transmitted over a measurable period of time, which result in the loss of BRCA1 containing protein/protein complexes from these structures, if not the loss of the structures themselves. These signals do not depend upon the cessation of DNA synthesis for accurate transmission and are, hence, not a specific result of replication arrest. Whether the dots are active in the absence of genome damage, playing an as yet unknown role in the replication process (and/or in postreplication events) or whether they are simply repositories of proteins that are active in the damage (and possibly other stress) response(s) is not clear. That BRCA1 appears to disperse from the dots after genome damage strongly suggests that BRCA1 itself plays a role in the response to DNA damage. Such a conclusion strongly supports the earlier speculation put forward on the occasion of the first detection of BRCA1/Rad 51 complexes (Scully et al., 1997a). Thus, the BRCA1/Rad51/BARD1 nuclear dots are an example of multiprotein-containing nuclear structures whose integrity is modified by modifiers of genome integrity.

Second, in parallel with the loss of the BRCA1 dots, DNA damage led to a specific alteration in the state of BRCA1 phosphorylation. The timing of the two events was similar, and both events were reversible in HU-treated cells, implying that they are linked and that both are reflections of the existence of unrepaired DNA damage. These findings indicate that BRCA1 is a substrate of one or more kinases activated specifically by DNA damage. They, therefore, place BRCA1 on an S phase DNA damage-initiated signaling pathway. G1 cells were able to respond with specific BRCA1 phosphorylation events following DNA damage, but there were clear differences in the substance of the responses between G1 and S phase cells. Whether the protein contributes to the enaction of both G1 and S (and possibly G2) checkpoint responses remains to be seen.

One class of genes implicated in such signaling pathways encode the "PIK" kinases, Atm, Atr, and p460 DNA-PK, each of which shows extensive conservation between yeast, drosophila and human (Bentley et al., 1996; Cimprich et al., 1996; Hari et al., 1995; Hartley et al., 1995; Keith and Schreiber, 1995; Morrow et al., 1995; Savitsky et al., 1995). Genetic analysis has suggested a role for Atm in multiple cell cycle checkpoints (Painter and Young, 1980; reviewed in Elledge, 1996). The yeast homologs of Atr, rad3^{sp}, and MEC1^{sc}, have been clearly implicated in S phase and other DNA damage checkpoints (Bentley et al., 1996; Paulovich and Hartwell, 1995). DNA-PK functions in double-stranded break repair and VDJ recombination (reviewed in Lieber et al., 1997). In addition, the products of these genes are protein kinases and they interact with yet other protein kinases. This combined evidence suggests that the "PIK" kinases are signal transducers, e.g., linking DNA damage with cell cycle events (reviewed in Elledge, 1996). Our observations on BRCA1 suggest that its phosphorylation after DNA damage might be an assay for the activity of one or more "PIK" kinases. There are data in the literature consistent with a model in which BRCA1 and Atr and, possibly, Atm interact on meiotic chromosomes (Keegan et al., 1996; Scully et al., 1997a).

The availability of tissue from ataxia-telangiectasia patients has provided cultured primary cells lacking Atm function. For each modality of DNA damage examined—HU treatment, UV, or ionizing radiation—S phase BRCA1 mobility slowed within 1 hr of exposure. Thus, Atm is not absolutely required for S phase DNA damage-induced phosphorylation of BRCA1. Whether the same is true for G1 cells is unclear at present. Similarly, p460 DNA-PK deficient cells responded normally to this same spectrum of DNA damaging agents. This implies that DNA-PK is not an absolute requirement for the S phase effect as well. The components of the S phase DNA damage/BRCA1 signaling pathway, therefore, remain to be identified. Based upon what is known from analyses of Drosophila and yeast, Atr must be considered a potential participant in this pathway. At present, however, there are no cell lines known to be functionally null for Atr.

Finally, BRCA1 appears to relocalize to replicating DNA structures after DNA damage. The interpretation of these observations can only be speculated upon at present. HU and UV induced the same relocalization behavior in BRCA1 (also in Rad51 and BARD1), again suggesting that the responses provoked by these two agents have fundamental similarities. One interpretation of these phenomena is that, in each case, a DNA repair process is initiated at the replication fork. In the case of UV-induced damage, DNA replication may be accompanied by a recombinational DNA damage response (Fornace, 1983; Friedberg et al., 1995). In the case of HU treatment, the replication fork likely contains a high density of "abnormal," or nonduplex, DNA structures, which might provoke a DNA damage response. If such speculations hold true, one might deduce that BRCA1 has an affinity for sites of specialized DNA structure, a conclusion supported by its localization to the axial element of the developing synaptonemal complex (Kleckner, 1996; Scully et al., 1997a).

If BRCA1 is recruited to certain abnormal DNA structures as part of a DNA damage response, a role for BRCA1 in DNA repair seems likely. This might or might not be linked to an inferred role of BRCA1 in transcription regulation, as evidenced by its transactivation domain and by its stable association with the RNA polymerase II holoenzyme (Scully et al., 1997b). Two paradigms, which are not mutually exclusive, could be considered.

First, BRCA1 may play a DNA repair role, even in the context of the RNA polymerase II holoenzyme, perhaps analogous to some components of TFIIH (reviewed in Bhatia et al., 1996). Second, BRCA1 may be truly bifunctional (or multifunctional), serving as both a factor in the processing of abnormal DNA structures and as a participant in the signaling which results in the activation of certain genes which follow DNA damage. The p53 tumor suppressor protein likely operates in such a bifunctional manner (reviewed in Ko and Prives, 1996).

How do these observations reflect upon the function of the BRCA1 dots in undamaged cells? One might speculate that the BRCA1 S/G2 phase dots are sites specialized for the processing of replicating or replicated DNA. It is worth noting, at this point, that BRCA1 is active during both the mitotic and meiotic cell cycle and interacts with developing synaptonemal complexes (Scully et al., 1997a). Given the functional parallel between meiotic interhomolog and mitotic intersister interactions (Kleckner, 1996), one wonders whether function in the BRCA1 dots is connected with intersister interactions.

Similarly obscure at present is the relationship that might exist between the mechanisms governing the behavior of BRCA1 in a replication checkpoint pathway and the tissue specificity of its role in tumor suppression. The connection may become clearer from a better understanding of the biology of breast and ovarian epithelium.

Experimental Procedures

Tissue Culture Methods

Cells were cultured in Dulbecco's modified Eagle's medium (DMEM)–10% fetal bovine serum (FBS). MCF7 cells were synchronized as described previously (Scully et al., 1997a). For late G1 synchronization, mimosine (200 μM final concentration) was added to MCF7 cells for 16 hr. Release into S phase produced tight synchrony through this segment of the cycle, allowing preparation of early or late S phase cultures.

DNA Damaging Agents

Cells were exposed to genotoxic agents and, unless otherwise stated, harvested 1 hr later. HU (Sigma) treatment was added to a final concentration of 1 mM. Mitomycin C (Sigma) was added to a final concentration of 20 μg/ml. UV doses were delivered in a single pulse using a Stratalinker (Stratagene). Prior to pulsing, medium was removed, being replaced immediately after treatment. Gamma irradiation was delivered using a Gammacell 1000 apparatus.

Immunoblotting and Immunoprecipitation of BRCA1

Cell extracts were prepared in EBC buffer (50 mM Tris, pH 8, 120 mM NaCl, 0.5% Nonidet P-40 [NP-40]), with the addition of 50 mM NaF, 1 mM sodium orthovanadate, 100 μg/ml polymethylsulfonyl fluoride (PMSF), 20 μg/ml aprotinin, and 10 μg/ml leupeptin. One hundred micrograms of whole cell extract were loaded per lane. To detect changes in the mobility of p220 BRCA1, prolonged 5 or 6% SDS-polyacrylamide gel electrophoresis (SDS-PAGE) was used (e.g., 100 V for 16 hr). Transfer to nitrocellulose was performed using a semidry transfer method (Novablot, Pharmacia), in 50 mM Tris base, 40 mM glycine, 0.37 g/l SDS, 20% methanol (for 3 hr at 1.5 mA/cm2). After blocking with 5% nonfat dried milk in TBS-T (20 mM Tris, pH 8, 0.9% NaCl, 0.05% Tween 20) with sodium azide (0.1%), the primary antibody, MS110 (Scully et al., 1996; Oncogene Science), was used at 2 μg/ml in PBS/1% nonfat dried milk/0.1% azide, for 1 hr at room temperature. The secondary antibody was peroxidase-conjugated goat anti-mouse IgG (H+L, Jackson Immunoresearch), at 1:10,000 in 1% nonfat milk/TBS-T. Signals were developed by ECL (Amersham). IP of BRCA1 was performed as described previously (Scully et al., 1997a).

Phosphatase Treatment of Immunoprecipitates

BRCA1 IPs were washed in extraction buffer in the absence of phosphatase inhibitors. Parallel samples were resuspended in λ-phosphatase buffer (New England Biolabs) either in the presence or absence of the phosphatase inhibitors, NaF (50 mM final concentration) and sodium orthovanadate (2 mM final concentration). After heating samples to 30°C for 1 min, 500 U of λ-phosphatase (New England Biolabs) was added to each sample, followed by incubation at 30°C for 1 hr. Samples were separated by SDS-PAGE and immunoblotted for BRCA1. In the same experiments, in vitro translation of the BRCA1 cDNA was performed using a TNT kit (Promega).

Antibodies, Immunostaining, and Confocal Microscopy

Cells were fixed for 10 min in PBS-buffered 3% paraformaldehyde/2% sucrose solution, followed by 5 min permeablization on ice in Triton buffer (0.5% Triton X-100 in 20 mM HEPES, pH 7.4, 50 mM NaCl, 3 mM MgCl, 300 mM sucrose). Alternatively, to visualize replication forks using PCNA Ab, methanol acetone (70%:30% v/v) fixation for 15 min at −20°C was performed. The latter coverslips were air dried and rehydrated in PBS prior to immunostaining. Methanol/acetone fixation produced poor results with the Rad51 Ab. To visualize replication forks in this case, cells were permeablized in Triton buffer (above) prior to paraformaldehyde fixation, to elute away the soluble PCNA fraction (a modification of Li et al., 1996).

BRCA1 was visualized using mAbs- MS13, MS110, or AP16 (Scully et al., 1996). PCNA was visualized using AK antiserum at 1:5000, or with PCNA mAb PC10 (Santa Cruz) at 1:100. BARD1 was visualized using an affinity-purified rabbit polyclonal antiserum to residues 141–388 of the gene product. This was shown to colocalize with BARD1-specific mAbs, confirming the identity of the signal. Cross-reactivity between this antiserum and BRCA1 protein was sought but not detected. Rad51 Ab was generated by immunization of rabbits with GST-Rad51 fusion protein. After absorption of anti-GST Abs, affinity purification was performed by standard methods using an aminolink column (Pierce) coupled to GST-Rad51. All secondary antibodies used were species-specific fluorochrome-conjugated Abs from Jackson Immunoresearch, used at 1:200 throughout.

Two-color immunostaining for BrdU and PCNA was performed as follows. Methanol-acetone fixed cells were stained with PCNA antiserum "AK" (from R. Ochs), followed by secondary Ab. After post-fixing in paraformaldehyde/sucrose solution (above) for 10 min at room temperature, cells were incubated for 5 min in 2 N HCl to expose incorporated BrdU. After multiple phosphate-buffered saline (PBS) washes, fluorescein isothiocyanate (FITC)-conjugated anti-BrdU mAb (Becton Dickenson) was used to develop a BrdU incorporation signal.

All antibody incubations were performed at 37°C for 20 min. Under the conditions used, no significant signal attributable to secondary antibody, alone, was detected. All images were collected by confocal microscopy (Zeiss) and processed using Adobe Photoshop software.

Cell Cycle Analysis

Cells were pulsed with BrdU (Boehringer-Mannheim) for 10 min prior to harvesting. Aliquots of harvested plates were trypsinized, neutralized, washed in PBS, and fixed in cold 70% ethanol while vortexing. After storage on ice, cells were vortexed into 2 N HCl/0.5% Tween-20. After 30 min of incubation, cells were washed twice in PBS/HEPES, pH 7.4, to restore physiological pH, and incubated with 50 μl of PBS/1% BSA/0.5% Tween-20 and 20 μl of FITC-conjugated anti-BrdU mAb (Becton-Dickenson), for 30 min at room temperature. After further washes, cells were incubated in 70 μM propidium diiodide dissolved in 38 mM sodium citrate, in the presence of DNAase-free RNAase (2.5 μg/ml final concentration, Boehringer-Mannheim) for 30 min at 37°C. Samples were analyzed immediately thereafter by FACS (Becton-Dickenson).

Acknowledgments

We are indebted to numerous colleagues whose generosity in sharing reagents and thoughts made this work possible. In particular, we

thank Dr. Richard Baer for generously making available antibodies to BARD1 and for informing us of his results revealing colocalization of BARD1 and BRCA1 in dots; Drs. David Weaver and Kurt Auger for gifts of cell lines; Dr. David Hill for antibody to DNA-PK; and Drs. Myles Brown, James DeCaprio, Mark Ewen, William Kaelin, and Richard Kolodner for critical and stimulating discussions.

Received June 11, 1997; revised July 1, 1997.

References

Allen, J.B., Zhou, Z., Siede, W., Friedberg, E.C., and Elledge, S.J. (1994). The SAD1/RAD53 protein kinase controls multiple checkpoints and DNA damage-induced transcription in yeast. Genes Dev. *8*, 2401–2415.

Ashley, T., Plug, A.W., Xu, J., Solari, A.J., Reddy, G., et al. (1995). Dynamic changes in Rad51 distribution on chromatin during meiosis in male and female vertebrates. Chromosoma *104*, 19–28.

Baumann, P., Benson, F.E., and West, S.C. (1996). Human Rad51 protein promotes ATP-dependent homologous pairing and strand transfer reactions in vitro. Cell *87*, 757–766.

Bentley, N.J., Holtzman, D.A., Keegan, K.S., Flaggs, G., DeMaggio, A.J., et al. (1996). The Schizosaccharomyces pombe rad3 checkpoint gene. EMBO J. *15*, 6641–6651.

Bhatia, P.K., Wang, Z., and Friedberg, E.C. (1996). DNA repair and transcription. Curr. Opin. Genet. Dev. *6*, 146–150.

Bishop, D.K. (1994). RecA homologues Dmc1 and Rad51 interact to form multiple nuclear complexes prior to meiotic chromosome synapsis. Cell *79*, 1081–1092.

Bork, P., Hofmann, K., Bucher, P., Neuwald, A.F., Altschul, S.F., and Koonin, E.V. (1997). A superfamily of conserved domains in DNA damage-responsive cell cycle checkpoint proteins. FASEB J. *11*, 68–76.

Bravo, R. (1986). Synthesis of the nuclear protein cyclin (PCNA) and its relationship with DNA replication. Exp. Cell. Res. *163*, 287–293.

Bravo, R., and Macdonald-Bravo, H. (1987). Existence of two populations of cyclin/proliferating cell nuclear antigen during the cell cycle: association with DNA replication sites. J. Cell. Biol. *105*, 1549–1554.

Callebaut, I., and Mornon, J.P. (1997). From BRCA1 to RAP1: a widespread BRCT module closely associated with DNA repair. FEBS Lett. *400*, 25–30.

Carr, A.M. (1995). DNA structure checkpoints in fission yeast. Semin. Cell Biol. *6*, 65–72.

Chapman, M.S., and Verma, I.M. (1996). Transcriptional activation by BRCA1. Nature *382*, 678–679.

Chen, Y.M., Farmer, A.A., Chen, C.F., Jones, D.C., Chen, P.L., and Lee, W.H. (1996). BRCA1 is a 220-kDa nuclear phosphoprotein that is expressed and phosphorylated in a cell cycle-dependent manner. Cancer Res. *56*, 3168–3172.

Cimprich, K.A., Shin, T.B., Keith, C.T., and Schreiber, S.L. (1996). cDNA cloning and gene mapping of a candidate human cell cycle checkpoint protein. Proc. Natl. Acad. Sci. USA *7*, 2850–2855.

Elledge, S.J. (1996). Cell cycle checkpoints: preventing an identity crisis. Science *274*, 1664–1672.

Feunteun, J., and Lenoir, G.M. (1996). BRCA1, a gene involved in inherited predisposition to breast and ovarian cancer. Biochim. Biophys. Acta *1242*, 177–180.

Fornace, A.J., Jr. (1983). Recombiation of parent and daughter strand DNA after UV-irradiation in mammalian cells. Nature *304*, 552–554.

Friedberg, E.C., Walker, G.C., and Siede, W. (1995). DNA Repair and Mutagenesis. (Washington: ASM Press).

Futreal, P.A., Liu, Q., Shattuck-Eidens, D., Cochran, C., Harshmann, K., et al. (1994). BRCA1 mutations in primary breast and ovarian carcinomas. Science *266*, 120–122.

Gowen, L.C., Johnson, B.L., Latour, A.M., Sulik, K.K., and Koller, B.H. (1996). BRCA1 deficiency results in early embryonic lethality characterized by neuroepithelial abnormalities. Nature Genet. *12*, 191–194.

Hakem, R., de la Pomba, J.L., Sirard, C., Mo, R., Woo, M., et al. (1996). The tumor suppressor gene *Brca1* is required for embryonic cellular proliferation in the mouse. Cell *85*, 1009–1023.

Hall, J.M., Lee, M.K., and Newmann, B. (1990). Linkage of early-onset breast cancer to chromosome 17q21. Science *250*, 1684–1689.

Hari, K.L., Santerre, A., Sekelsky, J.J., McKim, K.S., Boyd, J.B., and Hawley, R.S. (1995). The mei-41 gene of D. melanogaster is a structural and functional homolog of the human ataxia telangiectasia gene. Cell *82*, 815–821.

Hartley, K.O., Gell, D., Smith, G.C., Zhang, H., Divecha, N., et al. (1995). DNA-dependent protein kinase catalytic subunit: a relative of phosphatidylinositol 3-kinase and the ataxia telangiectasia gene product. Cell *82*, 849–856.

Humphrey, J.S., Salim, A., Erdos, M.R., Collins, F.S., Brody, L.C., and Klausner, R.D. (1997). Human *BRCA1* inhibits growth in yeast: potential use in diagnostic testing. Proc. Natl. Acad. Sci. USA *94*, 5820–5825.

Keegan, K.S., Holtzman, D.A., Plug, A.W., Christenson, E.R., Brainerd, E.E., et al. (1996). The Atr and Atm protein kinases associate with different sites along meiotically pairing chromosomes. Genes Dev. *10*, 2423–2437.

Keith, C.T., and Schreiber, S.L. (1995). PIK-related kinases: DNA repair, recombination, and cell cycle checkpoints. Science *270*, 50–51.

Kleckner, N. (1996). Meiosis: How could it work? Proc. Natl. Acad. Sci. USA *93*, 8167–8174.

Ko, L.J., and Prives, C. (1996). p53: puzzle and paradigm. Genes Dev. *10*, 1054–1072.

Koonin, V.F., Altschul, S.F., and Bork, P. (1996). BRCA1 protein products: functional motifs. Nature Genet. *13*, 266–267.

Lane, T.F., Deng, C., Elson, A., Lyu, M.S., Kozak, C.A., and Leder, P. (1995). Expression of BRCA1 is associated with terminal differentiation of ectodermally and mesodermally derived tissues in mice. Genes Dev. *9*, 2712–2722.

Lees-Miller, S.P., Godbout, R., Chan, D.W., Weinfeld, M., Day, R.S.I., et al. (1995). Absense of p350 subunit of DNA-activated protein kinase from a radiosensitive human cell line. Science *267*, 1183–1185.

Li, R., Hannon, G.J., Beach, D., and Stillman, B. (1996). Subcellular distribution of p21 and PCNA in normal and repair-deficient cells following DNA damage. Curr. Biol. *6*, 189–199.

Lieber, M.R., Grawunder, U., Wu, X., and Yaneva, M. (1997). Tying loose ends: roles of Ku and DNA-dependent protein kinase in the repair of double-strand breaks. Curr. Opin. Genet. Dev. *7*, 99–104.

Liu, C.Y., Flesken-Nikitin, A., Li, S., Zeng, Y., and Lee, W.-H. (1996). Inactivation of the mouse Brca1 gene leads to failure in the morphogenesis of the egg cylinder in early postimplantation development. Genes Dev. *10*, 1835–1843.

Marquis, S.T., Rajan, J.V., Wynshaw-Boris, A., Xu, J., and Yin, G.-Y. (1995). The developmental pattern of BRCA1 expression implies a role in differentiation of the breast and other tissues. Nature Genet. *11*, 17–26.

Miki, Y., Swensen, J., Shattuck-Eidens, D., Futreal, P.A., Harshman, K., et al. (1994). A strong candidate for the breast and ovarian cancer susceptibility gene BRCA1. Science *266*, 66–71.

Monteiro, A.N.A., August, A., and Hanafusa, H. (1996). Evidence for a transcriptional activation function of BRCA1 C-terminal region. Proc. Natl. Acad. Sci. USA *93*, 13595–13599.

Morrow, D.M., Tagle, D.A., Shiloh, Y., Collins, F.S., and Hieter, P. (1995). TEL1, an S. cerevisiae homolog of the human gene mutated in ataxia telangiectasia, is functionally related to the yeast checkpoint gene MEC1. Cell *82*, 831–840.

Nakamura, H., Morita, T., and Sato, C. (1986). Structural organizations of replicon domains during DNA synthetic phase in the mammalian nucleus. Exp. Cell Res. *165*, 291–297.

Neuhausen, S.L., and Marshall, C.J. (1994). Loss of heterozygosity in familial tumors from three BRCA1-linked kindreds. Cancer Res. *54*, 6069–6072.

Painter, R.B., and Young, B.R. (1980). Radiosensitivity in ataxia telangiectasia: a new explanation. Proc. Natl. Acad. Sci. USA *77*, 7315–7317.

Paulovich, A.G., and Hartwell, L.H. (1995). A checkpoint regulates the rate of progression through S phase in S. cerevisiae in response to DNA damage. Cell *82*, 841–847.

Ruffner, H., and Verma, I. (1997). BRCA1 is a cell cycle-regulated nuclear phosphoprotein. Proc. Natl. Acad. Sci. USA *94*, 7138–7143.

Sanchez, Y., Desany, B.A., Jones, W.J., Liu, Q., Wang, B., and Elledge, S.J. (1996). Regulation of RAD53 by the ATM-like kinases MEC1 and TEL1 in yeast cell cycle checkpoint pathways. Science *271*, 357–360.

Savitsky, K., Bar-Shira, A., Gilad, S., Rotman, G., Ziv, Y., et al. (1995). A single ataxia telangiectasia gene with a product similar to PI-3 kinase. Science *268*, 1749–1753.

Scully, R., Ganesan, S., Brown, M., De Caprio, J.A., Cannistra, S.A., et al. (1996). Location of BRCA1 in human breast and ovarian cell lines. Science *272*, 123–125.

Scully, R., Chen, J., Plug, A., Xiao, Y., Weaver, D., et al. (1997a). Association of BRCA1 with Rad51 in mitotic and meiotic cells. Cell *88*, 265–275.

Scully, R., Anderson, S.F., Chao, D.M., Wei, W., Ye, L., et al. (1997b). BRCA1 is a component of the RNA polymerase II holoenzyme. Proc. Natl. Acad. Sci. USA *94*, 5605–5610.

Sharan, S.K., Morimatsu, M., Albrecht, U., Lim, D.-S., Regel, E., et al. (1997). Embryonic lethality and radiation hypersensitivity mediated by Rad51 in mice lacking BRCA2. Nature *386*, 804–810.

Shinohara, A., Ogawa, H., and Ogawa, T. (1992). Rad51 protein involved in repair and recombination in Saccharomyces cerevisiae is a RecA-like protein. Cell *69*, 457–470.

Smith, S.A., Easton, D.F., Evans, D.G.R., and Ponder, B.A.J. (1992). Allele losses in the region 17q12-q21 in familial breast and ovarian cancer non-randomly involve the wild-type chromosome. Nature Genet. *2*, 128–131.

Sun, Z., Fay, D.S., Marini, F., Foiani, M., and Stern, D.F. (1996). Spk1/Rad53 is regulated by Mec1-dependent protein phosphorylation in DNA replication and damage checkpoint pathways. Genes Dev. *10*, 395–406.

Terasawa, M., Shinohara, A., Hotta, Y., Ogawa, H., and Ogawa, T. (1995). Localization of RecA-like recombination proteins on chromosomes of lily at various meiotic stages. Genes Dev. *9*, 925–934.

Wu, L.C., Wang, Z.W., Tsan, J.T., Spillman, M.A., Phung, A., et al. (1996). Identification of a RING protein that can interact in vivo with the BRCA1 gene product. Nature Genet. *14*, 430–440.

Cell, Vol. 105, 149–160, April 6, 2001, Copyright ©2001 by Cell Press

BACH1, a Novel Helicase-like Protein, Interacts Directly with BRCA1 and Contributes to Its DNA Repair Function

Sharon B. Cantor,* Daphne W. Bell,† Shridar Ganesan,* Elizabeth M. Kass,* Ronny Drapkin,* Steven Grossman,* Doke C.R. Wahrer,† Dennis C. Sgroi,‡ William S. Lane,§ Daniel A. Haber,† and David M. Livingston*‖

*The Dana-Farber Cancer Institute and the Harvard Medical School
Boston, Massachusetts 02115
†Center for Cancer Risk Analysis and
‡Molecular Pathology Unit
Massachusetts General Hospital
Charlestown, Massachusetts 02129
§Microchemistry and Proteomics Analysis Facility
Harvard University
Cambridge, Massachusetts 02138

Summary

BRCA1 interacts in vivo with a novel protein, BACH1, a member of the DEAH helicase family. BACH1 binds directly to the BRCT repeats of BRCA1. A BACH1 derivative, bearing a mutation in a residue that was essential for catalytic function in other helicases, interfered with normal double-strand break repair in a manner that was dependent on its BRCA1 binding function. Thus, BACH1/BRCA1 complex formation contributes to a key BRCA1 activity. In addition, germline *BACH1* mutations affecting the helicase domain were detected in two early-onset breast cancer patients and not in 200 matched controls. Thus, it is conceivable that, like *BRCA1*, *BACH1* is a target of germline cancer-inducing mutations.

Introduction

Germline mutations in *BRCA1* lead to an increased lifetime risk of breast and/or ovarian cancer. The gene encodes an 1863 residue nuclear protein with an N-terminal RING and C-terminal BRCT domains. BRCA1 contains little homology to known proteins. Evidence points to a role for this gene in the maintenance of genome integrity and in certain transcription regulation events (Deng and Brodie, 2000).

The C-terminal region of BRCA1 contains two BRCT (*BR*CA1 *C-T*erminal) motifs. These structures have been identified in many proteins engaged in genome integrity control (Koonin et al., 1996; Bork et al., 1997; Callebaut and Mornon, 1997) and, where studied, appear to participate in specific interactions with selected target proteins. For example, XRCC1 heterodimerizes with DNA ligase III in a base excision repair complex, and the BRCT motifs of both proteins are engaged in this interaction (Taylor et al., 1998).

For BRCA1, these motifs play a critical role in its ability to mediate double-strand break repair and homologous recombination (Moynahan et al., 1999; Scully et al., 1999; Zhong et al., 1999; Wu et al., 2000). They also possess a transcription activation function (Chapman and Verma, 1996; Monteiro et al., 1996), which is abrogated by clinically relevant mutations. In keeping with the latter observations, the BRCT-containing region can interact with the RNA polymerase holoenzyme (Scully et al., 1997a) and with CtIP, a partner of the transcriptional corepressor, CtBP (Yu et al., 1998). However, the physiological significance of these two interactions is unknown.

In this regard, disease-associated mutations exist throughout BRCA1, but the majority of them result in a truncated product with loss of the extreme C terminus and one or both BRCT motifs (Breast Cancer Information Core (BIC)). Clinically relevant missense mutations exist within each BRCT motif, implying a link between their function and the execution of BRCA1-mediated tumor suppression. These findings notwithstanding, there is little biochemical understanding of how BRCA1 functions as a tumor suppressor. Nonetheless, the evidence suggests that the genome integrity maintenance and the tumor suppression functions are linked (Welcsh et al., 2000).

In an effort to understand how the BRCT sequences function, we have screened for proteins that contact them directly. The search has led to the identification of BACH1, a novel member of the DEAH helicase family. From the results of a cell biological analysis and a clinical epidemiology study, it appears that BACH1 is a physiological partner of BRCA1, participating in the performance of both its DNA repair and its tumor suppressor functions.

Results

Screen for BRCT Binding Proteins

A GST fusion protein containing residues 1529–1863, which spans both BRCT motifs and extends to the BRCA1 C terminus (GST-BRCT; Figure 1A), was generated. The modified GST moiety was labeled by in vitro phosphorylation with protein kinase A and used in far Western blotting experiments (Blanar and Rutter, 1992; Kaelin et al., 1992) where it detected four bands ranging from 50 to 220 kDa (whole-cell extract (WCE), Figure 1B). Among them was a protein of ~130 kDa, which was also detected in 293T and U20S cell lysates (data not shown). This protein was also present in immunoprecipitates (IPs) generated with multiple BRCA1 monoclonal antibodies (mAbs) (for an example, see Figure 1B, lane 3).

Binding of the 130 kDa band to the GST-BRCT probe was compromised when clinically relevant point mutant derivatives were used as the probe. One mutation [P1749R] led to greatly reduced binding and another [M1775R] (see Figure 1A) completely abolished binding of the 130 kDa protein (Figure 1C). Unlike their wild-type (wt) counterpart, the GST-BRCT mutant proteins also failed to interact with this polypeptide in solution (data not shown).

‖To whom correspondence should be addressed (e-mail: david_livingston@dfci.harvard.edu).

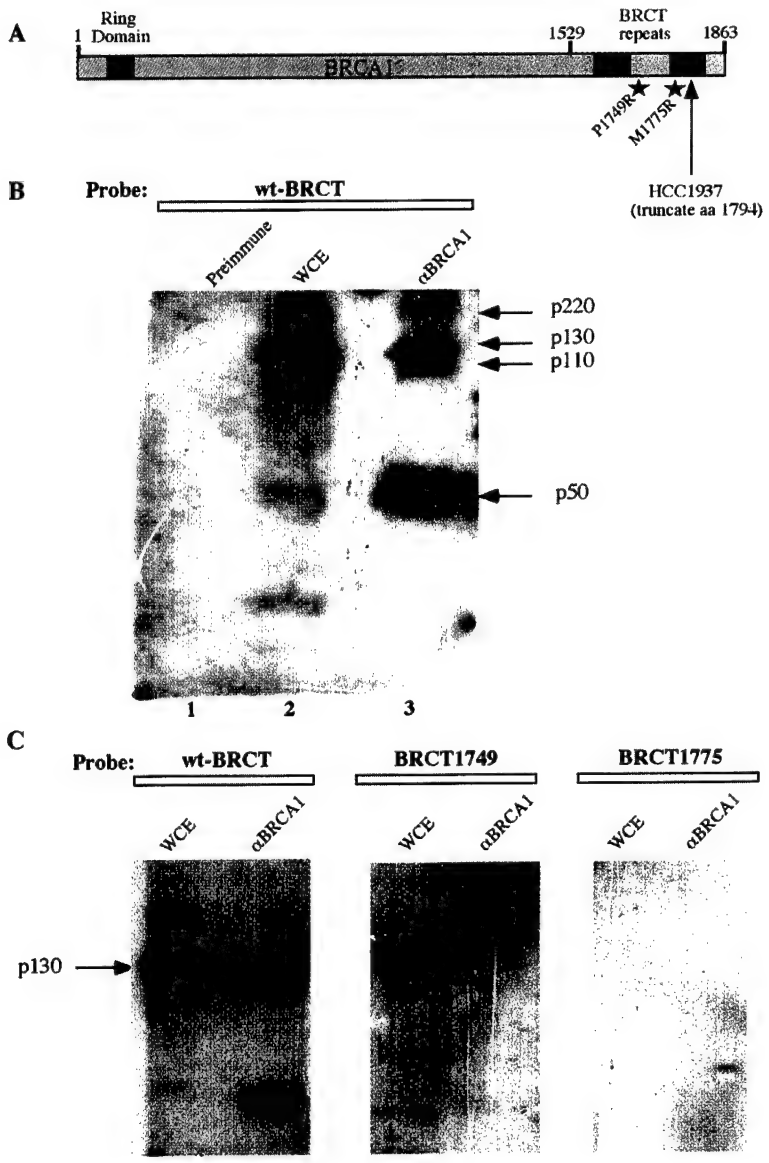

Figure 1. The BRCT Repeats of BRCA1 Interact with a Discrete Set of Polypeptides by Far Western Analysis

(A) Map of BRCA1 showing the BRCT motif-containing region (aa 1529–1863); this region also served as a probe in far Western analysis. Two different point mutations and the location of the BRCA1 truncation present in the HCC1937 cell line are noted with stars and an arrow, respectively.

(B and C) Far Western assays of Hela whole-cell lysates (WCE) and of immunoprecipitates (BRCA1 preimmune rabbit and rabbit immune, c23 polyclonal Ab). (B) A 130 kDa band is present in a HeLa cell lysate and in an anti-BRCA1 immunoprecipitate when wt BRCT probe was used. (C) BRCT probes containing the mutations, P1749R or M1775R, failed to recognize the 130 kDa band.

Purification of the 130 kDa BRCA1 Binding Protein

To purify the 130 kDa protein, a GST-BRCT fusion protein bound to glutathione sepharose beads (GSSH) was incubated with HeLa cell nuclear extract. After extensive washing, proteins bound to the beads were eluted by boiling in SDS-containing buffer, electrophoresed on a polyacrylamide SDS gel, and stained with Coomassie blue (data not shown). When sufficient quantities of nuclear extract were immunoprecipitated, the 130 kDa band was readily detected by this approach. By contrast, it was not detected when either of the above noted BRCT mutant derivatives ([P1749R] or [M1775R]) was substituted for the wt BRCT fusion protein.

The 130 kDa band was excised from the gel and subjected to tryptic digestion within the gel material. The digest was eluted and subjected to microcapillary reverse phase HPLC and nanoelectrospray tandem mass spectrometry (MS/MS). The ensuing MS/MS spectra revealed that the 130 kDa protein sequence contains peptide sequences (see Experimental Procedures) encoded by three different EST sequences present on chromosome 17 (GenBank accession numbers AA397978, R16443, AI218496). Based on this information, a full-length cDNA was generated, as described in Experimental Procedures. The open reading frame of this clone predicts the synthesis of a 1249 residue polypeptide (Figure 2B). When this cDNA was transcribed and translated in vitro, its product comigrated with the endogenous 130 kDa protein and interacted with the wt GST-BRCT fusion protein, as described above (for an example, see Figure 4).

The N-terminal 888 residues of the protein reveal strong homology to the catalytic and nucleotide binding domains of known members of the DEAH helicase family. Among others, this group includes the xeroderma pigmentosum complementing group D (XPD) protein (Weber et al., 1990; Vermeulen et al., 1997; Coin and Egly, 1998) and human CHL1 (Amann et al., 1997; Figure 2C). The 130 kDa protein sequence contains the seven helicase-specific motifs that are conserved among members of the DEAH family. This helicase domain is 48% homologous to the human CHL1 protein. Like the other members of this family, the helicase domain in-

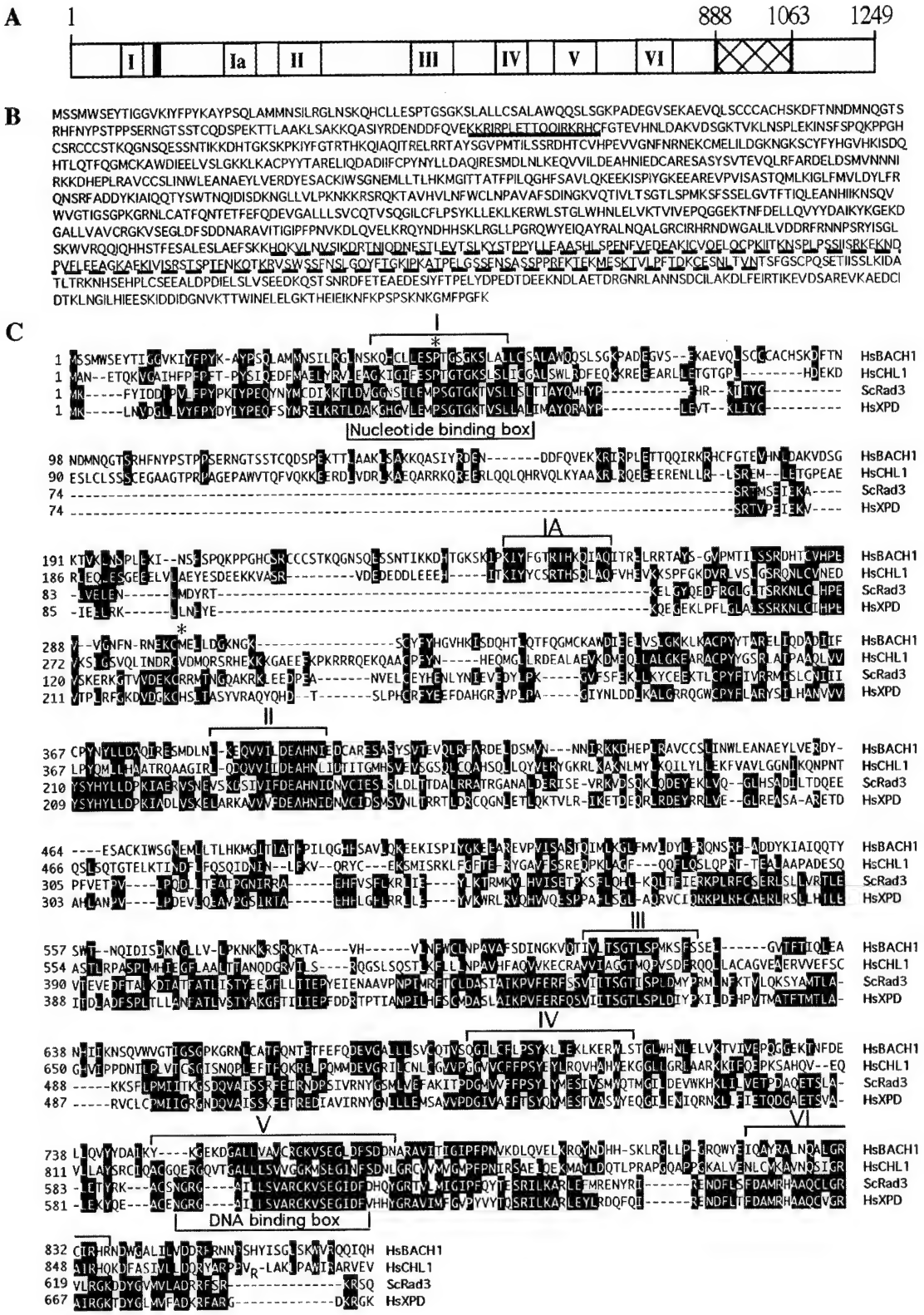

Figure 2. The BACH1 Sequence Is Significantly Homologous to that of DEAH Helicases

(A) DEAH helicase homology blocks are shown in roman numerals. The putative nuclear localization sequence (black rectangle) is shown. The helicase homology region of BACH1 spans residues 1–888. The BRCA1 binding domain spans residues 888–1063 (hatched box).

(B) The BACH1 amino acid sequence with its helicase homology region (1–888) (blue shaded region). The underlined, hatched area constitutes the BRCA1 binding domain, and the solid underlined region is predicted to contain a nuclear localization sequence.

(C) Homology alignment of the helicase domains of *Homo sapiens* BACH1 (HsBACH1), CHL1 (HsCHL1), and XPD (HsXPD), and *S. cerevisiae* Rad3 (ScRad3). Identical or similar amino acid residues are shaded. In addition, the seven conserved domains of known helicases are denoted above the sequence, and the nucleotide and DNA binding domains are shown below the alignment. BACH1 contains a canonical DEAH sequence in helicase box II. The (*) denotes the residues mutated in the cancer patients described in the text.

cludes a nuclear localization signal (Figure 2A). However, unlike other DEAH family members, the 130 kDa protein sequence contains a C-terminal extension of unknown function (Figure 2A). This particular sequence reveals 39% homology with synaptonemal complex protein 1, a major component of the transverse filaments of developing meiotic chromosomes (Schmekel et al., 1996).

Given the identical sequence properties of the gel-excised 130 kDa protein and the cloned polypeptide, their comigration in SDS gels, their ability to interact specifically with the BRCT-containing region of BRCA1, and the presence of a DEAH helicase domain, the 130 kDa protein was named BACH1 (for Brca1-Associated C-terminal Helicase). The *BACH1* gene was localized to chromosome 17q22 between markers D17S791 and D17S794, as defined by a Genemap 99 NCBI database search.

From a multiple-tissue cDNA panel (Clonetech), BACH1 is ubiquitously expressed, with highest RNA levels in testis (data not shown). This expression pattern is similar to that reported for BRCA1, which is present at some level in all tissues but highest in testis (Miki et al., 1994; Zabludoff et al., 1996).

BACH1 Is a Nuclear Protein that Interacts with BRCA1 In Vivo

Monoclonal antibodies to BACH1 were raised against recombinant GST-BACH1 (residues 647–1043) and against a BACH1 C-terminal peptide (NFKPSPSKNKGM FPGFK). Western blots of extracts from three different human cell lines probed with these antibodies revealed the presence of intact BACH1 in all extracts (data not shown). Furthermore, anti-BRCA1 or anti-BACH1 IPs of extracts from asynchronously growing MCF7 cells, independently performed with two BRCA1 and two BACH1 mAbs, coprecipitated BRCA1 and BACH1 (Figure 3A). These data strongly suggest that BRCA1 and BACH1 interact in vivo. The BRCA1 RING domain-associated protein, BARD1, was also present in the IPs generated with BACH1 mAbs and vice versa (Figure 3A), suggesting that BACH1 exists in complex with both BRCA1 and BARD1.

Immunofluorescence analysis using BACH1 mAbs revealed the presence of punctate nuclear staining in multiple human cell lines. Focal BACH1 staining was detected in numerous, albeit not all, cells present in asynchronous cultures. BRCA1 nuclear dots, as noted previously, were detected in S and G2 phase cells (Scully et al., 1997c). In the majority of cells containing both types of nuclear foci, many of these structures colocalized with one another (Figure 3B). In synchronized cell populations, nearly complete colocalization of BACH1 and BRCA1 was detected in late S-G2 cells. Exposure to gamma irradiation or hydroxyurea did not affect the co-IP of BACH1 and BRCA1, and, like BRCA1, BACH1 underwent dynamic relocation to PCNA-containing structures after hydroxyurea exposure (data not shown) (Scully et al., 1997b).

In a line of BRCA1 −/− cells (HCC1937) that synthesize a mutant BRCA1 species with a truncated C-terminal region affecting the integrity of the second BRCT motif (Tomlinson et al., 1998) (see Figure 1A), this BRCA1 species and BACH1 failed to coimmunoprecipitate (Figure 3A). The abundance of BACH1 in these cells was reduced by comparison with that detected in MCF7 or 293T cells (data not shown). Correspondingly, although punctate BACH1 nuclear staining was detectable (Figure 3B, compare the lowermost middle panel with panel 2/lane 2), the intensity of the BACH1 nuclear dot pattern was lower in HCC1937 cells than in other cell lines containing intact BRCA1 (like MCF7) (Figure 3B). In keeping with these observations, when we used higher concentrations of BACH1 mAb in HCC1937, BACH1 foci were also readily detectable (data not shown).

When HCC1937 cells were reconstituted with full-length BRCA1 by recombinant retroviral infection (Scully et al., 1999), BRCA1/BACH1 complexes and costaining nuclear dots were again readily detected (Figures 3A and 3B), even though the intracellular abundance of BACH1 was unchanged (data not shown).

These findings complement the far Western blotting results showing that two intact BRCT repeat units of BRCA1 are essential for a stable BRCA1/BACH1 interaction. They further imply that the intensity of the BACH1 nuclear dot pattern is dependent, at least in part, upon the ability of BACH1 to interact with BRCA1. Taken together, the data indicate that BACH1/BRCA1 complex formation is accompanied by an enhancement of the BACH1 immunostaining signal and the appearance of a prominent BACH1 nuclear dot pattern. Moreover, BARD1, absent from anti-BACH1 IPs of HCC1937 lysates, reappeared in BACH1 IPs of BRCA1-reconstituted HCC1937 cells (Figure 3A). The coimmunoprecipitation data and immunostaining results suggest that BRCA1 and BACH1 interact in vivo. They also suggest that the BARD1/BACH1 interaction is indirect, relying upon the independent association of each protein with BRCA1.

BRCA1 Binds to a Segment of the BACH1 Carboxy-Terminal Region

To search for a region of BACH1 necessary for binding BRCA1, a series of deletion mutants of BACH1 were generated and S^{35}-labeled products were synthesized by in vitro translation. These polypeptides were each incubated with the wt GST-BRCT (1529–1863) fusion protein bound to GSSH beads, and binding of the relevant BACH1 species was examined after SDS gel electrophoresis and autoradiography (Figure 4). The data reveal that a discrete region of BACH1, C-terminal to the helicase domain and spanning residues 888–1063, is sufficient for BRCA1 binding (Figure 4).

Dominant Negative BACH1 Disrupts Double-Strand Break Repair

Having established that BACH1 associates with BRCA1 in vivo, we asked whether the interaction between BACH1 and the BRCT-containing region of BRCA1 contributes to BRCA1 function. BRCA1 plays a major role in the repair of double-strand DNA breaks (Moynahan et al., 1999; Scully et al., 1999; Snouwaert et al., 1999). Since BACH1 interacts with BRCA1 and belongs to the DEAH helicase family, some members of which have a role in DNA repair (Wood, 1999; Cleaver, 2000), we asked whether BACH1 plays a role in double-strand break repair (DSBR). Specifically, we asked whether overexpression of a BACH1 mutant leads to a defect in DSBR. A

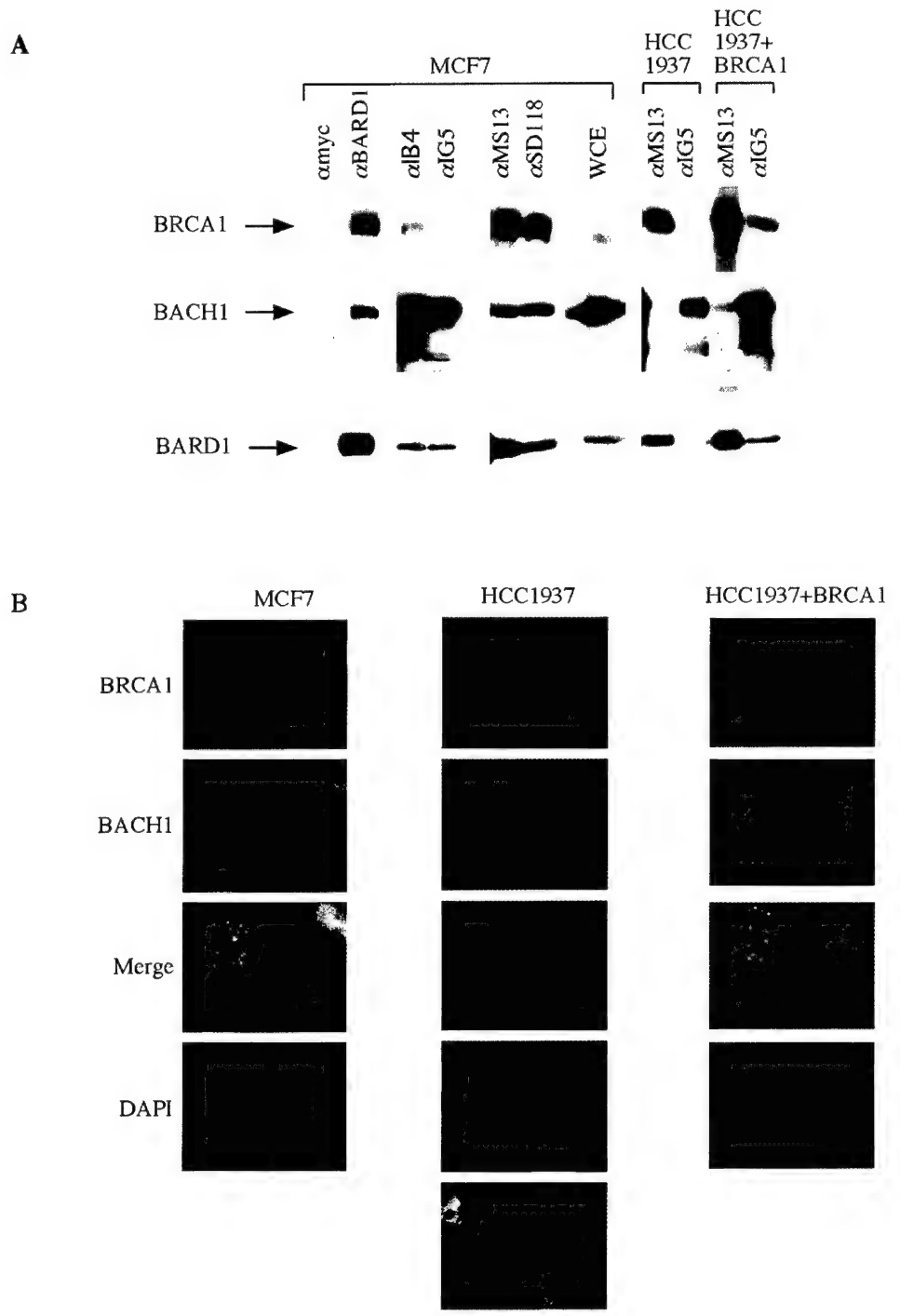

Figure 3. The BACH1/BRCA1 Interaction Depends on an Intact BRCA1 C-Terminal Region

(A) Immunoprecipitation/Western blot analyses of lysates of MCF7, HCC1937, and HCC1937 reconstituted with wt BRCA1. Immunoprecipitates, generated with the Abs denoted at the tops of the figures, were electrophoresed and blotted as described in Experimental Procedures. The blots were probed with αBRCA1 (MS110; upper third segment), αBACH1 (2G7; middle third segment), or αBARD1 (c20; bottom third segment). BACH1 was immunoprecipitated with either IB4 or IG5. BRCA1 was immunoprecipitated with either MS13 or SD118 . In the first experiment (left panel), BARD1 immunoprecipitation was generated with c20 (αBARD1), and control precipitation was achieved with anti-myc monoclonal antibody. The data presented in the other panels are from a second experiment.

(B) BACH1 and BRCA1 colocalize in nuclear dots in MCF7 cells, and colocalization in HCC1937 cells requires reconstitution with wt BRCA1. Asynchronous MCF7 or HCC1937−/− BRCA1 cells were dually stained for BRCA1 (using affinity-purified, rabbit polyclonal antiserum to BRCA1, red) and BACH1 (using monoclonal antibody to BACH1, green), as described in Experimental Procedures. Significant colocalization of BRCA1 and BACH1 nuclear dots in a subpopulation of cells is reflected by the presence of yellow nuclear dots in the merged images. BACH1 immunostaining was readily detected in the same HCC1937 cells (lowest middle panel) that were originally analyzed in lane 2/panel 2 when the intensity of exposure of the latter image was increased. BACH1 nuclear dots were also readily detected when the BACH1 antibody concentration was increased 100-fold above that used in the other panels (data not shown).

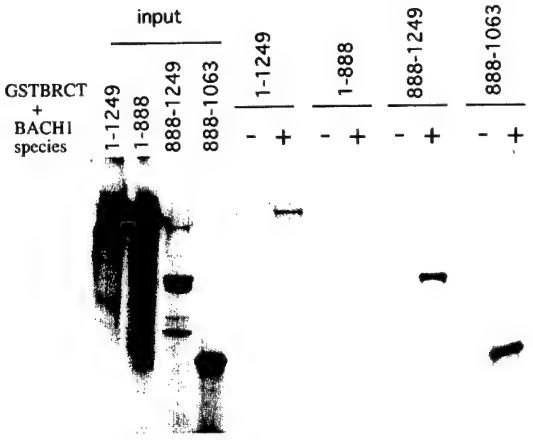

Figure 4. A Segment of the BACH1 C-Terminal Region Interacts with the BRCA1 BRCT Motifs

Various ^{35}S-labeled, in vitro translated BACH1 polypeptides were tested for binding to GST (−) or GST-BRCT:1529–1863 (+) fusion protein. Input lanes display 50% of the input of each in vitro translated BACH1 protein.

missense mutation that converts a lysine to an arginine was introduced at residue 52 (K52R). This residue is conserved in numerous ATPases and helicases, and has been shown to render the relevant protein incapable of hydrolyzing ATP (Sung et al., 1988; Ma et al., 1994). A double mutant, bearing both the K52R substitution and a second mutation (ΔC = dl 888–1249) that eliminates the BRCA1 binding domain of BACH1 (K52RΔC), was also generated.

To assess DSBR in cells overproducing wt or mutant BACH1, U2OS cells were transiently cotransfected with a GFP-encoding vector and an expression vector encoding wt, K52R, or K52R/ΔC BACH1. Transfected cultures were FACS sorted and the green fluorescing cells analyzed for expression of the relevant BACH1 species. Standardized Western blot analysis demonstrated comparable expression of the various proteins (Figure 5C). The sorted cells were either mock treated or gamma irradiated, and the abundance of double-strand breaks (DSB) in each culture was analyzed. Previous experience has shown that in multiple cell lines that synthesize wt BRCA1, there is nearly complete resolution of DSB by six hours after irradiation (Scully et al., 1999 and data not shown). Therefore, we analyzed DSB repair kinetics at 0, 3, and 6 hr following exposure to irradiation by pulsed field gel electrophoresis (Badie et al., 1995; Scully et al., 1999). As shown in Figure 5A, after exposure to 15 Gy, U2OS cells overproducing the K52R mutant of BACH1 displayed a marked delay in repair, as shown by an increase in the level of unrepaired breaks detectable at 3 and 6 hr. Importantly, cells synthesizing the double mutant, K52R/ΔC, which should neither hydrolyze ATP nor bind BRCA1, revealed normal DSB repair capacity at all time points (Figure 5A). With these kinetics in mind, we also performed a statistical analysis of these effects, employing multiple experiments in which U20S DSBR was tested after transfecting the vector, alone, or vector encoding wt BACH1, K52R, or K52R/ΔC BACH1. Statistically significant perturbation of repair was detected following expression of the K52R mutant. By contrast, it was not observed in the presence of equivalent levels of either the wt or the double mutant protein. These results indicate that K52R perturbs DSBR in a dominant negative fashion. They further show that this interfering effect is, in part, dependent on the ability of BACH1 to bind BRCA1. Therefore, BACH1, like BRCA1, appears to be important for DSBR, and the BACH1/BRCA1 interaction contributes to the execution of this BRCA1-dependent function.

Analysis of BACH1 Sequence Variants in Sporadic and Familial Breast Cancer

Human genome analysis localized the *BACH1* gene to chromosome 17q22. This region is frequently targeted by allelic losses in sporadic breast cancer, and failure to detect *BRCA1* mutations in these cases has suggested the presence of an additional tumor suppressor gene in this segment (Callahan, 1998). Given the evidence linking BACH1 to proper BRCA1-mediated DSBR and prior evidence suggesting a relationship between BRCA1-mediated DSBR and its tumor suppression function (Scully et al., 1999), we initiated a search for mutations in 21 cell lines derived from sporadic breast and ovarian tumors. In addition, we screened the germline DNAs of 65 individuals with early-onset breast cancer, of whom 35 had a strong family history of breast and/or ovarian cancer but lacked mutations in either *BRCA1* or *BRCA2* (Table 1). Mutational analysis involved direct nucleotide sequencing of RT-PCR amplified *BACH1* cDNA. The template for each cDNA was mRNA isolated from an immortalized B cell line generated with the relevant patient's peripheral blood B cells. Mutation confirmation was performed by sequence analysis of the relevant, individual exons, amplified from genomic DNA.

Two heterozygous missense mutations were detected in the germlines of two breast cancer patients. The first mutation, identified in a young woman with breast cancer who had a strong family history of breast and ovarian cancer, resulted in a proline to alanine substitution at codon 47 (P47A). Unfortunately, germline DNA was not available from any of this patient's family members to test for cosegregation of the mutation with breast cancer in this kindred. However, the P47A mutation was not detected in the germline DNAs of 200 control individuals, indicating that it is unlikely to be a polymorphism in the population (<1/400 alleles), although other polymorphisms were identified (see Table 1). The second germline *BACH1* mutation, M299I, was also detected in a case of early-onset breast cancer and absent in 200 control individuals (Table 1). Both mutations reside within the region encompassing the helicase domain of BACH1. Indeed, the P47A mutation resides within a region resembling the highly conserved nucleotide binding box of known DEAH helicases, while the M299I mutation is positioned between two other boxed motifs (see Figure 2C). Given its location within a conserved box motif, we further investigated the P47A mutation.

Specifically, we incorporated this mutation into an otherwise wt *BACH1* allele and expressed both mutant and wt gene products in U2OS cells. Remarkably, despite comparable expression of the two transcripts (data not shown), the abundance of the mutant gene product

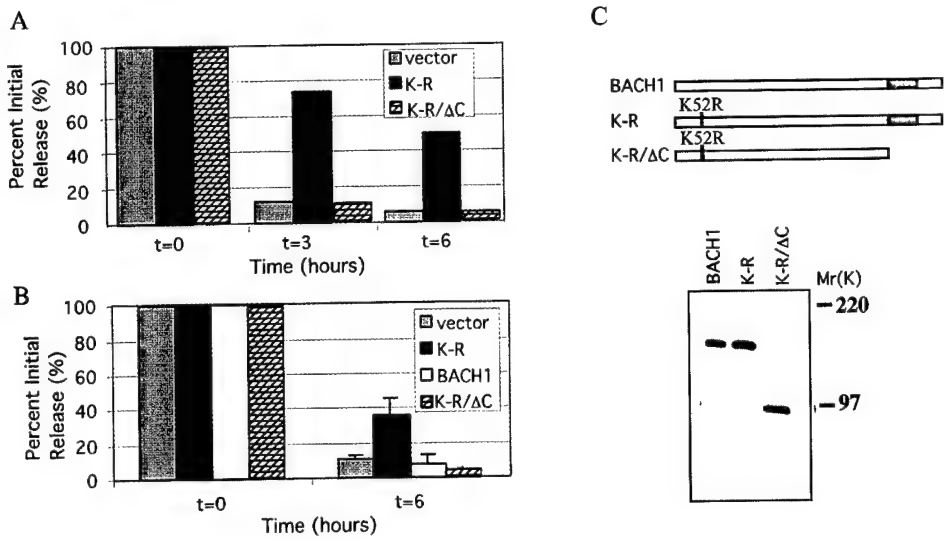

Figure 5. The BACH1 K52R Mutant Interferes with the Timely Repair of Double-Strand Breaks

(A) U2OS cells were transfected with a GFP-encoding vector and either K52R or K52RΔC, each expressed as a myc-6xhis-fusion protein. A control culture was transfected with vector alone. GFP-positive cells were FACS sorted and either exposed or not exposed to 15 Gy and harvested at the indicated times. Residual DSBs were determined by pulsed field electrophoresis as described in Experimental Procedures. Composite data analyzing results at three time points from two individual DSBR experiments are shown for K52R, K52RΔC, and vector. The data are the averages of 2–3 measurements at each time point.

(B) To further assess effects at the 6 hr time point, multiple experiments were performed using BACH1 (wt), K52R, K52RΔC, and vector alone, as described above. These data represent the mean and standard error of several independent experiments with at least 2–3 measurements per time point per experiment for each transfected culture.

(C) [Above], Maps of the primary structure of BACH1 (wt), K52R, and K52R/ΔC BACH1 are shown. [Below], FACS-sorted cells were lysed. Lysates were immunoprecipitated with myc antibody, and the relevant Western blot was probed with myc antibody. Western blot analysis showing that all three BACH1 proteins were expressed at the same level and were intact.

was considerably reduced, compared to the wt protein. To determine whether this was attributable to altered protein stability, the half-lives of the mutant and wt proteins were determined. Using the cycloheximide/chase method, the data indicated that BACH1 containing the P47A substitution was considerably less stable (t1/2: ~1 hr) than either the wild-type protein (t1/2: ~3 hr) or the K52R dominant negative mutant product (t1/2: ~4 hr) (Figure 6). These results suggest that the P47A alteration constitutes a functionally significant mutation and suggest that reduced protein levels attributable to this mutant allele may be linked to breast cancer predisposition.

Analysis of a laser capture microdissected sample from this patient's tumor did not reveal homozygosity for the P47A change. However, prior fixation of the specimen prevented screening of the full *BACH1* coding region for another mutation in the remaining allele or for any mutation that would restrict expression of the gene.

Discussion

Endogenous BACH1, a new member of the DEAH family of DNA helicases, interacts directly and specifically with the BRCT motif-containing domain of BRCA1. Moreover, BACH1 likely contributes to the DNA repair function of BRCA1, since a BACH1 derivative bearing a mutation in a key residue that is essential for catalytic function in other helicases interfered with normal DSBR in a manner that was dependent upon its ability to interact with BRCA1. Tumor-predisposing missense and deletion

Table 1. BACH1 Sequence Variations in Breast and Ovarian Cancer

		Frequency				
Sequence Variant	Effect on Protein	Familial Breast and Ovarian Cancer	Early-Onset Breast Cancer	Sporadic Breast Cancer	Sporadic Ovarian Cancer	Controls
C139G	PRO47ALA	1/35	0/30	0/13	0/8	0/200
G897A	MET299ILE	0/35	1/30	0/13	0/8	0/200
Polymorphisms						
G577A	VAL193ILE					3/200
C2755T	PRO919SER					11/21
G2637A	None					12/21
C3411T	None					10/23

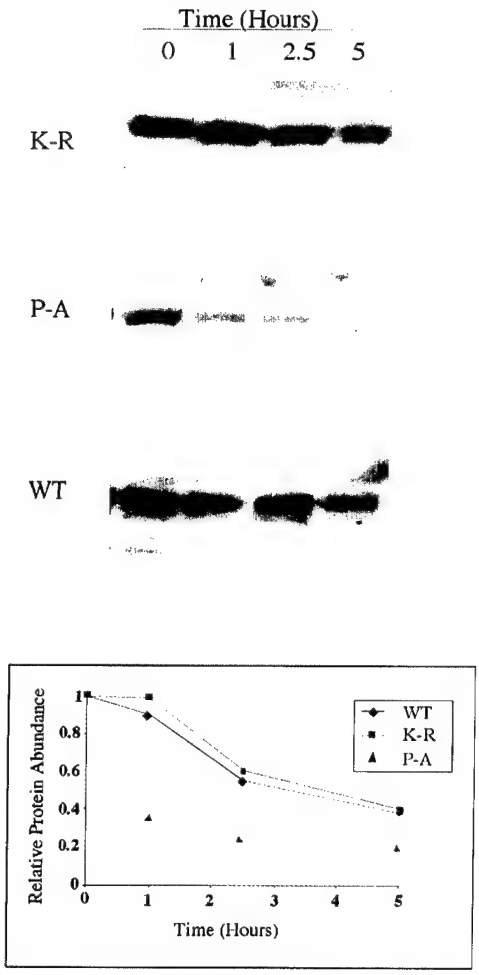

Figure 6. The BACH1 P47A Tumor-Associated Mutant Is Unstable

Stability of wt and various mutant species of BACH1 was assessed by cycloheximide-chase analysis. BACH1 wt, K52R, and P47A were each expressed as a myc-6xhis-fusion protein in U2OS cells (10 μg of each plasmid were transfected). Transfected cell lysates from each time point were immunoblotted for the c-myc epitope with 9E10 anti-myc Ab. The myc immunoblot was densitometrically scanned, and the intensity of each fusion protein band was plotted to determine the relevant half-lives. This experiment was repeated three times with similar results.

mutations in the BRCA1 BRCT domain, all of which render BRCA1 defective in its DSBR function, also disrupted BACH1 binding to BRCA1. These data imply that BACH1 is integral to the role of BRCA1 in DSBR.

Several lines of evidence suggest a role for BRCA1 in DSBR. BRCA1 interacts with several proteins that are intimately involved in this process, including Rad51 and the Mre11/Rad50/Nbs-1 (MRN) complex (Scully et al., 1997b; Carney et al., 1998; Stewart et al., 1999; Zhong et al., 1999; Wang et al., 2000; Wu et al., 2000). Moreover, BRCA1-deficient cells reveal a chromosome breakage syndrome and defective DSBR (Shen et al., 1998; Moynahan et al., 1999; Scully et al., 1999; Xu et al., 1999).

These findings notwithstanding, the mechanism by which BRCA1 participates in the DSBR process remains unclear. Events that are likely to be intrinsic to the repair process include the localized unwinding of DNA in the vicinity of a break. Enzymatic unwinding of DNA has already been shown to be an essential element in certain forms of DNA repair. For example, the XPD and XPB helicases associated with transcription-repair factor TFIIH are essential for nucleotide excision repair (reviewed in Coin and Egly, 1998), and this activity can be modulated by other proteins (Drapkin et al., 1994; Ohkuma and Roeder, 1994; Serizawa et al., 1994; Xiao et al., 1994; Wang et al., 1995; Qadri et al., 1996). In this context, the association of BRCA1 with a putative DNA helicase may help to shed light on the role of BRCA1 in the DSBR process.

Similarly, it will be interesting to determine whether binding of BRCA1 affects the putative enzymatic function of BACH1. Alternatively, it is conceivable that BACH1 operates upstream of BRCA1, influencing the DSBR-promoting function of the latter, or reciprocal BACH1 ↔ BRCA1 influence might exist after the creation of a DS break. What remains especially unclear is how and in what biochemical form the relevant influence is transmitted. Direct communication between a C-terminal segment of BACH1 and the BRCT motifs of BRCA1 would seem to be at least part of the story.

BRCA1 also functions in meiotic cells where it decorates the unsynapsed segments of developing synaptonemal complexes. In these regions, sister chromatids associate with one another in the presence of certain axial element proteins, BRCA1, BRCA2, Rad51, ATR, and other DNA replication/repair/checkpoint proteins (Keegan et al., 1996; Scully et al., 1997b; Chen et al., 1998; Yuan et al., 2000). Since the unsynapsed regions will eventually participate in appropriate pairing of homologous chromosomes, one or more proteins that are closely associated with them likely play(s) a role in the pairing/recombination process. Interestingly, the C-terminal region of BACH1 is homologous to SCP1 (Schmekel et al., 1996), an important component of the axial element, raising the question of whether BRCA1/BACH1 complexes may play a role in meiotic recombination.

The requirement for integrity of the BRCA1 BRCT motifs both for BACH1 binding and for BRCA1-mediated tumor suppression suggests a connection between these two functions. An association between loss of function of a helicase and either a decrease in cell viability or disease production is well established. The DEAH helicase family play significant roles in basal transcription, DNA repair, and chromosome transmission (reviewed in Hoeijmakers et al., 1996). In yeast, CHL1 appears to play a role in chromosome transmission, significant compromise of which can lead to nonviability. The *Saccharomyces cerevisiae* homolog of XPD, RAD3, is also essential for cell viability (Prakash and Prakash, 1989; Friedberg et al., 1995). In mammalian cells, XPD is part of TFIIH, which is required for both basal transcription and nucleotide excision repair (Weber et al., 1990; Drapkin et al., 1994; Coin and Egly, 1998). Nonlethal mutations of *XPD* are responsible for multiple genetic diseases including xeroderma pigmentosum, Cockayne Syndrome, and trichothiodystrophy (Coin and Egly, 1998). These examples highlight the diverse, yet key, roles played by members of the DEAH helicase family in biological processes dependent upon the mainte-

nance of proper DNA mechanics. They also underscore the close links that exist between abnormal/inadequate DNA mechanics and the emergence of disease.

In this context, it was interesting to detect an association between germline *BACH1* mutation and breast cancer development. In particular, two independent germline *BACH1* mutations were found among a cohort of 65 women with early-onset breast cancer, including one with a strong family history of breast and/or ovarian cancer but normal *BRCA1* and *BRCA2* genotypes. The mutation at proline 47, a highly conserved residue within the nucleotide binding domain of the DEAH family, is associated with BACH1 protein destabilization. Thus, the P47A sequence change is most likely a loss-of-function mutation. While there is clearly no evidence indicating that mutation at *BACH1* is a common source of inherited breast cancer, the fact that *BACH1* mutations exist in certain early-onset breast cancer patients and not in 200 normal controls heightens speculation that, like the case of DSBR, BACH1 activity is linked to BRCA1 tumor-suppressing function. Of note, loss of heterozygosity (LOH) was not observed in cells from the tumor of the patient with a *BACH1* P47A germline mutation. However, inherent limitations in the method of analysis make it unclear whether or not the other *BACH1* allele is intact. If *BACH1* is intact, this would raise the question of whether heterozygosity at *BACH1* translates into haploinsufficiency. In such a case, somatic mutations in other genes might follow, with the subsequent mutation collection contributing to the emergence of a neoplastic phenotype in the relevant tumor cells.

The potential existence of a clinical association between a germline mutation in BACH1 and early-onset breast cancer is intriguing and leads to speculation of a more general role for *BACH1* in cancer suppression. Unquestionably, broader epidemiological and formal human genetic analyses, as well as targeted mutation of the *Bach1* gene in the mouse, will be needed to address this possibility.

Experimental Procedures

Glutathione S-transferase (GST) Fusion Proteins

GST and GST fusion proteins were expressed in *E. coli* BLR (Novagen) transformed with pGEX2TK, pGST-BRCT, pGST-BRCT1749, or pGST-BRCT1775. Fusion proteins were purified by affinity chromatography using glutathione Sepharose beads (Pierce) as described (Kaelin et al., 1992). The relative protein concentration was estimated by Coomassie blue staining. Purified GST proteins were used in affinity/protein binding experiments (Chen et al., 1998) using either HeLa cell nuclear extracts or in vitro translated ^{35}S-labeled proteins. The latter were generated with the TNT system (Promega). Beads were extensively washed in NET-N buffer [150 mM NaCl, 0.5% NP-40, 20 mM Tris-HCl (pH8), 1 mM EDTA]. Bound proteins were separated by SDS-PAGE (10% gels) and/or visualized by autoradiography. For far Western blotting experiments, the pGEX2TK fusion proteins were labeled with ^{32}P-ATP as described (Amersham Pharmacia Biotech) and used as radioactive probes (Kaelin et al., 1992).

BACH1 Purification and Sequencing

Ten liters of HeLa cells, purchased from Cell Culture Science (Minneapolis, MN), were resuspended in low salt NET-N buffer. After a slow speed spin (1100 RPM), the pellet was lysed in 300 mM NaCl-containing NET-N buffer for 20 min on ice and then centrifuged at 15,000 RPM for 20 min. These supernatants were incubated with ~60 μl of packed glutathione agarose beads loaded with approximately 1 μg/μl of GST protein for 2 hr at 4°C. Following this preclearing step, the supernatants were further incubated with ~60 μl of packed glutathione agarose beads loaded with approximately 20 μg of GST-BRCT fusion protein for 2 hr at 4°C. The beads were then collected by centrifugation and washed four times in NET-N containing 300 mM NaCl. Finally, the beads were boiled in SDS loading buffer containing 10% β-mercaptoethanol and analyzed by SDS-PAGE (10% gels). The gels were either stained or transferred to nitrocellulose (Schleicher & Schuell) and subjected to far Western blotting analysis. Where indicated, the 130 kDa BACH1 band was visualized with Coomassie blue, excised from the gel, and subjected to sequence analysis.

Mass Spectrometry

The excised BACH1 gel bands were subjected to reduction, carboxyamidomethylation, and tryptic digestion (Promega) within the relevant gel strips. Multiple peptide sequences were determined in a single run by microcapillary reverse phase chromatography directly coupled to an LCQ quadruple ion trap mass spectrometer (Finnigan), equipped with a custom nanoelectrospray source. The column was packed in-house with 5 cm of C18 support into a one-piece 75 μm ID column terminating in a 15 μm tip (New Objective). Flow rate was 190 nl/min. The ion trap was programmed to acquire three successive scan modes consisting of: full scan MS over alternating ranges of 395–800 m/z and 800–1300 m/z, followed by two data-dependent scans on the most abundant ion in those full scans. These dependent scans allowed the automatic acquisition of a high resolution (zoom) scan to determine charge state, exact mass, and MS/MS spectra for peptide sequence information at <10 fmol. MS/MS spectra were acquired with a relative collision energy of 30%, an isolation width of 2.5 Da, and recurring ions were dynamically excluded. Interpretation of the resulting MS/MS spectra was facilitated by programs developed in the Harvard Microchemistry Facility (Chittum et al., 1998) and by database correlation with the algorithm SEQUEST (Eng et al., 1994). The following peptides were identified: TNFDELLQVYYDAIK, VSIGLDFSDDNAR, AVITIGIPFPNVK, WLSTGLWHNLELVK, TVIVEPQGGEK, IDATLTR, TTWINELELGK, DLFEIR, ALNQALGR, QWYEIQAYR.

Immunoprecipitation, Immunoblotting, and Stability Analysis

Cultured cells were washed once with 10 mM sodium phosphate buffer (pH 7.4) containing 150 mM NaCl (PBS) and lysed in NET-N buffer. In a typical immunoprecipitation reaction, 100–300 μg of whole-cell extract was incubated with 1 μg of antibody and 20 μl of protein A Sepharose beads (1:1) at 4°C for 1–2 hr. Beads were washed four times in 1 ml of NET-N buffer. Proteins bound to the beads were eluted by boiling in SDS sample buffer, separated by SDS-PAGE, and transferred to nitrocellulose membranes (Schleicher & Schuell) using a semidry blotter (milliBlot-SDE system; Millipore). The membranes were used for far Western blotting (Kealin et al., 1992) or for immunoblotting as described (Chen et al., 1998). Cycloheximide-chase experiments on transfected cells were performed as described (Maki and Howley, 1997).

Plasmids

Full-length BACH1 cDNA was constructed from two phage containing partial cDNA fragments and a 5′ RACE product generated as described by the manufacturer of the relevant kit (Gibco BRL). The fragments were digested and ligated together to produce a full-length BACH1 sequence in a pBluescript II KS+/− vector (Stratagene). It was sequenced fully and found to be intact before use in experiments described here. To generate a mammalian expression plasmid encoding myc+ his-tagged full-length BACH1, the pBluescript vector containing wt BACH1 cDNA was digested with Not1 and Apa1 to release the full-length BACH1 sequence. The excised, full-length BACH1 sequence was subcloned into the pCDNA3myc-6xhis vector (Invitrogen) to generate an in-frame polypeptide fused with the C-terminal myc-6xhis tag.

Sequences encoding truncated derivatives of BACH1 were generated by PCR using the wt BACH1 pBluescript vector as a template and the following primers: for the helicase domain derivative, [TTG CGGCCGCGCCACCATGGCACTTCATCAACTTGTCAAGATT] and [TTG GGCCCGGAAAATTCAGCCAAGGACTCCAG]; for the C-terminal domain-containing derivative, [TTGCGGCCGCGCCACCATGGATCCA

AAAAAGAAGAGAAAGGTATCCTTGGCTGAATTTTCCAAAAAG] and [AAGGGCCCCTTAAAACCAGGAAACATGCCTTTATTTTTGG]; and for the BRCA1 binding domain-containing derivative, [TTGCGGCCGCG CCACCATGGATCCAAAAAAGAAGAGAAAGGTATCCTTGGCTGAA TTTTCCAAAAAG] and [AAGGGCCCTGTGTTTACTGTCAGATTTGA GGATTC].

These products were subcloned into a pCDNA3myc-6xhis vector (Invitrogen) in frame with the C-terminal myc-6xhis tag. To insure that the BACH1 C-terminal and BRCA1 binding domain fusion proteins localized to nuclei, an SV40 nuclear localization sequence was included in the 5′ primer.

To inactivate the putative ATPase activity of BACH1, the lysine residue at position 52 was changed to an arginine, using a Quikchange site-directed mutagenesis kit (Stratagene). Two primers were used in this process: [CCCACAGGAAGTGGAAGGAGCTT AGCCTTAGCC] and [GGCTAAGGCTAAGCTCCTTCCACTTCCTGT GGG]. To generate the (K52RΔC) mutation, the helicase primers, listed above, were used with the (K52R) mutant BACH1 template. All newly generated recombinants were sequenced. To generate the tumor-associated mutant, the proline at position 47 was changed to an alanine by Quikchange site-directed mutagenesis (Stratagene) using the following primers: [CATTGTTTGTTGGAGAGTGCCACA GGAAGTGGAAAAGC] and [GCTTTTTCCACTTCCTGTGGCACTCTC CAACAAACAATG]

The BRCT-GST fusion protein was generated by PCR using the following primers: [ATCGGATCCATTAAGGTTGTTGATGTGGAG] and [AAGGATCCTCAGTAGTGCTGTGGGGGATCTG]. The product was digested with BamH1/Sal1 and subcloned into pGEX2TK. The generation of M1775R and P1749R derivatives was carried out by standard PCR cloning techniques. Each derivative was verified by standard sequencing techniques. Templates containing these mutations were used with above-noted primers to introduce the BRCT1775 and BRCT1749 mutations into the pGEX2TK vector.

In Vitro Protein Binding Reactions

Expression plasmids encoding the full-length BACH1 and BACH1 polypeptides, generated as described above, were in vitro translated (TNT kit, Promega) and tested for binding to GST (−) or GST-BRCT:1529–1863 (+) fusion protein.

Cell Culture

U20S and 293T cells were cultivated in Dulbecco's modified Eagle's medium (DMEM) containing 10% fetal calf serum (HyClone) at 37°C in a 10% CO_2-containing atmosphere. MCF7 cells were maintained in DMEM supplemented with 10% fetal bovine serum (HyClone). For transfection, a standard calcium phosphate precipitation method was used (Chen and Okayama, 1987). Cells were collected 48 hr after transfection.

Immunostaining

MCF7 cells were grown on coverslips, fixed with 3% paraformaldehyde/2% sucrose in PBS for 10 min., and permeabilized with 0.5% Triton X-100 as described previously (Scully et al., 1997c). Cells were then incubated with mouse monoclonal antibodies to BACH1 (2G7 or 1G5 at 1:50–1:100) and polyclonal anti-sera to BRCA1 (at 1:500) in PBS with 1% bovine serum albumin. After washing, appropriate species-specific, fluorochrome-conjugated secondary antibodies (Jackson ImmunoResearch Laboratories) were applied as recommended by the manufacturer, and fluorescence was visualized using a Nikon microscope.

Antibodies

Some of the anti-BRCA1 mAbs used were described previously (Scully et al., 1996; Chen et al., 1998). BARD1 antibody was made by subcloning a BglII-XhoI fragment of BARD1 cDNA, encoding residues 201–777, into the BamHI-XhoI sites of pGEX-4T-1 to generate the vector for the expression of GST-BARD1 fusion protein. GST fusion protein purification, antibody production, and purification were performed as described previously (Scully et al., 1996; Chen et al., 1998). Two mouse monoclonal antibodies, generated against a specific BACH1 peptide (NFKPSPSKNKGMFPGFK) (PP15-IB4 and PP112G7), and a third raised against GST-BACH1 (647–1043) (GO-IG5) were also used where indicated.

Double-Strand Break Repair Assay

Cells were cotransfected with BACH1 species and GFP, sorted after 24 hr by virtue of their GFP-associated fluorescence, and plated at 400,000 cells per 60 cm dish. 40 hr after transfection, the cells were either irradiated or mock irradiated and allowed to recover for various time points and then analyzed for their ability to perform DSBR, as described (Scully et al., 1999). Cells were irradiated with a 137 Cs source at 4°C and allowed to repair DNA breaks at 37°C. At the indicated times, cellular DNA was analyzed by pulse field gel electrophoresis as described (Badie et al., 1995). After electrophoresis, the gel was processed and stained with SYBR green as described (Kiltie and Ryan, 1997). Fluorescence was quantitated with a Molecular Dynamics Storm Scanner using the blue fluorescence channel and ImageQuant software (Molecular Dynamics). The fraction of DNA entering the gel was measured using the formula: Percent release = (signal in lane)/[(signal in lane) + (signal in plug)]/100. The quantity of signal present in unirradiated, parallel control cultures (<10% of total input DNA in a given lane) was taken as a measure of background signal and subtracted from the measured values. For kinetic studies, the data presented were normalized to the percent DNA released into the gel at T = 0.

Clinical Study Population

EBV-immortalized lymphoblastoid cell lines from 65 women diagnosed with breast cancer before the age of 40 were analyzed for BACH1 germline mutations. Sixteen cases had a definitive (3 or more affected individuals over 2 or more generations) family history of breast cancer, and 19 other individuals had a positive family history of breast-ovarian cancer. The remaining cases of early-onset breast cancer represent a subset of the general population at high risk for genetic predisposition. These individuals were part of a larger cohort of 408 women with early-onset breast cancer from Boston area hospitals (FitzGerald et al., 1996). Control EBV-immortalized lymphoblastoid cell lines were established from healthy blood donors registered in the blood banks of these hospitals. Both the early-onset breast cancer study group and the control population represent individuals within the Boston area. The two groups are well matched with respect to ethnicity as confirmed by equal contribution in the two populations of multiple polymorphic sequences. Thirteen sporadic breast cancer cell lines and 8 ovarian cancer cell lines were obtained from the American Type Culture Collection (Manassas, VA). They are: MDA-MB-415, MDA-MB-436, MDA-MB-453, MDA-MB-231, MDA-MB-157, MDA-MB-468, MDA-MB-435, MDA-MB-175, HS157, MCF7-ADR, HS275, T47D, BT549, OVCAR-3, OVCAR-4, OVCAR-5, OVCAR-8, OV1063, IGROV-1, MDA-2774.

Mutation Detection

Denaturing HPLC was used to detect mutations within the BACH1 coding region. Total mRNA was isolated using STAT-60 (Tel-test, Inc., Friendswood, TX). The entire BACH1 transcript was amplified in an RT-PCR reaction with primers BACH1-PRIM-F (GAATCGGAG CTCAGAGCGTTGCTTCG) and BACH1-PRIM-R (GGGCAACAGAC CAAGACTCTGTCTC) for 25 cycles at 95°C for 30 s, 58°C for 30 s, and 72°C for 4 min. Products of this reaction were diluted 100-fold and used as templates in subsequent nested PCR analyses to generate 14 overlapping fragments for dHPLC analysis. Primers and PCR conditions are available upon request. Wavemaker software (Transgenomic, Ohmaha, NE) and the Stanford prediction program (available at http://insertion.stanford.edu/melt.html) were used to predict the optimal temperatures for mutational analysis of each amplicon. Aberrant dHPLC profiles were confirmed by sequencing after reamplification of the fragment with primers that included M13-tailed primers. For sequencing analysis, PCR products were resolved by gel electrophoresis, treated with exonuclease I (Amersham Life Sciences) and with shrimp alkaline phosphatase (United States Biochemical). They were then diluted 6-fold prior to sequencing. Energy Transfer Dye Primer (Amersham Pharmacia Biotech) sequencing was performed according to the manufacturer's instructions. Potentially heterozygous nucleotides were marked and displayed for evaluation by Factura and Sequence Navigator (Applied Biosystems). Specifically, base positions at which the height of the secondary peak was >30% that of the primary peak were marked as heterozy-

gous and were confirmed by analysis of both sense and antisense strands. For LOH analysis, as reflected by the nature of the sequence at the codon responsible for residue 47, paraffin-embedded tumor blocks were sectioned and subjected to laser capture microdissection to isolate homogeneous regions of histologically normal cells and tumor cells. DNA was extracted using phenol-chloroform followed by ethanol precipitation. A genomic DNA fragment spanning codon 47 was amplified using forward (GATTAAACAGCAAGCAA CATTGTTTG) and reverse (CATGCTAAAGCAGAACAAAGTAAGG) primers. PCR conditions consisted of: 35 cycles of 95°C for 30 s, 58°C for 30 s, 72°C for 30s.

Acknowledgments

We are particularly grateful to all of our laboratory colleagues for helpful advice and discussions. We also wish to thank Jim DeCaprio for the preparation of BACH1 antibodies, Ralph Scully for the BRCA1 reconstituted HCC1937 cells, and Kerry Pierce for expert HPLC and mass spectrometry analysis. We also thank Junjie Chen for providing the BARD1 antibody. This work was supported by grants from the National Cancer Institute to D. M. L. and S. C. as well as a grant from the Dana Farber-Partners Gillette Women's Cancer Program and the Dana Farber/Harvard Specialized Program of Research Excellence (SPORE) in breast cancer from the National Cancer Institute (P50 CA89393). S. G. is a recipient of a Howard Hughes Medical Institute postdoctoral fellowship for physicians. R. D. is funded by NIH training grant T32 HL07627-16.

Received November 27, 2000; revised February 21, 2001.

References

Amann, J., Kidd, V.J., and Lahti, J.M. (1997). Characterization of putative human homologues of the yeast chromosome transmission fidelity gene. CHL1. J. Biol. Chem. *272*, 3823–3832.

Badie, C., Iliakis, G., Foray, N., Alsbeih, G., Cedervall, B., Chavaudra, N., Pantelias, G., Arlett, C., and Malaise, E.P. (1995). Induction and rejoining of DNA double-strand breaks and interphase chromosome breaks after exposure to X rays in one normal and two hypersensitive human fibroblast cell lines. Radiat. Res. *144*, 26–35.

Blanar, M.A., and Rutter, W.J. (1992). Interaction cloning: identification of a helix-loop-helix zipper protein that interacts with c-Fos. Science *256*, 1014–1018.

Bork, P., Hofmann, K., Bucher, P., Neuwald, A.F., Altschul, S.F., and Koonin, E.V. (1997). A superfamily of conserved domains in DNA damage-responsive cell cycle checkpoint proteins. FASEB J. *11*, 68–76.

Breast Cancer Information Core (BIC). http://www.nhgri.nih.gov/Intramural_research/Lab_transfer/Bic/.

Callahan, R. (1998). Somatic mutations that contribute to breast cancer. Biochem. Soc. Symp. *63*, 211–221.

Callebaut, I., and Mornon, J.P. (1997). From BRCA1 to RAP1: a widespread BRCT module closely associated with DNA repair. FEBS Lett. *400*, 25–30.

Carney, J.P., Maser, R.S., Olivares, H., Davis, E.M., Le Beau, M., Yates, J.R., 3rd, Hays, L., Morgan, W.F., and Petrini, J.H. (1998). The hMre11/hRad50 protein complex and Nijmegen breakage syndrome: linkage of double-strand break repair to the cellular DNA damage response. Cell *93*, 477–486.

Chapman, M.S., and Verma, I.M. (1996). Transcriptional activation by BRCA1. Nature *382*, 678–679.

Chen, C., and Okayama, H. (1987). High-efficiency transformation of mammalian cells by plasmid DNA. Mol. Cell. Biol. *7*, 2745–2752.

Chen, J., Silver, D.P., Walpita, D., Cantor, S.B., Gazdar, A.F., Tomlinson, G., Couch, F.J., Weber, B.L., Ashley, T., Livingston, D.M., and Scully, R. (1998). Stable interaction between the products of the BRCA1 and BRCA2 tumor suppressor genes in mitotic and meiotic cells. Mol. Cell *2*, 317–328.

Chittum, H.S., Lane, W.S., Carlson, B.A., Roller, P.P., Lung, F.D., Lee, B.J., and Hatfield, D.L. (1998). Rabbit beta-globin is extended beyond its UGA stop codon by multiple suppressions and translational reading gaps. Biochemistry *37*, 10866–10870.

Cleaver, J.E. (2000). Common pathways for ultraviolet skin carcinogenesis in the repair and replication defective groups of xeroderma pigmentosum. J. Dermatol. Sci. *23*, 1–11.

Coin, F., and Egly, J.M. (1998). Ten years of TFIIH. Cold Spring Harb. Symp. Quant. Biol. *63*, 105–110.

Deng, C.X., and Brodie, S.G. (2000). Roles of BRCA1 and its interacting proteins. Bioessays *22*, 728–737.

Drapkin, R., Reardon, J.T., Ansari, A., Huang, J.C., Zawel, L., Ahn, K., Sancar, A., and Reinberg, D. (1994). Dual role of TFIIH in DNA excision repair and in transcription by RNA polymerase II. Nature *368*, 769–772.

Eckner, R., Ewen, M.E., Newsome, D., Gerdes, M., DeCaprio, J.A., Lawrence, J.B., and Livingston, D.M. (1994). Molecular cloning and functional analysis of the adenovirus E1A-associated 300-kD protein (p300) reveals a protein with properties of a transcriptional adaptor. Genes Dev. *8*, 869–884.

Eng, J.K., McCormick, A.L., and Yates, J.R., III (1994). An approach to correlate tandem mass spectral data of peptides with amino acid sequences in a protein database. J. Am. Soc. Mass Spectrom. *5*, 976–989.

FitzGerald, M.G., MacDonald, D.J., Krainer, M., Hoover, I., O'Neil, E., Unsal, H., Silva-Arrieto, S., Finkelstein, D.M., Beer-Romero, P., Englert, C., et al. (1996). Germ-line BRCA1 mutations in Jewish and non-Jewish women with early-onset breast cancer. N. Engl. J. Med. *334*, 143–149.

Friedberg, E.C., Bardwell, A.J., Bardwell, L., Feaver, W.J., Kornberg, R.D., Svejstrup, J.Q., Tomkinson, A.E., and Wang, Z. (1995). Nucleotide excision repair in the yeast Saccharomyces cerevisiae: its relationship to specialized mitotic recombination and RNA polymerase II basal transcription. Philos. Trans. R. Soc. Lond. B. Biol. Sci. *347*, 63–68.

Hoeijmakers, J.H., Egly, J.M., and Vermeulen, W. (1996). TFIIH: a key component in multiple DNA transactions. Curr. Opin. Genet. Dev. *6*, 26–33.

Kaelin, W.G., Jr., Krek, W., Sellers, W.R., DeCaprio, J.A., Ajchenbaum, F., Fuchs, C.S., Chittenden, T., Li, Y., Farnham, P.J., Blanar, M.A., et al. (1992). Expression cloning of a cDNA encoding a retinoblastoma-binding protein with E2F-like properties. Cell *70*, 351–364.

Keegan, K.S., Holtzman, D.A., Plug, A.W., Christenson, E.R., Brainerd, E.E., Flaggs, G., Bentley, N.J., Taylor, E.M., Meyn, M.S., Moss, S.B., et al. (1996). The Atr and Atm protein kinases associate with different sites along meiotically pairing chromosomes. Genes Dev. *10*, 2423–2437.

Kiltie, A.E., and Ryan, A.J. (1997). SYBR green I staining of pulsed field agarose gels is a sensitive and inexpensive way of quantitating DNA double-strand breaks in mammalian cells. Nucleic Acids Res. *25*, 2945–2946.

Koonin, E.V., Altschul, S.F., and Bork, P. (1996). BRCA1 protein products. Functional motifs. Nat. Genet. *13*, 266–268.

Ma, L., Westbroek, A., Jochemsen, A.G., Weeda, G., Bosch, A., Bootsma, D., Hoeijmakers, J.H., and van der Eb, A.J. (1994). Mutational analysis of ERCC3, which is involved in DNA repair and transcription initiation: identification of domains essential for the DNA repair function. Mol. Cell. Biol. *14*, 4126–4134.

Maki, C.G., and Howley, P.M. (1997). Ubiquitination of p53 and p21 is differentially affected by ionizing and UV radiation. Mol. Cell. Biol. *17*, 355–363.

Miki, Y., Swenson, J., Shattuck-Eiden, D., Futreal, P.A., Harshman, K., Tavtigian, S., Liu, Q.Y., Cochran, C., Bennett, L.M., Ding, W., et al. (1994). A strong candidate for the breast and ovarian cancer susceptibility gene BRCA1. Science *266*, 66–71.

Monteiro, A.N., August, A., and Hanafusa, H. (1996). Evidence for a transcriptional activation function of BRCA1 C-terminal region. Proc. Natl. Acad. Sci. USA *93*, 13595–13599.

Moynahan, M.E., Chiu, J.W., Koller, B.H., and Jasin, M. (1999). Brca1 controls homology-directed DNA repair. Mol. Cell *4*, 511–518.

Ohkuma, Y., and Roeder, R.G. (1994). Regulation of TFIIH ATPase

and kinase activities by TFIIE during active initiation complex formation. Nature *368*, 160–163.

Prakash, L., and Prakash, S. (1989). Excision repair genes of Saccharomyces cerevisiae. Ann. Ist. Super. Sanita *25*, 99–113.

Qadri, I., Conaway, J.W., Conaway, R.C., Schaack, J., and Siddiqui, A. (1996). Hepatitis B virus transactivator protein, HBx, associates with the components of TFIIH and stimulates DNA helicase activity of TFIIH. Proc. Natl. Acad. Sci. USA *93*, 10578–10583.

Schmekel, K., Meuwissen, R.L., Dietrich, A.J., Vink, A.C., van Marle, J., van Veen, H., and Heyting, C. (1996). Organization of SCP1 protein molecules within synaptonemal complexes of the rat. Exp. Cell Res. *226*, 20–30.

Scully, R., Ganesan, S., Brown, M., De Caprio, J.A., Cannistra, S.A., Feunteun, J., Schnitt, S., Livingston, D.M. (1996). Location of BRCA1 in human breast and ovarian cancer cells. Science *272*, 123–125.

Scully, R., Anderson, S.F., Chao, D.M., Wei, W., Ye, L., Young, R.A., Livingston, D.M., and Parvin, J.D. (1997a). BRCA1 is a component of the RNA polymerase II holoenzyme. Proc. Natl. Acad. Sci. USA *94*, 5605–5610.

Scully, R., Chen, J., Plug, A., Xiao, Y., Weaver, D., Feunteun, J., Ashley, T., and Livingston, D.M. (1997b). Association of BRCA1 with Rad51 in mitotic and meiotic cells. Cell *88*, 265–275.

Scully, R., Chen, J., Ochs, R.L., Keegan, K., Hoekstra, M., Feunteun, J., and Livingston, D.M. (1997c). Dynamic changes of BRCA1 subnuclear location and phosphorylation state are initiated by DNA damage. Cell *90*, 425–435.

Scully, R., Ganesan, S., Vlasakova, K., Chen, J., Socolovsky, M., and Livingston, D.M. (1999). Genetic analysis of BRCA1 function in a defined tumor cell line. Mol. Cell *4*, 1093–1099.

Serizawa, H., Conaway, J.W., and Conaway, R.C. (1994). An oligomeric form of the large subunit of transcription factor (TF) IIE activates phosphorylation of the RNA polymerase II carboxyl-terminal domain by TFIIH. JBC *269*, 20750–20756.

Shen, X.-S., Weaver, Z., Xu, X., Li, C., Weinstein, M., Chen, L., Guan, X.-Y., Ried, T., and Deng, C.-X. (1998). A targeted disruption of the murine Brca1 gene causes a γ-irradiation hypersensitivity and genetic instability. Oncogene *17*, 3115–3124.

Snouwaert, J.N., Gowen, L.C., Latour, A.M., Mohn, A.R., Xiao, A., DiBiase, L., and Koller, B.H. (1999). BRCA1 deficient embryonic stem cells display a decreased homologous recombination frequency and an increased frequency of non-homologous recombination that is corrected by expression of a brca1 transgene. Oncogene *18*, 7900–7907.

Stewart, G.S., Maser, R.S., Stankovic, T., Bressan, D.A., Kaplan, M.I., Jaspers, N.G., Raams, A., Byrd, P.J., Petrini, J.H., and Taylor, A.M. (1999). The DNA double-strand break repair gene hMRE11 is mutated in individuals with an ataxia-telangiectasia-like disorder. Cell *99*, 577–587.

Sung, P., Higgins, D., Prakash, L., and Prakash, S. (1988). Mutation of lysine-48 to arginine in the yeast RAD3 protein abolishes its ATPase and DNA helicase activities but not the ability to bind ATP. EMBO J. *7*, 3263–3269.

Taylor, R.M., Wickstead, B., Cronin, S., and Caldecott, K.W. (1998). Role of a BRCT domain in the interaction of DNA ligase III-alpha with the DNA repair protein XRCC1. Curr. Biol. *8*, 877–880.

Tomlinson, G.E., Chen, T.T., Stastny, V.A., Virmani, A.K., Spillman, M.A., Tonk, V., Blum, J.L., Schneider, N.R., Wistuba, I.I., Shay, J.W., et al. (1998). Characterization of a breast cancer cell line derived from a germ-line BRCA1 mutation carrier. Cancer Res. *58*, 3237–3242.

Vermeulen, W., de Boer, J., Citterio, E., van Gool, A.J., van der Horst, G.T., Jaspers, N.G., de Laat, W.L., Sijbers, A.M., van der Spek, P.J., Sugasawa, K., et al. (1997). Mammalian nucleotide excision repair and syndromes. Biochem. Soc. Trans. *25*, 309–315.

Wang, X.W., Yeh, H., Schaeffer, L., Roy, R., Moncollin, V., Egly, J.-M., Wang, Z., Friedberg, E.C., Evans, M.K., Taffe, B.G., et al. (1995). P53 modulation of TFIIH-associated nucleotide excision repair activity. Nat. Genet. *10*, 188–195.

Wang, Y., Cortez, D., Yazdi, P., Neff, N., Elledge, S.J., and Qin, J. (2000). BASC, a super complex of BRCA1-associated proteins involved in the recognition and repair of aberrant DNA structures. Genes Dev. *14*, 927–939.

Weber, C.A., Salazar, E.P., Stewart, S.A., and Thompson, L.H. (1990). ERCC2: cDNA cloning and molecular characterization of a human nucleotide excision repair gene with high homology to yeast RAD3. EMBO J. *9*, 1437–1447.

Welcsh, P.L., Owens, K.N., and King, M-C. (2000). Insights into the functions of BRCA1 and BRCA2. Trends Genet. *16*, 69–74.

Wood, R.D. (1999). DNA damage recognition during nucleotide excision repair in mammalian cells. Biochimie *81*, 39–44.

Wu, X., Petrini, J.H.J., Heine, W.F., Weaver, D.T., Livingston, D.M., and Chen, J. (2000). Independence of R/M/N focus formation and the presence of intact BRCA1. Science *289*, 11a.

Xiao, H., Pearson, A., Coulombe, B., Truant, R., Zhang, S., Regier, J., Triezenberg, S.J., Reinberg, D., Flores, O., Ingles, C.J., and Greenblatt, J. (1994). Binding of basal transcription factor TFIIH to the acidic activation domain of VP16 and p53. Mol. Cell. Biol. *14*, 7013–7024.

Xu, X., Weaver, Z., Linke, S.P., Li, C., Gotay, J., Wang, X.-W., Harris, C.C., Ried, T., and Deng, C.-X. (1999). Centrosome amplification and a defective G2-M cell cycle checkpoint induce genetic instability in BRCA1 exon 11 isoform-deficient cells. Mol. Cell *3*, 389–395.

Yu, X., Wu, L.C., Bowcock, A.M., Aronheim, A., and Baer, R. (1998). The C-terminal (BRCT) domains of BRCA1 interact in vivo with CtIP, a protein implicated in the CtBP pathway of transcriptional repression. J. Biol. Chem. *273*, 25388–25392.

Yuan, L., Liu, J.G., Zhao, J., Brundell, E., Daneholt, B., and Hoog, C. (2000). The murine SCP3 gene is required for synaptonemal complex assembly, chromosome synapsis, and male fertility. Mol. Cell *5*, 73–83.

Zabludoff, S.D., Wright, W.W., Harshman, K., and Wold, B.J. (1996). BRCA1 mRNA is expressed highly during meiosis and spermiogenesis but not during mitosis of male germ cells. Oncogene *13*, 649–653.

Zhong, Q., Chen, C.F., Li, S., Chen, Y., Wang, C.C., Xiao, J., Chen, P.L., Sharp, Z.D., and Lee, W.H. (1999). Association of BRCA1 with the hRad50-hMre11-p95 complex and the DNA damage response. Science *285*, 747–750.

GenBank Accession Number

The GenBank accession number for the BACH1 sequence reported in this paper is AF360549.

Molecular Cell, Vol. 2, 317–328, September, 1998, Copyright ©1998 by Cell Press

Stable Interaction between the Products of the *BRCA1* and *BRCA2* Tumor Suppressor Genes in Mitotic and Meiotic Cells

Junjie Chen,* Daniel P. Silver,* Deepika Walpita,† Sharon B. Cantor,* Adi F. Gazdar,‡ Gail Tomlinson,‡ Fergus J. Couch,‖ Barbara L. Weber,§ Terry Ashley,† David M. Livingston,*# and Ralph Scully*
*The Dana Farber Cancer Institute
Harvard Medical School
Boston, Massachusetts 02115
†Department of Genetics
Yale University School of Medicine
New Haven, Connecticut 06520
‡Hamon Center for Therapeutic Oncology Research
University of Texas Southwestern Medical Center
Dallas, Texas 75235
§Department of Medicine
University of Pennsylvania
Philadelphia, Pennsylvania 19104
‖Department of Laboratory Medicine and Pathology
Mayo Clinic and Foundation
Rochester, Minnesota 55905

Summary

***BRCA1* and *BRCA2* account for most cases of familial, early onset breast and/or ovarian cancer and encode products that each interact with hRAD51. Results presented here show that BRCA1 and BRCA2 coexist in a biochemical complex and colocalize in subnuclear foci in somatic cells and on the axial elements of developing synaptonemal complexes. Like BRCA1 and RAD51, BRCA2 relocates to PCNA$^+$ replication sites following exposure of S phase cells to hydroxyurea or UV irradiation. Thus, BRCA1 and BRCA2 participate, together, in a pathway(s) associated with the activation of double-strand break repair and/or homologous recombination. Dysfunction of this pathway may be a general phenomenon in the majority of cases of hereditary breast and/or ovarian cancer.**

Introduction

BRCA1 or *BRCA2* germline mutations predispose women to early onset, familial breast cancer (Hall et al., 1990; Narod et al., 1991; Miki et al., 1994; Wooster et al., 1994, 1995; Tavtigian et al., 1996). Disease risk is inherited as an autosomal dominant trait (Newman et al., 1988; Claus et al., 1991). The majority of tumors arising in *BRCA1*- or *BRCA2*-linked family members show loss of heterozygosity (LOH) at the relevant loci with retention of the mutant allele (reviewed in Zhang et al., 1998). Thus, the behavior of these two genes follows the Knudson model of tumor suppressor genetics.

The *BRCA1* and *BRCA2* products are large nuclear proteins, whose primary amino acid sequences yield few clues to their function. An exception is a motif at the C terminus of BRCA1, termed BRCT (Koonin et al., 1996). BRCT is a relatively common feature of proteins involved in DNA repair and/or in cell cycle checkpoint function (Koonin et al., 1996; Bork et al., 1997; Callebaut and Mornon, 1997). Although there is some similarity between the exon structures of *BRCA1* and *BRCA2*, there is no appreciable sequence homology between the proteins.

There is evidence suggesting that *BRCA1* and *BRCA2* function in an analogous manner (reviewed in Zhang et al., 1998). Both gene products interact with hRAD51 in vivo (Scully et al., 1997a; Sharan et al., 1997). RAD51 plays a key role in homologous recombination and double-strand break repair (Radding, 1991; Shinohara et al., 1992; Sung, 1994; Sung and Robberson, 1995; Baumann et al., 1996). In the developing mouse embryo, the patterns of *BRCA1*, *RAD51*, and *BRCA2* gene expression are almost identical (Lane et al., 1995; Marquis et al., 1995; Rajan et al., 1997; Sharan et al., 1997). In human cell lines, the expression of each gene increases as cells enter S phase, suggesting that at least some of the biological function(s) of these genes are exerted during or following DNA replication (Gudas et al., 1995, 1996; Rajan et al., 1996; Vaughn et al., 1996; Chen et al., 1997; Blackshear et al., 1998).

BRCA1, *BRCA2*, or *RAD51* nullizygous mice all reveal early embryonic lethality, associated with a proliferation deficit (Gowen et al., 1996; Hakem et al., 1996; Lim and Hasty, 1996; Liu et al., 1996; Tsuzuki et al., 1996; Ludwig et al., 1997; Sharan et al., 1997; Suzuki et al., 1997). Death occurs at E6.5 in *RAD51*, E7.5 in *BRCA1*, and E8.5 in *BRCA2* nullizygotes. Preceding death of either *BRCA1* or *BRCA2* nullizygotes, there is increased expression of the DNA damage-responsive, cell cycle inhibitor, *p21* (Hakem et al., 1996; Connor et al., 1997; Suzuki et al., 1997). For *RAD51*, *BRCA1*, and *BRCA2*, the lethal nullizygous phenotype is partially suppressed by coincident, homozygous *p53* germline mutation (Lim and Hasty, 1996; Hakem et al., 1997; Ludwig et al., 1997). Homozygous *p21* germline mutations also partially suppress the *BRCA1* or *BRCA2* nullizygous phenotype (Hakem et al., 1997). Hence, viability of these embryos is likely limited by activation of the p53-mediated checkpoint control system with subsequent nonproliferation.

These observations imply that BRCA1 and BRCA2 function in related pathways. If these pathways were linked to genome integrity control, abnormal DNA structures might emerge as a consequence of their dysfunction (Scully et al., 1997a). Abnormal DNA structures, in turn, might lead to DNA damage-dependent, p53/p21-mediated cell cycle arrest, leading to the genetic relationships noted above. Consistent with this model, *BRCA2* nullizygous embryos exhibited X-ray supersensitivity (Sharan et al., 1997). Cells of *BRCA2* mutant mice reveal inefficient repair of DNA breaks and aberrant chromosomal structures (Connor et al., 1997; Patel et al., 1998). They are also hypersensitive to DNA-adducting agents (Patel et al., 1998). These findings suggest a role for BRCA2 in recombinational responses to DNA damage, as was suggested for BRCA1 (Scully et al., 1997a, 1997c). Moreover, the cells of *BRCA1*- and

To whom correspondence should be addressed.

BRCA2-deficient tumors are especially aneuploid (Marcus et al., 1996), consistent with both loci participating in the maintenance of genome stability.

Here we report the interaction of endogenous BRCA2 with endogenous BRCA1 in cultured human cell lines, their nuclear colocalization, and similar responses of these proteins to DNA damage. These data indicate that endogenous BRCA1 and BRCA2 coexist in a biochemical complex, suggesting their joint participation in at least one DNA damage pathway that is frequently inactivated in hereditary breast and ovarian cancer.

Results

Characterization of Anti-BRCA2 Antibodies

Three affinity-purified polyclonal rabbit antibodies (Ab), anti-BRCA2A, -2B, and -2C were raised against GST BRCA2 proteins encoding aa 1425–1973, 2422–2976, and 3245–3418, respectively. To learn whether these antibodies recognize endogenous BRCA2, blots of U2OS cell extracts were probed with the BRCA1 mAb, MS110, or a BRCA2 Ab (Figure 1A, left panel). All three BRCA2 antibodies recognized a protein larger than BRCA1 (400 kDa; see Figure 1A, and data not shown). To learn whether the 400 kDa protein was hBRCA2, we generated a full-length cDNA encoding hBRCA2 fused to an N-terminal influenza hemagglutinin (HA) epitope. The abundance of the 400 kDa protein, detected by immunoblotting with anti-BRCA2, was significantly increased in cells transfected with an HA-BRCA2 expression plasmid (Figure 1B, left panel). HA antibody also immunoprecipitated a 400 kDa protein from transfected cells but not from untransfected cells (data not shown), suggesting that this protein is HA-tagged, full-length BRCA2. HA-BRCA2 comigrated with the 400 kDa protein precipitated by BRCA2 antibody from untransfected cell extracts (Figure 1B, right panel).

To determine whether BRCA2 antibody can immunoprecipitate intact BRCA2, extracts of untransfected cells or cells transfected with HA-BRCA2 were immunoprecipitated with a control anti-mIgG Ab or anti-BRCA2C (Figure 1C). Blotted immunoprecipitates were probed with anti-HA mAb (12CA5). The 400 kDa protein was detected by anti-HA immunoblotting only in transfected cell extracts, and it was also immunoprecipitated by anti-BRCA2 antibody, thereby showing that the BRCA2 antiserum can immunoprecipitate hBRCA2 (Figure 1C).

CAPAN-1 is a human pancreatic carcinoma cell line that carries a 6174delT BRCA2 mutation and has lost the wild-type *BRCA2* allele (Goggins et al., 1996). This mutation should result in the loss of BRCA2 residues 1982–3418 and the concomitant disappearance of the anti-BRCA2B (residues 2422–2976) and 2C epitopes (residues 3245–3418). An IP/immunoblotting protocol was used with anti-BRCA2C to search for BRCA2 in various human cell lines, including CAPAN-1. Full-length BRCA2 proteins were detected in 293T, MCF-7, HCC1937, and U2OS cells, but not in CAPAN-1 (Figure 1D, upper left panel), implying that anti-BRCA2C Ab recognizes intact, endogenous BRCA2. While anti-BRCA2B also failed to recognize truncated BRCA2 in CAPAN-1 cells (Figure 1D, upper right panel), anti-BRCA2A, raised against a more N-terminal region of BRCA2, did recognize this fast-migrating BRCA2 species (Figure 1D, upper right panel; Figure 3B). The 220 kDa BRCA1 protein levels in CAPAN-1 cells were similar to those detected in the control cell lines 293T, MCF-7, and U2OS (Figure 1D, lower panel).

HCC1937 was established from the primary infiltrating breast ductal carcinoma of a 24-year-old female who had a germline BRCA1 mutation, insert C at nt 5382 (G. T. et al., unpublished data). HCC1937 has lost the wild-type *BRCA1* allele. The mutant sequence predicts a frameshift in codon 1756 of the *BRCA1* ORF, leading to the synthesis of a truncated product lacking the BRCA1 C terminus. Consistent with this, HCC1937 extracts revealed no full-length BRCA1 protein (Figure 1D, lower panel). HCC1937 extracts did, however, contain low levels of a 210 kDa BRCA1 species (Figure 1D, lower right panel). The BRCA2 levels in HCC1937 cells were similar to those in 293T, MCF-7, and U2OS extracts (Figure 1D, upper left panel).

Association of BRCA1 and BRCA2 In Vivo

MCF7 cell extracts were subjected to immunoprecipitation using multiple BRCA1 Abs, each raised against a different region of BRCA1 (Figure 2A). While an E1A mAb, M73, and control rabbit IgG failed to precipitate BRCA1 or BRCA2, all BRCA1 Abs coimmunoprecipitated BRCA1 and BRCA2 (Figure 2A, left panel). Identical results were obtained with 293T or U2OS extracts (data not shown). Each BRCA1 Ab recognized in vitro translated BRCA1, but not in vitro translated BRCA2 (data not shown), indicating that they do not recognize BRCA2 directly. These observations suggest that endogenous BRCA1 and BRCA2 interact, directly or indirectly.

To test further for evidence of BRCA1/2 antibody cross-reactivity, we investigated the coimmunoprecipitation of BRCA1 and BRCA2 in HCC1937 cells. The mAb, SG11, was raised against the C-terminal 17 residues of BRCA1 (Scully et al., 1996). As noted above, this epitope should be absent from the 210 kDa truncated *BRCA1* product detected in HCC1937 cells. While monoclonal antibodies against more N-terminal epitopes of BRCA1 immunoprecipitated this truncated form of BRCA1, SG11 did not (Figure 2A, right panel and data not shown). In addition, unlike SG11, MS13, a mAb raised against an N-terminal segment of BRCA1 (Scully et al., 1996), also coimmunoprecipitated BRCA2 from HCC1937 extracts (Figure 2A, right panel). These results rule out the possibility that SG11 cross-reacts with BRCA2. They also suggest that the extreme C terminus of BRCA1 is not required for the proposed BRCA1/BRCA2 interaction.

In search of additional evidence that BRCA1 and BRCA2 can form a complex in vivo, we generated a full-length *BRCA1* cDNA bearing an N-terminal myc epitope. Myc-tagged BRCA1 and HA-tagged BRCA2 were transiently transfected, individually and together, into 293T cells. A myc mAb, 9E10, coimmunoprecipitated HA-BRCA2 from cells cotransfected with both expression vectors, but not from cells transfected with HA-BRCA2, alone (Figure 2B). A BRCA1 mutant (Mut) with an 11-residue truncation of its extreme C terminus (Y1853term) also coprecipitated with BRCA2 in these assays (Figure

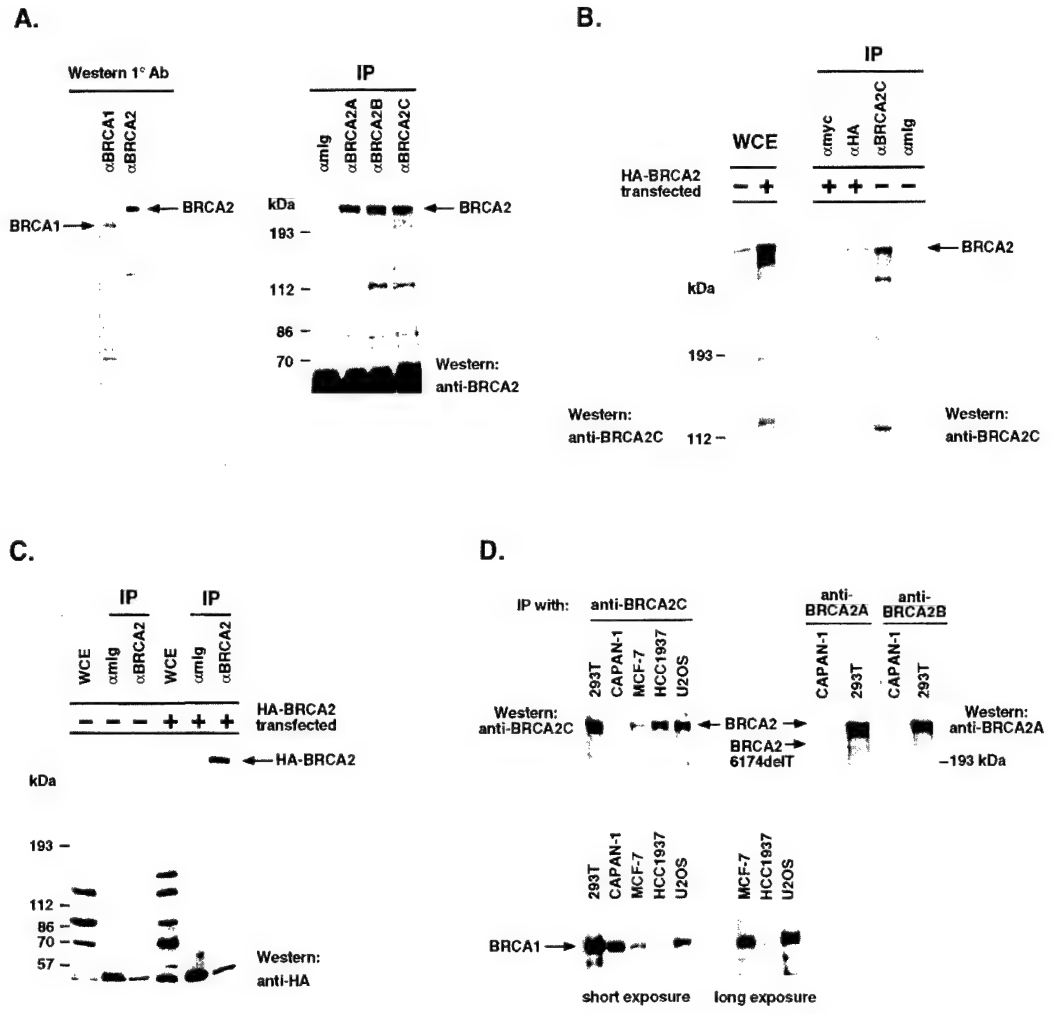

Figure 1. Characterization of Anti-BRCA2 Antibodies

(A) Left, whole-cell extracts of U2OS cells were separated by SDS-PAGE and immunoblotted with either anti-BRCA1 mAb MS110 or anti-BRCA2C antibody. Right, 293T cell extracts were subjected to immunoprecipitation (IP) with control antibody (rabbit anti-mouse IgG) or three independent anti-BRCA2 antibodies (A, B, and C), and the immunoblot was probed with anti-BRCA2C antibody.

(B) Aliquots of whole-cell extract (WCE, 50 μg/lane) from untransfected 293T (−) cells or cells transfected with expression plasmids encoding HA-BRCA2 (+) were separated by SDS-PAGE and immunoblotted with anti-BRCA2 antibody (left panel). Aliquots of extract from cells transfected with expression plasmids encoding HA-BRCA2 were subjected to immunoprecipitation by a control anti-myc antibody (9E10) or anti-HA mAb 12CA5, and extracts of untransfected 293T cells were subjected to immunoprecipitation with anti-BRCA2C antibody or a control rabbit anti-mouse IgG Ab. Immunoblotting was performed with anti-BRCA2C antibody (right panel).

(C) Whole-cell extracts (50 mcg) of untransfected 293T cells (−) or 293T cells transfected with an HA-BRCA2 expression plasmid (+) were subjected to immunoprecipitation with control (anti-mouse IgG) or anti-BRCA2C antibodies, separated by SDS-PAGE, and immunoblotted using anti-HA antibody (12CA5).

(D) Top, extracts of 293T, CAPAN-1, MCF-7, HCC1937, and U2OS cells were immunoprecipitated and immunoblotted with anti-BRCA2C antibody (left panel). Extracts of 293T and CAPAN-1 cells were immunoprecipitated with anti-BRCA2A or anti-BRCA2B antibodies and immunoblotted with anti-BRCA2A (right panel). Bottom, extracts of 293T, CAPAN-1, MCF-7, HCC1937, and U2OS cells were immunoprecipitated with an affinity-purified, polyclonal anti-BRCA1 antibody (raised against residues 758–1313 of BRCA1) and immunoblotted with a monoclonal anti-BRCA1 antibody, MS110. A longer exposure in the lower panel is shown here to illustrate the truncated BRCA1 protein present in HCC1937 cells.

2B). This is in agreement with the above-noted finding that the extreme C terminus of BRCA1 is not required for BRCA1/BRCA2 coprecipitation. These data indicate that authentic, clonal BRCA1 and BRCA2 can interact in vivo.

Finally, reciprocal immunoprecipitation experiments were performed with anti-BRCA2 antibodies raised against three different regions of BRCA2. Both BRCA1 and RAD51 were detected in all three anti-BRCA2 immunoprecipitates from naive MCF7 or 293T cells (Figures 3A and 3B, and data not shown), confirming that BRCA1 and BRCA2 interact in unperturbed cells. Anti-RAD51 immunoprecipitates generated from an extract of MCF7 cells contained both BRCA1 and BRCA2 (Figure 3A, left panel). To determine whether anti-BRCA2 Abs cross-react with BRCA1, we repeated these experiments in

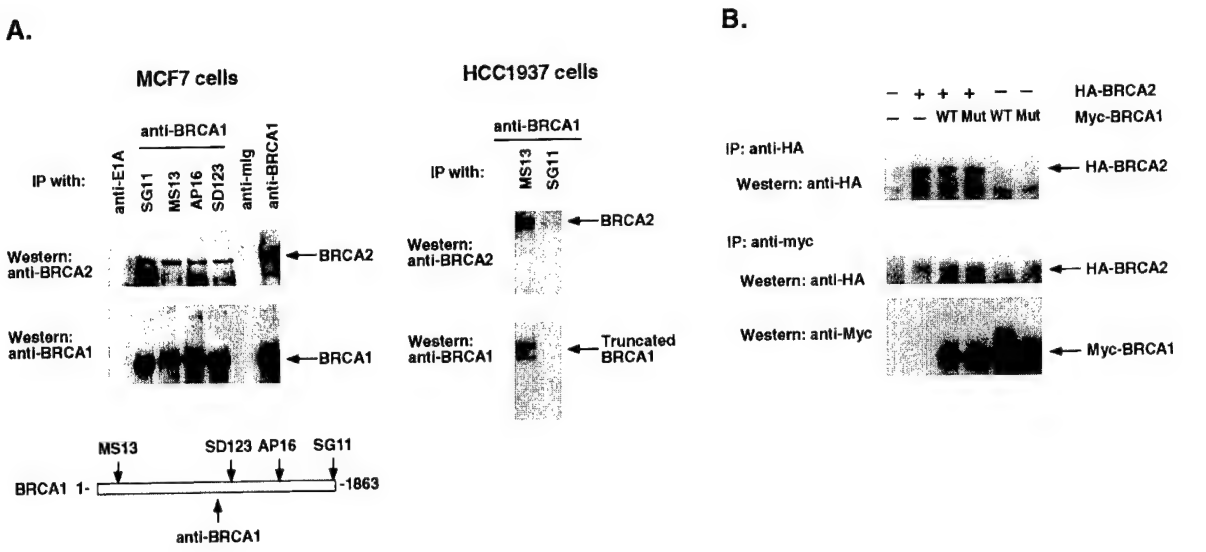

Figure 2. Coimmunoprecipitation of BRCA2 and BRCA1

(A) Left, extracts of MCF-7 cells were subjected to immunoprecipitation with control anti-E1A mAb M73, anti-BRCA1 mAbs SG11, MS13, AP16, and SD123, a control rabbit antibody (anti-mIg), or with an affinity-purified anti-BRCA1 rabbit polyclonal Ab. Right, extracts of HCC1937 cells were subjected to immunoprecipitation with N-terminal-specific BRCA1 mAb MS13 or with mAb SG11 (raised against a peptide corresponding to the C-terminal 17 amino acids of BRCA1) and immunoblotted with either anti-BRCA1 mAb MS110 or anti-BRCA2C Ab. The locations of the epitopes recognized by each of the BRCA1 antibodies used in these immunoprecipitation experiments are shown below.

(B) 293T cells were transfected with a plasmid encoding HA-BRCA2, a plasmid encoding myc-BRCA1 (WT), a plasmid encoding myc-BRCA1Y1853term (Mut), or plasmids encoding HA-BRCA2 and myc-BRCA1 (WT or Mut). Top, extracts were subjected to immunoprecipitation with anti-HA antibody and immunoblotting with anti-HA mAb 12CA5 to indicate the synthesis of HA-BRCA2. Middle and bottom, extracts were subjected to immunoprecipitation with anti-myc mAb 9E10. Immunoprecipitates were separated by SDS-PAGE and immunoblotted with either anti-HA mAb 12CA5 to illustrate the associated HA-BRCA2 (middle) or anti-myc mAb 9E10 to indicate the synthesis of myc-BRCA1 (WT or MUT; lower panel).

CAPAN-1 cells. As noted above, CAPAN-1 cells lack the epitopes against which anti-BRCA2C Ab was raised, and anti-BRCA2C Ab failed to immunoprecipitate BRCA1, BRCA2, or RAD51 from extracts of these cells (Figure 3A right panel), implying that anti-BRCA2C Ab does not cross-react with BRCA1 or RAD51.

The anti-BRCA2A epitope should be still present in the truncated BRCA2 species present in CAPAN-1 cells. Indeed, anti-BRCA2A immunoprecipitated a 230 kDa BRCA2 species from CAPAN-1 cells (Figure 3B, right panel; also see Figure 1D), along with both BRCA1 and RAD51 (Figure 3B, right panel). The presence of complexes containing BRCA1 and a BRCA2 species truncated at residue 1981 suggests that BRCA1 interacts with sequences present in the N-terminal half of BRCA2.

Sequences Adjacent to, but Not at the Extreme C Terminus of, BRCA1 Mediate BRCA2 Binding

We generated six overlapping BRCA1 fragments spanning the entire BRCA1 primary sequences as GST fusion proteins (Figure 4A; also see Scully et al., 1997a) and used them to determine whether there are discrete regions of the BRCA1 structure that mediate BRCA2 binding. It has already been shown that GST-BRCA1 fragment #4 (GST-B1F4), which contains BRCA1 residues 758–1064, can bind to RAD51 in vitro (Scully et al., 1997a). Since RAD51 interacts with both BRCA1 and BRCA2 (Figure 3A; also see review Zhang et al., 1998), one might imagine that RAD51 mediates the interaction between BRCA1 and BRCA2. We tested this hypothesis by employing the same ligand affinity binding assay used to define the RAD51/BRCA1 interaction (Scully et al., 1997a). If RAD51 mediates the interaction between BRCA1 and BRCA2, then GST-B1F4, the fragment of BRCA1 that interacts with RAD51, should also bind to BRCA2. Equivalent quantities of each fusion protein, bound to glutathione-sepharose beads, were incubated with extracts of MCF7 cells. Proteins bound to the beads were recovered, separated electrophoretically, and immunoblotted with either anti-RAD51 or anti-BRCA2 antibodies. While RAD51 again bound to GST-B1F4 (Figure 4B, lower panel), BRCA2 did not. Instead, it bound to GST-B1F6 (Figure 4B, upper panel). Identical results were obtained with extracts of CV-1P and DU-145 cells (data not shown).

As a test of the significance of this observation, we generated mammalian expression vectors encoding the six BRCA1 fragments, noted above. In this instance, the GST moiety at the N terminus of each was substituted with an amino-terminal myc epitope and a nuclear localization sequence when necessary. B1F2 and B1F3 have their own nuclear localization sequences. After transient transfection into 293T cells, myc-tagged BRCA1 fragments were recovered by anti-myc immunoprecipitation, and any bound BRCA2 was sought by immunoblotting with anti-BRCA2 antibody. As a positive control, full-length BRCA1 was also tested, and, as expected, it interacted with BRCA2. Moreover, the only BRCA1 fragment that interacted with BRCA2 was B1F6, the

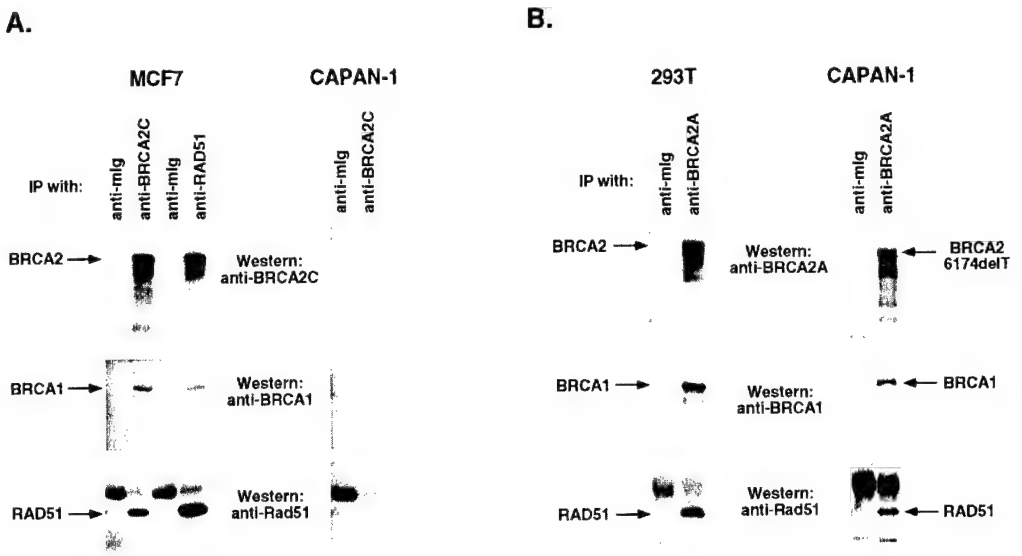

Figure 3. Association of BRCA1 and RAD51 with BRCA2

(A) Left, extracts of MCF-7 cells were subjected to immunoprecipitation with control (anti-mIg), anti-BRCA2C, or anti-RAD51 antibodies. Right, extracts of CAPAN-1 cells were subjected to immunoprecipitation with control (anti-mIg) or anti-BRCA2C Abs. All immunoprecipitates were immunoblotted with anti-BRCA1 mAb MS110, anti-BRCA2C Ab, or anti-RAD51 Ab.

(B) Extracts of 293T or CAPAN-1 cells were immunoprecipitated with anti-mIg Ab or with anti-BRCA2A. Immunoprecipitates were immunoblotted with anti-BRCA1 mAb MS110, anti-BRCA2A Ab, or anti-RAD51 Ab.

same segment that bound to BRCA2 in vitro (Figure 4C). In keeping with these results, a mutant BRCA1 species (BRCA1ΔBAMH I) deleted for residues 1314–1863, the residues present in B1F6, failed to bind BRCA2 (Figure 4D, right panel). These results strongly suggest that RAD51 does not serve as an essential bridge between BRCA1 and BRCA2. On the other hand, sequences at or near the BRCA1 C terminus are important for BRCA1/BRCA2 complex formation.

Colocalization of BRCA1 and BRCA2 in S Phase Nuclear Foci

BRCA1 and RAD51 colocalize in nuclear dots in S and G2 cells (Scully et al., 1997a, 1997c). Since BRCA2 interacted with and coprecipitated with both BRCA1 and RAD51, we asked whether nuclear dots detected by anti-BRCA1 or anti-RAD51 staining also contain BRCA2. Two-color immunostaining was performed using anti-BRCA1 and anti-BRCA2 Abs and visualized by confocal microscopy. BRCA2 immunostaining revealed a nuclear dot pattern, consistent with previous work suggesting that BRCA2 is a nuclear protein (Bertwistle et al., 1997; Chen et al., 1998). Figure 5A shows the results of an experiment using the BRCA1 mAb, SD118 (green), and anti-BRCA2C Ab (red) in DU145 cells. Extensive colocalization of BRCA1 and BRCA2 in nuclear dot structures is apparent (Figure 5A). Anti-BRCA2C staining was blocked by preincubation with the GST-BRCA2 fusion protein against which anti-BRCA2C was raised, but not by preincubation with GST (data not shown). Similar colocalization results were obtained in other cell lines (MCF-7, SaOS2, and CV1-P) and with each of the three affinity-purified anti-BRCA2 antibodies (data not shown).

To test whether affinity-purified BRCA2 antibody recognizes endogenous BRCA2 and not any cross-reacting protein(s), we repeated the aforementioned experiments in CAPAN-1 cells. CAPAN-1 cells contain only a truncated form of BRCA2 that has lost the epitopes recognized by anti-BRCA2C (see above). In these cells, anti-BRCA2C did not produce a signal, unlike anti-BRCA1, which revealed the previously described BRCA1 dot pattern (data not shown).

The BRCA1 S-phase dot pattern undergoes dynamic changes after DNA damage (Scully et al., 1997c). When S phase cells were treated with hydroxyurea (HU), most lost their punctate BRCA1 immunostaining. Only in late S phase cells, where PCNA immunostaining is punctate, did BRCA1 immunostaining remain punctate, and it now colocalized with these PCNA-containing replication centers (Scully et al., 1997c). We asked whether BRCA2 immunostaining undergoes similar changes. As shown in Figure 5B, there was very limited overlap between the PCNA staining pattern and the BRCA2 dot pattern before HU treatment. However, after exposure to HU for 1 hr, extensive colocalization of BRCA2 and PCNA was apparent (Figure 5B).

Colocalization of BRCA1 and BRCA2 on Meiotic Chromosomes

Colocalization of BRCA1 and RAD51 has also been detected on human meiotic chromosomes (Scully et al., 1997a). *BRCA2* and *BRCA1* mRNA expression is coordinately regulated in mitotic and meiotic cells (Rajan et al., 1996; Blackshear et al., 1998). Given the biochemical interactions between BRCA1 and BRCA2 and their colocalization in mitotic cells, we asked whether BRCA2 is concentrated on meiotic chromosomes.

BRCA2 immunostaining of human spermatocyte nuclei was sought using anti-BRCA2B and 2C. While the

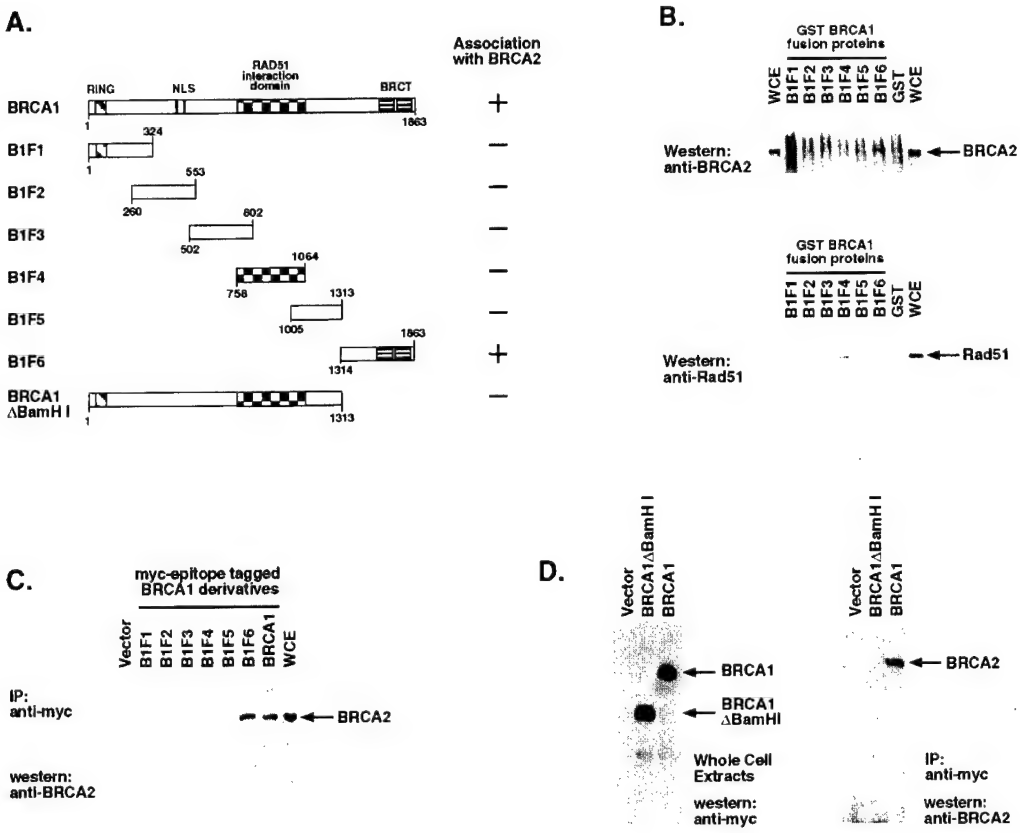

Figure 4. The C Terminus of BRCA1 Associates with BRCA2

(A) Schematic diagram of BRCA1 and its derivatives. Ring domain, two nuclear localization sequences (NLS), the RAD51 interaction domain, and the two BRCT repeats are indicated. Corresponding BRCA1 residues are marked.

(B) Top, beads coated with GST-BRCA1 fusion proteins were incubated with aliquots of an MCF-7 cell extract. Proteins bound to the beads were washed, eluted, separated by SDS-PAGE, and immunoblotted using anti-BRCA2C Ab. The smudges on the top of the gel are nonspecific signals resulting from the GST fusion protein preparation. Bottom, the same ligand affinity binding assay was repeated, and immunoblotting was performed using anti-RAD51 antibody.

(C) 293T cells were transfected with either vector plasmids or plasmids encoding myc-BRCA1 or myc-BRCA1 fragments (B1F1-B1F6). Extracts were subjected to immunoprecipitation with anti-myc mAb 9E10, separated by SDS-PAGE, and immunoblotted with anti-BRCA2C Ab.

(D) 293T cells were transfected with either vector plasmids or plasmids encoding myc-BRCA1 or myc-BRCA1ΔBAMH I (deleted for residues 1314–1863, the residues present in B1F6). Left, whole-cell extracts from transfected cells were separated by SDS-PAGE and immunoblotted using anti-myc mAb 9E10 to examine the synthesis of myc-epitope-tagged proteins. After transfection, both myc-BRCA1 and myc-BRCA1Δ BAMH I localized in nuclei (data not shown). Right, extracts were subjected to immunoprecipitation with the anti-myc mAb 9E10, separated by SDS-PAGE, and immunoblotted with anti-BRCA2C Ab.

2B Ab gave a stronger signal, both antibodies elicited nuclear staining. Cells were costained with anti-BRCA2B (red) and antibody to the axial element protein, SCP3 (white). In early zygonema nuclei, there was BRCA2 staining at discrete sites on unsynapsed axial elements (data not shown). Figure 6A shows a late zygonema–early pachynema nucleus where the majority of axes have synapsed. Although there was no BRCA2 detected on synapsed axes, significant staining was detected on the unsynapsed axial element (arrow head–bubble area). BRCA2 staining also was detected on the unpaired X and Y chromosomes (arrow on X chromosome). Since X and Y have no homologs, they remain unsynapsed throughout pachynema. These data indicate that, like BRCA1, BRCA2 is present on unsynapsed axial elements.

The specificity of anti-BRCA2B and anti-BRCA2C for BRCA2 recognition was analyzed by preincubating each Ab with its respective GST-fused antigen and then testing the axial element staining capabilities of the adsorbed serum. The relevant BRCA2 segment blocked its cognate antibody from staining unsynapsed axial elements (data not shown). In contrast, preincubation of anti-BRCA2 antibodies with an unrelated GST-fusion protein or GST failed to block anti-BRCA2 antibodies from staining axial elements (data not shown). Therefore, the anti-BRCA2 antibodies revealed the localization of BRCA2 protein.

BRCA1 and RAD51 colocalize on unsynapsed axial elements (Scully et al., 1997a). Given the above-noted results on BRCA2 and the physical association of BRCA2 with BRCA1 and RAD51, we asked whether BRCA2 colocalizes with BRCA1 and RAD51 on meiotic chromosomes. Human spermatocytes were costained with a BRCA1 mAb (green) and affinity-purified anti-BRCA2B antibody (red). As shown in Figure 6B, there is

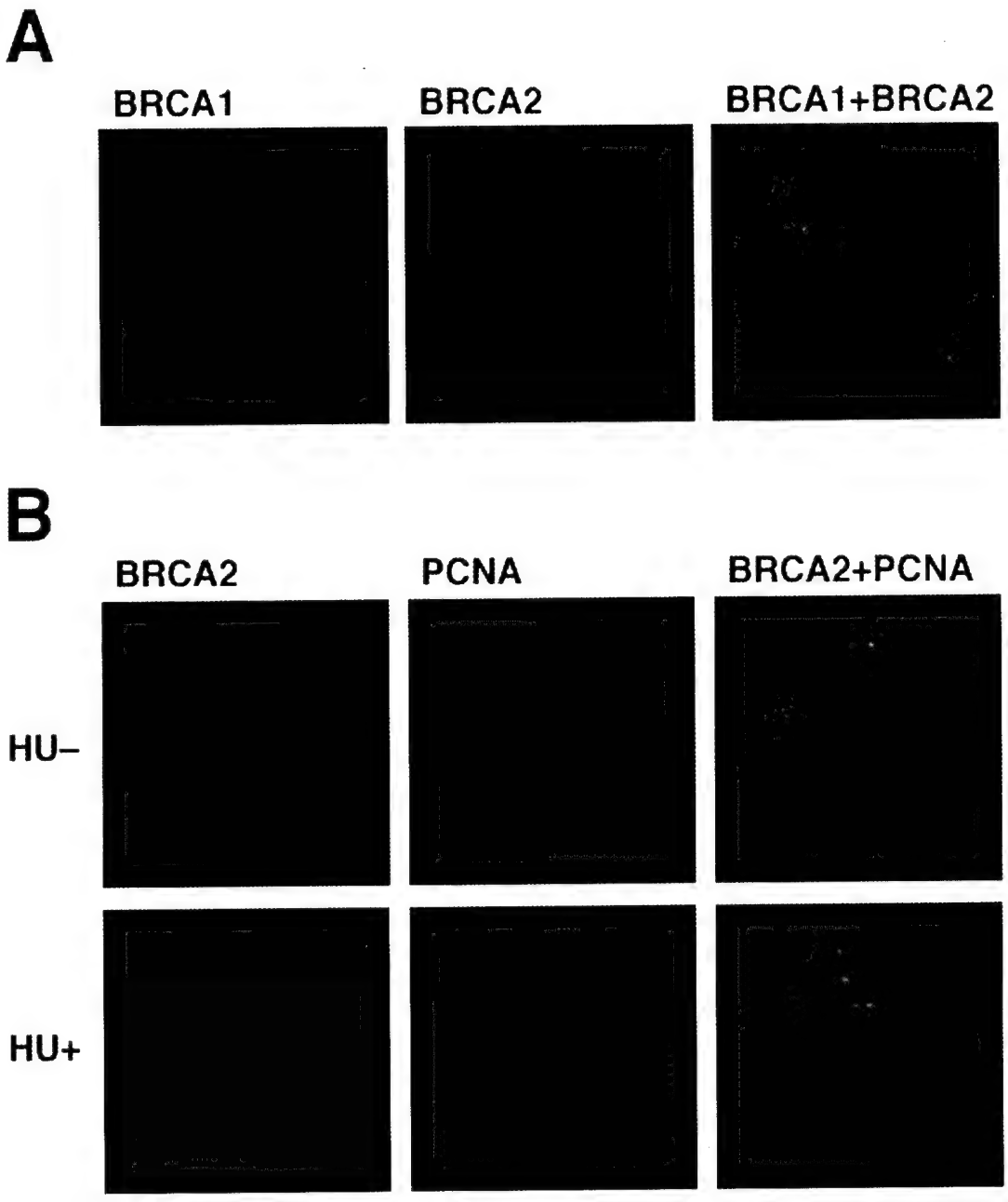

Figure 5. Colocalization of BRCA1 and BRCA2 in Somatic Cells

(A) Colocalization of BRCA1 and BRCA2 in discrete nuclear dots. DU145 cells were prepared as described in Experimental Procedures, stained with anti-BRCA1 mAb SD118 (green) and affinity-purified anti-BRCA2C Ab (red), and imaged by confocal microscopy. Where green and red signals overlap, a yellow pattern is observed, indicating the colocalization of BRCA1 and BRCA2.

(B) Recruitment of BRCA2 to replication foci following hydroxyurea (HU) treatment. MCF-7 cells were double-stained with anti-BRCA2C Ab (green) and anti-PCNA antiserum (AK serum, red). In untreated cells, BRCA2 dots (green) did not overlap significantly with PCNA foci (red). In HU-treated cells, there was extensive colocalization of BRCA2 (green) and PCNA (red) as indicated by yellow signals in the composite picture.

extensive colocalization of BRCA1 and BRCA2. RAD51 also colocalized with BRCA2 on unsynapsed axial elements (data not shown). The colocalization of BRCA1, BRCA2, and RAD51 on synaptonemal complexes further suggests that complexes containing BRCA1, BRCA2, and RAD51 participate in one or more signaling pathways.

Discussion

The results presented here reveal a specific physical association between the products of the two major hereditary breast cancer genes, *BRCA1* and *BRCA2*. This interaction was revealed by coimmunoprecipitation of

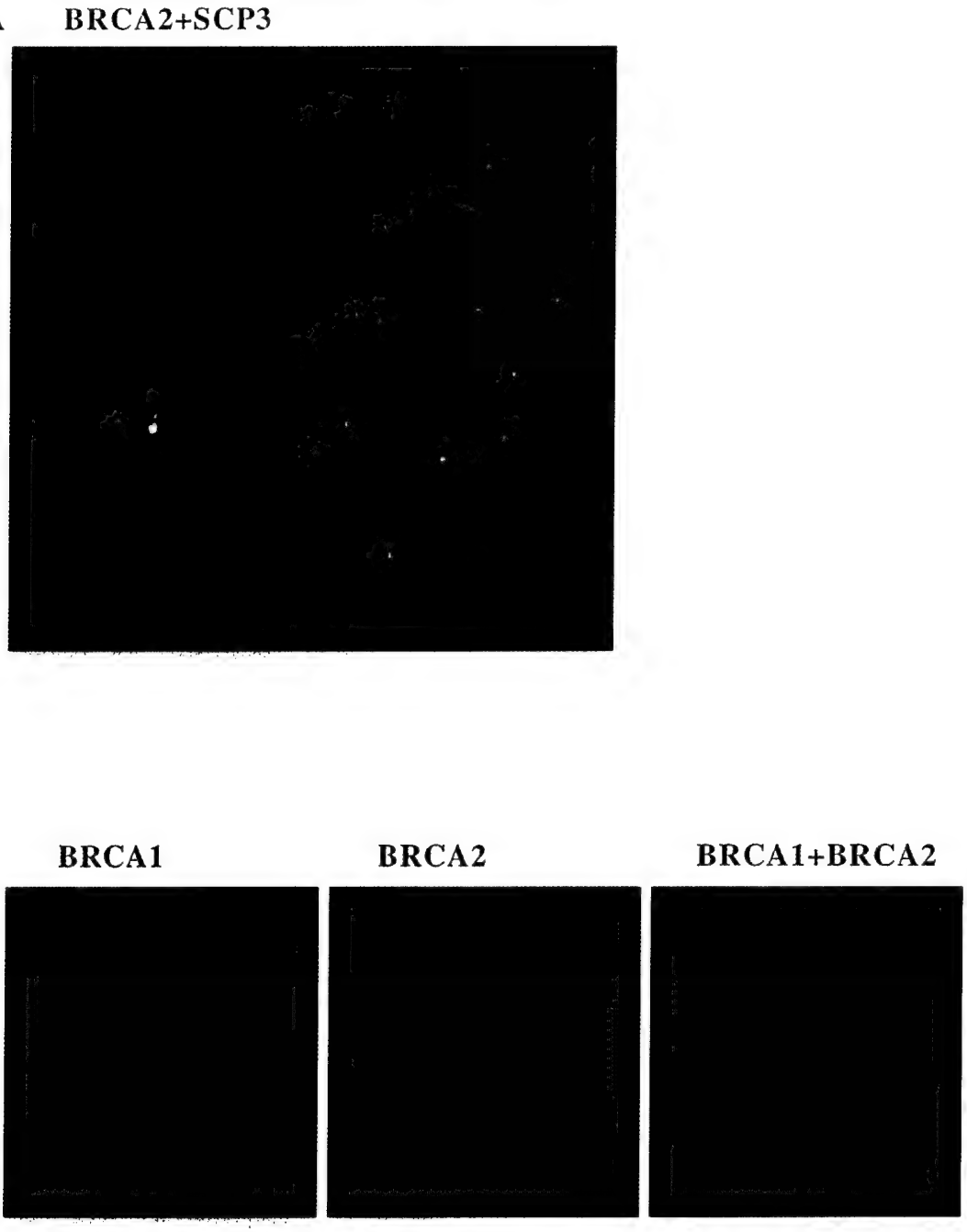

Figure 6. Colocalization of BRCA2 and BRCA1 on Meiotic Chromosomes

(A) A late human zygotene/early pachytene nucleus was costained with anti-BRCA2B Ab (red) and anti-SCP3 antibody (white). BRCA2 (red) localized to unsynapsed regions of a synapsing axial element (indicated by arrowhead) and the unsynapsed X (indicated by arrow) and Y chromosomes.

(B) Meiotic cells were stained with anti-BRCA1 mAb MS110 (green) and affinity-purified anti-BRCA2B Ab (red). Where green and red foci overlap, a yellow signal is observed, confirming the colocalization of BRCA1 and BRCA2.

the two proteins from untransfected cells, using antibodies specific for BRCA1 to coprecipitate BRCA2, and antibodies specific for BRCA2 to coprecipitate BRCA1. Moreover, RAD51 antibodies coimmunoprecipitated both BRCA1 and BRCA2.

In mitotic cells, we found that BRCA2 and BRCA1 coexist in nuclear dot structures before DNA damage, and in PCNA-containing replicating structures thereafter, implying that their physical association is linked to their joint performance of certain form(s) of biological work. In this regard, they were also found to codecorate synaptonemal complexes, further extending the repertoire of their conjoint activities to meiotic cells. Whether there is a unique species of complex containing all three

proteins or whether there are multiple complexes containing BRCA1/BRCA2/RAD51 and yet other proteins is unclear.

The structural basis for the various protein/protein contacts within these multiprotein complexes is not fully understood. However, it would appear that the C-terminal segment of BRCA1 has an intrinsic ability to interact with BRCA2. The actual sequences within these 550 residues (aa 1314–1863) that are responsible for this interaction have not yet been identified. Intact BRCT repeats are not essential for the interaction, because one of them is deleted in the mutant BRCA1 of HCC1937 cells, which coimmunoprecipitated normally with BRCA2. Furthermore, data presented above indicate that a mutant form of BRCA1 (Y1853term), possibly affecting one of the two BRCT domains and rendering BRCA1 transactivation-defective (Chapman and Verma, 1996; Monteiro et al., 1996), bound BRCA2 in transient transfection assays. Unlike wild-type BRCA1, the same mutant also failed to bind the RNA polymerase II holoenzyme (Scully et al., 1997b). These results suggest that the transactivation function of BRCA1 is not required for its interaction with BRCA2. They similarly dissociate BRCA2 binding to BRCA1 and the ability of BRCA1 to copurify with RNA polymerase II holoenzyme. Thus, the relevant BRCA2 binding domain can be localized within a 440 residue segment (residues 1314–1756) at the N-terminal end of B1F6 (Figure 4A). The fact that a specific, C-terminal BRCA1 fragment can interact with BRCA2 in vitro and in vivo reinforces the impression that BRCA2 binding directly or indirectly is an intrinsic property of BRCA1. In a similar vein, although RAD51 does not appear to be the bridge between BRCA1 and BRCA2, data presented here (anti-RAD51 coprecipitation of endogenous BRCA1 [Figure 3A]) reinforce the view that RAD51 and BRCA1 interact, although it is still not clear whether the interaction is direct or indirect.

The detailed stoichiometry of the BRCA1/BRCA2/RAD51 interaction is not yet clear. It is apparent, however, that anti-RAD51 antibodies were as efficient as anti-BRCA2 antibodies in immunoprecipitating BRCA2. Thus, it is possible that BRCA2 is quantitatively bound to RAD51 in the cell. The reverse relationship is apparently not the case, since there appears to be a pool of cellular RAD51 uncomplexed with BRCA2. Interestingly, RAD51 expression increases as cells undergo immortalization (Xia et al., 1997), and one might speculate that the existence of "free" RAD51 is a manifestation of cell immortalization. However, similar proportions of free and "bound" RAD51 were detected in extracts of primary human diploid fibroblasts (data not shown). Whatever the reason for the rise in RAD51 with immortalization, it is possible that free and "BRCA2-bound" RAD51 have different biochemical functions.

The interaction between BRCA1 and BRCA2 appears to be substoichiometric. Based on a comparison of immunoblot intensities of whole-cell extracts versus coimmunoprecipitated protein, we estimate that 2%–5% of cellular BRCA1 is complexed to BRCA2 and that a similar percentage of BRCA2 is complexed with BRCA1 in MCF-7 cell extracts. It is not yet known whether this reflects a regulated interaction between BRCA1 and BRCA2, whether our current immunopurification strategy is inefficient at preserving these complexes, or whether free and bound BRCA1 and/or BRCA2 behave differently in vivo.

Taken together, these results imply that BRCA1 and BRCA2 function, at least in part, as a biochemical complex together with at least one other protein. One might imagine that such a complex plays a role in one or more DNA damage response pathways, particularly in the control of double-strand break repair and homologous recombination. This is supported by the change of localization of both BRCA1 and BRCA2 following DNA damage in mitotic cells and the presence of both proteins (with RAD51) on the axial elements of developing synaptonemal complexes in meiotic cells. Conceivably, dysfunction of this pathway is required for the evolution of most hereditary breast and ovarian cancers. If so, mutations in another gene(s) involved in such a pathway might also contribute to hereditary breast/ovarian cancer.

Somatic mutation of the *BRCA1* and *BRCA2* genes does not accompany sporadic breast or ovarian cancer. Hence, it is not yet apparent whether the *BRCA1/BRCA2* DNA damage response pathway, described above, is dysfunctional in sporadic breast cancer. However, LOH is commonly observed in the regions of 17q and 13q within which *BRCA1* and *BRCA2* are located, possibly reflecting a role for haploinsufficiency at either or both of these loci in the evolution of certain forms of sporadic breast/ovarian cancer (Futreal et al., 1994; Neuhausen and Marshall, 1994; Cleton-Jansen et al., 1995; Beckmann et al., 1996; Kelsell et al., 1996; Lancaster et al., 1996; Miki et al., 1996; Teng et al., 1996; Bieche et al., 1997; Kerangueven et al., 1997). In addition, new results suggest that the level of BRCA1 is markedly reduced in many high-grade invasive breast cancers (C. Wilson, personal communication). As with the possibility of haploinsufficiency, these findings, too, elicit speculation that there is a role for a reduction in the normal amplitude of BRCA1 and/or BRCA2 function during the evolution of a significant fraction of sporadic breast/ovarian cancers.

Since BRCA1 and BRCA2 colocalize and interact before and after DNA damage, our original speculations on the nature of BRCA1 function, based upon localization data and association with RAD51, can now be extended to BRCA2. In this regard, hydroxyurea or UV treatment of S phase cells may generate persistent regions of parental ssDNA, in close proximity to replication forks. These ssDNA regions or their derivatives (dsDNA breaks) may be recombinogenic—possibly accounting, in part, for the recruitment of RAD51/BRCA1/BRCA2/BARD1 complexes to PCNA-containing sites in these circumstances (see also Scully et al., 1997c). These complexes may, therefore, function in a process analogous to prokaryotic "daughter strand gap repair," an error-free, *RecA*-dependent homologous recombinational response to ssDNA lesions generated during attempted replication across a DNA adduct (Rupp and Howard-Flanders, 1968; Hanawalt et al., 1979). Defects in such a process, possibly arising from insufficient BRCA1 or BRCA2 function, could explain some of the spontaneous anomalies in chromosome structure and sensitivity to DNA adducting agents noted recently in cells of *BRCA2* mutant mouse embryos (Patel et al., 1998). If this homologous recombinational process were

saturable, then either a high "load" to the replication machinery of adducted DNA or a quantitative defect in the homologous recombinational pathway might translate into inefficient gap repair and, hence, increased cancer risk.

The concept of a common, *BRCA1/BRCA2* hereditary breast and ovarian cancer pathway suggests at least one hypothesis for understanding the tissue specificity of BRCA1/BRCA2-linked disease. A potentially "universal" carcinogen can give rise to tissue-specific disease, if it is concentrated in certain specialized cell types (so-called "remote carcinogenesis," reviewed in Friedberg et al., 1995). Conceivably, the breast ductal epithelium accumulates such a carcinogen and, therefore, suffers an unusually high rate of DNA damage of a type that stresses postreplication homologous recombination (such as DNA adduction). Lifetime estrogen exposure is a risk factor in breast cancer. Some estrogen metabolites can adduct DNA, and animal models suggest that they are carcinogens in estrogen-responsive tissue (Liehr et al., 1986; Fishman et al., 1995). Additional, as yet unidentified extrinsic/environmental agents might also be implicated as "remote carcinogens" in the etiology of some breast cancers. In this setting, the tissue specificity of *BRCA1/BRCA2*-linked disease might, in part, reflect an inadequate DNA repair response to tissue-specific DNA adduction.

Experimental Procedures

Plasmids

To generate vectors for the expression of myc epitope-tagged BRCA1 in mammalian cells, sequences encoding the tag were generated by PCR using pA3M (a pcDNA3 derivative vector containing three repeats of sequences that encode the myc epitope; Makela et al., 1995) as a template and the following primers: 5′-CACAAGCTT GGCCGCCAGTGTGCTGGA-3′ and 5′-ATAGGATCCATAACCGGTC AAGTCTTCTTC-3′. The product was ligated, in place of the HA-encoding sequences, into the HindIII-BamHI site of pcDNA3β/HA plasmids containing either wild type or the Y1853term mutant of BRCA1 (Scully et al., 1997a, 1997b). A BamHI fragment of BRCA1, encoding residues 1–1313 of BRCA1, was inserted in-frame into a new pcDNA3β-myc vector to generate myc-tagged BRCA1ΔBAMH I (deleting residues 1314–1863 of BRCA1).

BRCA2 full-length cDNA was assembled from fragments derived from five human cDNA libraries—including breast, placenta, thymus and brain. cDNA fragments were ligated to produce a full-length *BRCA2* cDNA. It was sequenced fully and found to be intact before use in the experiments described here. To generate a mammalian expression plasmid encoding HA-tagged full-length BRCA2, a pcDNA3β/HA vector containing wild-type *BRCA1* cDNA was digested with BamHI and XhoI to remove the full-length *BRCA1* sequence. A BamHI–EcoRV-XhoI linker was ligated into this cleaved/excised vector to generate a new mammalian expression vector termed pcDNA3β/HA-2. A 10 Kb SalI fragment containing the sequences encoding the full-length BRCA2 was inserted in-frame into the XhoI site of the pcDNA3β/HA-2 to generate an expression plasmid encoding HA-tagged BRCA2.

To generate plasmids encoding myc epitope-tagged BRCA1 fragments #1–#6, which correspond to the previously described GST-BRCA1 #1–#6 (Scully et al., 1997a), BamHI-EcoRI fragments encoding, respectively, BRCA1 fragments #1–#6 were individually ligated, in parallel, into pcDNA3 digested with HindIII and EcoRI, along with the HindIII-BamHI fragment encoding the myc epitope tag from pcDNA3β-myc-BRCA1. BRCA1 fragments #2 and #3 contain nuclear localization sequences and localized to the nucleus when synthesized in vivo. To ensure that BRCA1 fragment #1, #4, #5, and #6 also localized to nuclei, the SV40 nuclear localization sequence was inserted between the sequence encoding the myc epitope tag and the sequence encoding each relevant BRCA1 fragment.

Antibodies

Some of the anti-BRCA1 mAbs used here were described previously (Scully et al., 1996). SD118 and SD123 are monoclonal antibodies raised against GST fusion proteins encoding residues 758–1313 of BRCA1. Rabbit polyclonal antisera for BRCA1 were raised against GST fusion proteins encoding residues 758–1313 of BRCA1. Rabbit polyclonal antisera for BRCA2, anti-BRCA2A, anti-BRCA2B, and anti-BRCA2C were, respectively, raised against GST-BRCA2 fusion proteins encoding residues 1425–1973, 2422–2976, and 3245–3418. All polyclonal antisera were affinity-purified using an AminoLink kit, as suggested by the manufacturer (Pierce). "AK" anti-PCNA antisera is a generous gift of Dr. Robert L. Ochs (the Scripps Research Institute, La Jolla, CA).

Cell Culture

In general, cells were grown in DMEM supplemented with 10% fetal bovine serum. CAPAN-1 and HCC1937 were cultivated in RPMI supplemented with 10% fetal bovine serum. For transfection, the standard calcium phosphate precipitation method was used. Cells were collected 48 hr after transfection.

Immunoprecipitation and Immunoblotting

NETN buffer (150 mM NaCl, 1 mM EDTA, 20 mM Tris [pH 8.0], 0.5% NP-40) was normally used for cell lysis. For a typical immunoprecipitation reaction, 1–2 mg of whole-cell extract was incubated with 1 μg of antibody and 20 μl of protein A Sepharose beads (1:1) at 4°C for 1–2 hr. Beads were washed four times in 1 ml of NETN buffer. Proteins bound to the beads were eluted by boiling in SDS gel sample buffer, separated by SDS-PAGE, and transferred to Immobilon-P (Millipore). Immunoblotting was performed using the ECL kit as suggested by the manufacturer (Amersham). The primary antibodies were routinely used at a concentration of 1 μg/ml, and the HRP-conjugated secondary antibodies were used either at 1:2000 (HRP-conjugated protein A; Amersham) or 1:5000 dilution (HRP-conjugated goat anti-mouse Ig; Jackson ImmunoResearch laboratories, Inc.).

Immunostaining

Cells were fixed and permeabilized as described previously (Scully et al., 1997a, 1998c). Monoclonal anti-BRCA1 antibodies were used at a 1:10 to 1:50 dilution of the hybridoma culture supernatant. Affinity-purified anti-BRCA2 antibodies were used at a concentration of 1–2 μg/ml. The preparation and immunostaining of human spermatocytes, antibody incubation, and detection were performed according to Wessel and McClay (1986), or as described previously (Scully et al., 1997a). Fluorochrome-conjugated secondary antibodies were obtained from Jackson Immunoresearch or Pierce, and were used according to the manufacturer's instructions.

Acknowledgments

We are grateful to Matt Fred for his expert technical assistance, Dr. David Hill for his gift of the CAPAN-1 cell line, Dr. Robert L. Ochs for anti-PCNA AK sera, Dr. James A. DeCaprio and Jianmin Gan for their help in generating monoclonal antibodies, and Dr. Sean V. Tavtigian and Albert Wong for providing reagents. In addition, we are grateful to all of our laboratory and divisional colleagues for many helpful and stimulating conversations. J. C. was supported by NIH training grant. R. S. was supported by DOD IDEA award. This work was supported by grants from DOD IDEA award and the National Cancer Institute to D. M. L.

Received May 19, 1998; revised August 3, 1998.

References

Baumann, P., Benson, F.E., and West, S.C. (1996). Human Rad51 protein promotes ATP-dependent homologous pairing and strand transfer reactions in vitro. Cell *87*, 757–766.

Beckmann, M.W., Picard, F., An, H.X., Van Roeyen, C.R.C., Dominik,

S.I., et al. (1996). Clinical impact of detection of loss of heterozygosity of BRCA1 and BRCA1 markers in sporadic breast cancer. Br. J. Cancer *73*, 1220–1226.

Bertwistle, D., Swift, S., Marston, N.J., Jackson, L.E., Crossland, S., et al. (1997). Nuclear location and cell cycle regulation of the BRCA2 protein. Cancer Res. *57*, 5485–5488.

Bieche, I., Nogues, C., Rivoilan, S., Khodja, A., Latil, A., and Lidereau, R. (1997). Prognostic value of loss of heterozygosity at BRCA2 in human breast carcinoma. Br. J. Cancer *76*, 1416–1418.

Blackshear, P.E., Goldsworthy, S.M., Foley, J.F., McAllister, K.A., Bennett, L.M., et al. (1998). Brca1 and Brca2 expression patterns in mitotic and meiotic cells of mice. Oncogene *16*, 61–68.

Bork, P., Hofmann, K., Bucher, P., Neuwald, A.F., Altschul, S.F., and Koonin, E.V. (1997). A superfamily of conserved domains in DNA damage-responsive cell cycle checkpoint proteins. FASEB J. *11*, 68–76.

Callebaut, I., and Mornon, J.P. (1997). From BRCA1 to RAP1: a widespread BRCT module closely associated with DNA repair. FEBS Lett. *400*, 25–30.

Chapman, M.S., and Verma, I.M. (1996). Transcriptional activation by BRCA1. Nature *382*, 678–679.

Chen, F., Nastasi, A., Shen, Z., Brenneman, M., Crissman, H., and Chen, D.J. (1997). Cell cycle-dependent protein expression of mammalian homologs of yeast DNA double-strand break repair genes *Rad51* and *Rad52*. Mutat. Res. *384*, 205–211.

Chen, P.L., Chen, C.F., Chen, Y., Xiao, J., Sharp, Z.D., and Lee, W.H. (1998). The BRC repeats in BRCA2 are critical for RAD51 binding and resistance to methyl methanesulfonate treatment. Proc. Natl. Acad. Sci. USA *95*, 5287–5292.

Claus, E.B., Risch, N., and Thompson, W.D. (1991). Genetic analysis of breast cancer in the cancer and steroid hormone study. Am. J. Hum. Genet. *48*, 232–241.

Cleton-Jansen, A.M., Collins, N., Lakhani, S.R., Weissenbach, J., Devilee, P., et al. (1995). Loss of heterozygosity in sporadic breast tumours at the BRCA2 locus on chromosome 13q12-q13. Br. J. Cancer *72*, 1241–1244.

Connor, F., Bertwistle, D., Mee, P.J., Ross, G.M., Swift, S., et al. (1997). Tumorigenesis and a DNA repair defect in mice with a truncating Brca2 mutation. Nat. Genet. *17*, 423–430.

Fishman, J., Osborne, M.P., and Telang, N.T. (1995). The role of estrogen in mammary carcinogenesis. Ann. N Y Acad. Sci. *768*, 91–100.

Friedberg, E.C., Walker, G.C., and Siede, W. (1995). DNA repair and mutagenesis. (Washington, DC: ASM Press).

Futreal, P.A., Liu, Q., Shattuck-Eidens, D., Cochran, C., Harshmann, K., et al. (1994). BRCA1 mutations in primary breast and ovarian carcinomas. Science *266*, 120–122.

Goggins, M., Schutte, M., Lu, J., Moskaluk, C.A., Weinstein, C.L., et al. (1996). Germline *BRCA2* gene mutations in patients with apparently sporadic pancreatic carcinomas. Cancer Res. *56*, 5360–5364.

Gowen, L.C., Johnson, B.L., Latour, A.M., Sulik, K.K., and Koller, B.H. (1996). BRCA1 deficiency results in early embryonic lethality characterized by neuroepithelial abnormalities. Nat. Genet. *12*, 191–194.

Gudas, J.M., Nguyen, H., Li, T., and Cowan, K. (1995). Hormone-dependent regulation of BRCA1 in human breast cancer cells. Cancer Res. *55*, 4561–4565.

Gudas, J.M., Li, T., Nguyen, H., Jensen, D., Rauscher, F.J.I., and Cowan, K.H. (1996). Cell cycle regulation of BRCA1 messenger RNA in human breast epithelial cells. Cell Growth Differ. *7*, 717–723.

Hakem, R., de la Pompa, J.L., Sirard, C., Mo, R., Woo, M., Hakem, A., Wakeham, A., Potter, J., Reitmair, A., Billia, F., et al. (1996). The tumor suppressor gene *Brca1* is required for embryonic cellular proliferation in the mouse. Cell *85*, 1009–1023.

Hakem, R., de la Pompa, J.L., Elia, A., Potter, J., and Mak, T.W. (1997). Partial rescue of Brca1 (5–6) early embryonic lethality by p53 or p21 null mutation. Nat. Genet. *16*, 298–302.

Hall, J.M., Lee, M.K., and Newmann, B. (1990). Linkage of early-onset breast cancer to chromosome 17q21. Science *250*, 1684–1689.

Hanawalt, P.C., Cooper, P.K., Ganesan, A., and Smith, C.A. (1979). DNA repair in bacteria and mammalian cells. Annu. Rev. Biochem. *48*, 783–836.

Kelsell, D.P., Spurr, N.K., Barnes, D.M., Gusterson, B., and Bishop, D.T. (1996). Combined loss of BRCA1/BRCA2 in grade 3 breast carcinomas. Lancet *347*, 1554–1555.

Kerangueven, F., Eisinger, F., Noguchi, T., Allione, F., Wargniez, V., et al. (1997). Loss of heterozygosity in human breast carcinomas in the ataxia telangiectasia, Cowden disease and *BRCA1* gene regions. Oncogene *14*, 339–347.

Koonin, V.F., Altschul, S.F., and Bork, P. (1996). BRCA1 protein products: functional motifs. Nat. Genet. *13*, 266–267.

Lancaster, J.M., Wooster, R., Mangion, J., Phelan, C.M., Cochran, C., et al. (1996). BRCA2 mutations in primary breast and ovarian cancers. Nat. Genet. *13*, 238–240.

Lane, T.F., Deng, C., Elson, A., Lyu, M.S., Kozak, C.A., and Leder, P. (1995). Expression of BRCA1 is associated with terminal differentiation of ectodermally and mesodermally derived tissues in mice. Genes Dev. *9*, 2712–2722.

Liehr, J.G., Avitts, T.A., Randerath, E., and Randerath, K. (1986). Estrogen-induced endogenous DNA adduction: possible mechanism of hormonal cancer. Proc. Natl. Acad. Sci. USA *83*, 5301–5305.

Lim, D.S., and Hasty, P. (1996). A mutation in mouse rad51 results in an early embryonic lethal that is suppressed by a mutation in p53. Mol. Cell. Biol. *16*, 7133–7143.

Liu, C.Y., Flesken-Nikitin, A., Li, S., Zeng, Y., and Lee, W.-H. (1996). Inactivation of the mouse *Brca1* gene leads to failure in the morphogenesis of the egg cylinder in early postimplantation development. Genes Dev. *10*, 1835–1843.

Ludwig, T., Chapman, D.L., Papaioannou, V.E., and Efstratiadis, A. (1997). Targeted mutations of breast cancer susceptibility gene homologs in mice: lethal phenotypes of Brca1, Brca2, Brca1/Brca2, Brca1/p53, and Brca2/p53 nullizygous embryos. Genes Dev. *11*, 1226–1241.

Makela, T.P., Parvin, J.D., Kim, J., Huber, L.J., Sharp, P.A., and Weinberg, R.A. (1995). A kinase-deficient transcription factor TFIIH is functional in basal and activated transcription. Proc. Natl. Acad. Sci. USA *92*, 5174–5178.

Marcus, J.N., Watson, P., Page, D.L., Narod, S.A., Lenoir, G., et al. (1996). Hereditary breast cancer: pathobiology, prognosis, and *BRCA1* and *BRCA2* gene linkage. Cancer *77*, 697–709.

Marquis, S.T., Rajan, J.V., Wynshaw-Boris, A., Xu, J., and Yin, G.-Y. (1995). The developmental pattern of BRCA1 expression implies a role in differentiation of the breast and other tissues. Nat. Genet. *11*, 17–26.

Miki, Y., Swensen, J., Shattuck-Eidens, D., Futreal, P.A., Harshman, K., et al. (1994). A strong candidate for the breast and ovarian cancer susceptibility gene *BRCA1*. Science *266*, 66–71.

Miki, Y., Katagiri, T., Kasumi, F., Yoshimoto, T., and Nakamura, Y. (1996). Mutation analysis in the *BRCA2* gene in primary breast cancers. Nat. Genet. *13*, 245–247.

Monteiro, A.N.A., August, A., and Hanafusa, H. (1996). Evidence for a transcriptional activation function of BRCA1 C-terminal region. Proc. Natl. Acad. Sci. USA *93*, 13595–13599.

Narod, S.A., Feunteun, J., Lynch, H.T., Watson, P., Conway, T., Lynch, J., and Lenoir, G. (1991). Familial breast-ovarian cancer locus on chromosome 17q12–23. Lancet *338*, 82–83.

Neuhausen, S.L., and Marshall, C.J. (1994). Loss of heterozygosity in familial tumors from three BRCA1-linked kindreds. Cancer Res. *54*, 6069–6072.

Newman, B., Austin, M.A., Lee, M., and King, M.-C. (1988). Inheritance of breast cancer: evidence for autosomal dominant transmission in high risk families. Proc. Natl. Acad. Sci. USA *85*, 1–5.

Patel, K.J., Yu, V.P.C.C., Lee, H., Corcoran, A., Thistlethwaite, F.C., Evans, M.J., Colledge, W.H., Friedman, L.S., Ponder, B.A.J., and Venkitaraman, A.R. (1998). Involvement of Brca2 in DNA repair. Mol. Cell *1*, 347–357.

Radding, C.M. (1991). Helical interactions in homologous pairing and strand exchange driven by RecA protein. J. Biol. Chem. *266*, 5355–5358.

Rajan, J.V., Wang, M., Marquis, S.T., and Chodosh, L.A. (1996). Brca2 is coordinately regulated with Brca1 during proliferation and differentiation in mammary epithelial cells. Proc. Natl. Acad. Sci. USA *93*, 13078–13083.

Rajan, J.V., Marquis, S.T., Gardner, H.P., and Chodosh, L.A. (1997). Developmental expression of Brca2 colocalizes with Brca1 and is associated with proliferation and differentiation in multiple tissues. Dev. Biol. *184*, 385–401.

Rupp, W.D., and Howard-Flanders, P. (1968). Discontinuities in the DNA synthesised in an excision-defective strain of *Escherichia coli* following ultraviolet irradiation. J. Mol. Biol. *31*, 291–304.

Scully, R., Ganesan, S., Brown, M., DeCaprio, J.A., Cannistra, S.A., Feunteun, J., Schnitt, S., and Livingston, D.M. (1996). Location of BRCA1 in human breast and ovarian cell lines. Science *272*, 123–125.

Scully, R., Chen, J., Plug, A., Xiao, Y., Weaver, D., Feunteun, J., Ashley, T., and Livingston, D.M. (1997a). Association of BRCA1 with Rad51 in mitotic and meiotic cells. Cell *88*, 265–275.

Scully, R., Anderson, S.F., Chao, D.M., Wei, W., Ye, L., Young, R.A., Livingston, D.M., and Parvin, J.D. (1997b). BRCA1 is a component of the RNA polymerase II holoenzyme. Proc. Natl. Acad. Sci. USA *94*, 5605–5610.

Scully, R., Chen, J., Ochs, R.L., Keegan, K., Hoekstra, M., Feunteun, J., and Livingston, D.M. (1997c). Dynamic changes of BRCA1 subnuclear location and phosphorylation state are initiated by DNA damage. Cell *90*, 425–435.

Sharan, S.K., Morimatsu, M., Albrecht, U., Lim, D.-S., Regel, E., et al. (1997). Embryonic lethality and radiation hypersensitivity mediated by Rad51 in mice lacking BRCA2. Nature *386*, 804–810.

Shinohara, A., Ogawa, H., and Ogawa, T. (1992). Rad51 protein involved in repair and recombination in *Saccharomyces cerevisiae* is a RecA-like protein. Cell *69*, 457–470.

Sung, P. (1994). Catalysis of ATP-dependent homologous DNA pairing and strand exchange by yeast Rad51 protein. Science *265*, 1241–1243.

Sung, P., and Robberson, D.L. (1995). DNA strand exchange mediated by a Rad51-ssDNA nucleoprotein filament with polarity opposite to that of RecA. Cell *82*, 453–461.

Suzuki, A., de la Pompa, J.L., Hakem, R., Elia, A., Yoshida, R., et al. (1997). Brca2 is required for embryonic cellular proliferation in the mouse. Genes Dev. *11*, 1242–1252.

Tavtigian, S.V., Simard, J., Rommens, J., Couch, F., Shattuck-Eidens, D., et al. (1996). The complete *BRCA2* gene and mutations in chromosome 13q-linked kindreds. Nat. Genet. *12*, 333–337.

Teng, D.H., Bogden, R., Mitchell, J., Baumgard, M., Bell, R., et al. (1996). Low incidence of BRCA2 mutations in breast carcinoma and other cancers. Nat. Genet. *13*, 241–244.

Tsuzuki, T., Fujii, Y., Sakumi, K., Tominaga, Y., Nakao, K., et al. (1996). Targeted disruption of the *Rad51* gene leads to lethality in embryonic mice. Proc. Natl. Acad. Sci. USA *93*, 6236–6240.

Vaughn, J.P., Davis, P.L., Jarboe, M.D., Huper, G., Evans, A.C., et al. (1996). BRCA1 expression is induced before DNA synthesis in both normal and tumor-derived breast cells. Cell Growth Differ. *7*, 711–715.

Wessel, G.M., and McClay, D.R. (1986). Two embryonic, tissue-specific molecules identified by a double-label immunofluorescence technique for monoclonal antibodies. J. Histochem. Cytochem. *34*, 703–706.

Wooster, R., Neuhausen, S.L., Mangion, J., Quirk, Y., Ford, D., et al. (1994). Localization of a breast cancer susceptibility gene, *BRCA2*, to chromosome 13q12–13. Science *265*, 2088–2090.

Wooster, R., Bignell, G., Lancaster, J., Swift, S., Seal, S., et al. (1995). Identification of the breast cancer susceptibility gene *BRCA2*. Nature *378*, 789–792.

Xia, S.J., Shammas, M.A., and Reis, R.J. (1997). Elevated recombination in immortal human cells is mediated by HsRAD51 recombinase. Mol. Cell. Biol. *17*, 7151–7158.

Zhang, H., Tombline, G., and Weber, B.L. (1998). BRCA1, BRCA2, and DNA damage response: collision or collusion? Cell *92*, 433–436.

THE PRODUCTS OF THE BRCA1 AND BRCA2 TUMOR SUPPRESSOR GENES INTERACT STABLY IN MITOTIC AND MEIOTIC CELLS

Junjie Chen[1], Daniel P. Silver[1], Deepika Walpita[1], Sharon B. Cantor[1], Adi F. Gazdar[4], Gail Tomlinson[4], John D. Minna[4], Fergus J. Couch[1], Barbara L. Weber[1], Terry Ashley[2], David M. Livingston[1] and Ralph Scully[1]

[1]Dana-Farber Cancer Institute, Harvard Medical School, Boston, MA 02115; [2]Department of Genetics, Yale University School of Medicine, New Haven, CT 06520; [3]Department of Medicine, University of Pennsylvania, Philadelphia, PA 19104; [4]Hamon Center for Therapeutic Oncology Research, University of Texas Southwestern Medical Center, Dallas, TX 75235-8593

The two major hereditary breast cancer susceptibility genes, *BRCA1* and *BRCA2*, are associated with early onset breast and/or ovarian cancer and encode products which each interact with the product of the eukaryotic *RecA* homolog, *hRad51*. This and other data has led to speculation that BRCA1 and BRCA2 function in a related manner. Here, we report a specific physical association between the BRCA1 and BRCA2 proteins. This interaction was revealed by co-immunoprecipitation of the two endogenous proteins from extracts of untransfected cells, using antibodies specific for BRCA1 to co-precipitate BRCA2, and antibodies specific for BRCA2 to co-precipitate BRCA1. Moreover, Rad51 antibodies co-immunoprecipitated both BRCA1 and BRCA2 from extracts of untransfected cells. Two different, non-overlapping segments of BRCA1 appear to serve as interaction domains for BRCA2 and Rad 51, respectively, implying that BRCA2 does not serve solely as a linker protein bringing Rad 51 to the surface of BRCA1. BRCA 1 and BRCA2 also colocalize in subnuclear foci in mitotic cells, as well as on the (unsynapsed) axial elements of developing synaptonemal complexes in meiotic cells. Finally, like BRCA1 and Rad51, BRCA2 relocated to $PCNA^+$ replication sites following exposure of S phase cultures to either hydroxyurea or UV irradiation. Thus, one can hypothesize that BRCA1 and BRCA2 functionally communicate and participate in a common DNA damage response pathway associated with the activation of homologous recombination and double strand break repair. Dysfunction of this pathway may be a general phenomenon in the majority of cases of hereditary breast and/or ovarian cancer.

A NOVEL HELICASE, BAH1, INTERACTS WITH A TUMOR SUPPRESSION DOMAIN OF BRCA1 AND CONTRIBUTES TO ITS DOUBLE STRAND BREAK REPAIR FUNCTION.

Sharon Cantor, Shridar Ganesan, Elizabeth Kass, and David M. Livingston. The Dana-Farber Cancer Institute and the Harvard Medical School, Boston, MA

BRCA1 is mutated in a subset of families with inherited breast and/or ovarian cancer. Several lines of evidence suggest a role for this gene in the maintenance of genome integrity and in repairing double strand breaks. To date, several proteins have been identified as BRCA1- interacting elements. Most fall into the categories of repair, checkpoint control, DNA synthesis, or transcription regulation proteins. Yet, how these proteins participate in BRCA1 biochemical function and, where relevant, in its tumor suppression function remains unclear.

In search of proteins that interact with BRCA1 regions active in tumor suppression, we performed a screen for polypeptides that interact with the extreme BRCA1 carboxyl-terminal region, a segment that contains 2 BRCT repeat elements and is often compromised by tumor inducing mutations. A new, BRCA1 interacting protein was identified and cloned,. This 140 kd protein, BAH1, binds directly to the C-terminal BRCT unit, and two, clinically relevant point mutations in this domain, P1749R and M1775R, each disrupted BRCA1/BAH1 binding. BAH1 belongs to the DEAH family of DNA helicases, which have roles in basal transcription, DNA repair, and chromosome segregation.

The BAH1 gene maps to chromosome 17q22 and is ubiquitously expressed. Endogenous BAH1 is nuclear; regularly co-IPs with wt BRCA1, BRCA2, and BARD1; and colocalizes with these proteins in nuclear dots in S and G2 cells. In HCC1937 (BRCA1 -/-) cells, which synthesize only a truncated BRCA1 species with a defective C-terminal BRCT domain, the mutant protein failed to co-IP with BAH1, and the BAH1 nuclear dot pattern was perturbed. However, in wt BRCA1-transduced HCC cells, intact BRCA1/BAH1 complexes reappeared, and costaining nuclear dots were readily detected. Thus, an intact BRCT region of BRCA1 is essential for stable interactions with BAH1. In addition, a discrete, C-terminal segment of BAH1 is necessary for BRCA1 binding.

BRCA1 plays a major role in ds DNA break repair (DSBR). In this regard, U20S (BRCA1+/+) cells, transfected with an ATPase domain mutant of BAH1, capable of binding to wt BRCA1, were rendered defective in double strand break repair (DSBR). By contrast, a BAH1 double mutant, defective in both ATPase and BRCA1 binding and expressed at the same level as the single mutant, was inactive in this assay, despite its nuclear localization. Thus, in one of the first models of functional interplay between BRCA1 and an associated protein, BAH1 interacts with BRCA1 in a manner that contributes to a major BRCA1 activity. The latter correlates well with expression of its tumor suppression function.

FUNCTIONAL ANALYSIS OF THE BRCA1 GENE PRODUCT

S. Cantor, J. Chen, S. Ganesan, V. Joukov, R. Scully, W. ElShamy, D. Silver, Xiaohua Wu, Y.-L. Yang, and D. M. Livingston, Dana-Farber Cancer Institute and Harvard Medical School, Boston, MA 02115.

BRCA1 is a large, nuclear protein dedicated, in part, to the suppression of breast and ovarian cancer. BRCA1 participates in certain DNA damage responses and is a significant contributor to genome integrity control. It is an ATM substrate, a contributor to mitotic checkpoint control, a participant in the transcription-coupled repair of oxidative DNA damage, and interacts through specific domains with a variety of proteins dedicated to DNA repair and transcription control.

Presently unclear are the answers to two prime questions: how does BRCA1 exert its tumor suppressing function(s) and why are BRCA1 tumors manifest primarily in the breast and ovary? To address the former, we performed genetic analyses of certain BRCA1 functions. The approach was based on the observation that a BRCA1 -/- human breast tumor cell line (HCC 1937) is hypersensitive to gamma irradiation (IR), i.e. its DNA is hypernickable after standardized doses of IR, and it performs double strand break repair (DSBR) inefficiently, before but not after wt BRCA1 reconstitution. The method allows one to probe the behavior of selected mutant alleles expressed at physiological levels in these cells. Synthesis of species containing single, clinically relevant missense mutations which, in the aggregate, affect a diverse set of functional domains each failed to correct both the hypernickability and the DSBR defect of HCC. Thus, one can speculate that multiple BRCA1 domains cooperate to exert a common function(s), suggesting that BRCA1 operates, at least in part, as a scaffold, focusing diverse functions of multiple associated proteins on limiting nickability and promoting DSBR. In this regard, we have recently discovered and cloned a new BRCA1-associated protein (p130) which, although unique, contains a large, DNA-dependent helicase motif. BRCA1/p130 binding, like BRCA1 tumor suppression, depends upon the integrity of the BRCA1 C-terminal BRCT motifs, and a genetic analysis in BRCA1 -/- cells strongly suggests that a physiological interaction with p130, a putative helicase, contributes to BRCA1-mediated DSBR. This result implies that the facilitory role of BRCA1 on DSBR is linked, in part, to an indirect influence on DNA mechanics. Given these and the above-noted genetic data, one might hypothesize that at least part of the BRCA1 contribution to tumor suppression involves proper limitation of DNA nickability and regulation of DSBR. [This abstract has also been submitted to another meeting.]